UTILISATION OF NOVEL MAGNETIC RESONANCE IMAGING FEATURES IN THE DIAGNOSIS AND UNDERSTANDING OF MULTIPLE SCLEROSIS

Niraj Mistry

MA MB BChir, Downing College

A DISSERTATION SUBMITTED FOR THE DEGREE OF
DOCTOR OF MEDICINE OF THE UNIVERSITY OF CAMBRIDGE

MARCH 2016

Abstract

Background

There is no single test clinically available that is independently diagnostic for multiple sclerosis (MS). Currently MS is diagnosed using a combination of clinical evaluation and investigations including magnetic resonance imaging (MRI), interpreted in accordance with diagnostic criteria, to demonstrate the requisite dissemination of lesions in (anatomical) space and time.

Lesions comprising inflammatory demyelination in the central nervous system are a core pathological feature of MS. Ultra-high field (e.g. 7 Tesla or 7T) T2*-weighted MRI can demonstrate in vivo a central vein in most of these lesions. This is a histopathologically specific feature which could be exploited to improve diagnostic workup in cases of suspected inflammatory demyelination.

Central nervous system white matter not involved in demyelinating lesions is nevertheless affected in MS. The mechanisms inflicting injury to this normal appearing white matter (NAWM) and how they relate to focal lesions are unclear. Damage to NAWM seems important, because it correlates well with disability. Any association between cortical lesions, focal white matter lesions (WML) and diffuse damage to NAWM is difficult to investigate in vivo in MS, principally because MRI is relatively insensitive to cortical lesions. Investigation of such associations may also be confounded by the presence of small focal lesions within the "NAWM" that may remain undetected when using conventional MRI to define NAWM. Advantages inherent to ultra-high field MRI might help mitigate both of these problems.

Objectives and methods

For any diagnostic test to be useful, it must be sensitive and specific at the onset of disease (not just adept at distinguishing long-established cases). We therefore prospectively investigated whether a single 7T T2*-weighted MRI brain scan could predict accurately (based on the presence of a central vein in brain lesions) an eventual diagnosis of MS in a group of patients referred to the Neurology clinic with diagnostic uncertainty.

Even if a 7T MRI brain scan can be used to predict an eventual diagnosis of MS, 7T MRI scanners remain the preserve of research institutions, and are not used in routine clinical practice. In order to translate any benefit to clinical practice, such a technique must work using clinically available scanners. We therefore investigated whether a version of the protocol optimised for use with a standard clinical 3T MRI scanner could distinguish known cases of MS from brain lesions due to microangiopathic (i.e. small-vessel ischaemic) changes.

One postulated explanation for some of the damage to NAWM in MS is that occult focal lesions do exist within the NAWM, which are beyond the resolution of conventional MRI scanners. We therefore compared lesion detection using 7T magnetisation prepared rapid acquisition gradient echo (MPRAGE) and 3T fluid attenuation inversion recovery (FLAIR) MRI brain scans in known cases of MS.

To investigate potential associations between cortical lesions, WML and diffuse damage to NAWM we analysed 7T MRI brain scans of people with MS, which were segmented into cortical lesion, WML, and NAWM compartments. Cortical lesions were identified using both MPRAGE and magnetisation transfer ratio (MTR) images. WML were detected and NAWM segments were defined using MPRAGE images. The extent of damage to NAWM was ascertained by measuring its MTR.

Results

A single 7T T2*-weighted MRI brain scan was performed at baseline on 29 patients suspected to have MS, but in whom initial conventional diagnostic workup proved inconclusive. By calculating the proportion of brain lesions containing a central vein on the 7T MRI scan, we were able to correctly predict whether the eventual clinical diagnosis arrived at by their treating neurologist was MS or not MS (after a median follow-up period of 26 months), in all 22 out of 29 participants who had received a clinical diagnosis.

For the cross-sectional study comparing an optimised 3T T2*-weighted MRI brain scan index test (against the diagnosis already established by the patient's neurologist), 20 patients were recruited for the test cohort. Ten of them had MS and the other 10 patients were known to have microangiopathic WML related to small-vessel ischaemic disease (in 7 cases) or migraine (in 3 cases). The MS group had a significantly higher proportion of lesions with perivenous appearance compared to the non-MS group. All MS patients had central veins visible in >45% of brain lesions. All non-MS patients had central veins visible in <45% of lesions. Based on this technique, a “rule of six” was devised that quickly and accurately characterised MS cases in a further validation cohort of another 20 individuals with brain lesions (13 with MS, the rest had WML related to hypertension associated small-vessel ischaemic disease or migraine).

In order to assess whether focal multiple sclerosis lesions can be found using 7T MPRAGE MRI in NAWM defined using 3T FLAIR MRI, 14 patients with clinically definite MS underwent 3T and 7T MRI brain scans. Although the majority of lesions were detected both on 3T FLAIR and 7T MPRAGE images, 22% of the lesions were only detected using 7T MPRAGE.

To evaluate association between cortical lesions, WML, and diffuse damage to NAWM 19 people with MS were recruited to undergo a 7T MRI brain scan. Cortical lesion volume and counts on both

MPRAGE and MTR images correlated significantly with NAWM MTR. WML load did not correlate significantly with NAWM MTR.

Conclusions

For the cohort of patients in whom conventional methods left initial diagnostic doubt, a single early 7T T2*-weighted MRI had 100% positive and negative predictive value for MS.

Optimised 3T T2*-weighted MRI can be used to differentiate between individuals with MS and those with microangiopathic brain lesions. If validated in a large prospective cohort, this technique could complement existing diagnostic algorithms by improving the specificity with which MRI demonstrates inflammatory demyelinating brain lesions.

MRI with 7T MPRAGE enables detection of MS lesions in areas defined as NAWM using 3T FLAIR MRI. Focal MS lesions contribute to the abnormalities known to exist in what has previously been classified as the NAWM. In future, inclusion of 7T MRI lesion maps may refine segmentation of NAWM and augment accuracy of analyses involving NAWM metrics.

Cortical lesion load determined using 7T MRI has a significant correlation with NAWM MTR. Although it does not prove causation, the correlation implicates cortical lesions in the pathogenesis of NAWM injury, which underlies progression and disability in MS.

Keywords: “Multiple Sclerosis”, “Magnetic Resonance Imaging”, “Diagnosis”, “Sensitivity and Specificity”

Table of Contents

Publications and presentations related to this thesis

Publications

Imaging central veins in brain lesions with 3-T T2-weighted magnetic resonance imaging differentiates multiple sclerosis from microangiopathic brain lesions.*

Mistry N, Abdel-Fahim R, Samaraweera A, Mougin O, Tallantyre EC, Tench C, *et al.* Mult. Scler. J. 2016; 22(10): 1289-96

Cortical lesion load correlates with diffuse injury of multiple sclerosis normal appearing white matter.

Mistry N, Abdel-Fahim R, Mougin O, Tench C, Gowland P, Evangelou N.

Mult. Scler. J. 2014; 20: 227–233.

Central veins in brain lesions visualized with high-field magnetic resonance imaging: a pathologically specific diagnostic biomarker for inflammatory demyelination in the brain.

Mistry N, Dixon J, Tallantyre EC, Tench C, Abdel-Fahim R, Jaspan T, *et al.*

JAMA Neurol. 2013; 70: 623–628.

The above was a "Research Highlight" in Nature reviews neurology:

Multiple sclerosis: Imaging of central veins in brain lesions can be used to predict multiple sclerosis.

Nat. Rev. Neurol. 2013; 9: 240–240.

Focal multiple sclerosis lesions abound in 'normal appearing white matter'.

Mistry N, Tallantyre EC, Dixon JE, Galazis N, Jaspan T, Morgan PS, *et al.*

Mult. Scler. J. 2011; 17: 1313–1323.

Platform presentations

3T T2 MRI distinguishes MS from microangiopathic lesions*

Mistry N, Abdel-Fahim R, Samaraweera A, Mougin O, Tallantyre EC, Tench C, *et al.*

Association of British Neurologists Annual Meeting 2014, Cardiff

A Single 7 Tesla MRI Brain Scan Predicts Multiple Sclerosis in Cases with Initial Diagnostic Uncertainty

Mistry N, Dixon J, Tallantyre EC, Tench C, Abdel-Fahim R, Jaspan T, *et al.*

Presented at

American Academy of Neurology 64th Annual Meeting 2012, New Orleans **(also included in meeting scientific highlights)**

AND

Association of British Neurologists Annual Meeting 2011, Newcastle

Ultra high-field MRI (7T) uncovers many multiple sclerosis lesions undetected with clinical 3 Tesla MRI

Mistry N, Galazis N, Tallantyre EC, Dixon J, Jaspan T, Morgan P, *et al.*

26th Congress of the European Committee for Treatment and Research in Multiple Sclerosis (ECTRIMS) 2010, Gothenburg

Poster presentations

A corticocentric model for MS pathogenesis

Mistry N, Abdel-Fahim R, Tench C, Mougin O, Gowland P

Association of British Neurologists Annual Meeting 2014, Cardiff

3 Tesla T2 brain MRI distinguishes multiple sclerosis from incidental white matter lesions*

Mistry N, Dixon J, Tallantyre EC, Tench C, Abdel-Fahim R, Jaspan T, *et al.*

29th Congress of the European Committee for Research and Treatment in Multiple Sclerosis (ECTRIMS) 2013, Copenhagen

(Top scoring poster and included in meeting scientific highlights)

A single 7T MRI brain scan accurately predicts eventual diagnosis of MS in cases with initial diagnostic uncertainty

Mistry N, Dixon J, Tallantyre EC, Jaspan T, Morgan P, Morris P *et al.*

Presented at

5th Joint triennial congress of the European and Americas Committees for Treatment and Research in Multiple Sclerosis 2011, Amsterdam

AND

Neuroscience @ Nottingham Poster and Lecture Day 2011 **(won first prize)**

Abbreviations

3D	3-dimensional
3T	3 Tesla
7T	7 Tesla
ABN	The Association of British Neurologists
ADC	apparent diffusion coefficient
ANOVA	analysis of variance
B_0	the constant, homogeneous magnetic field used to polarize proton spins
B_1	the applied radiofrequency field
BBB	blood-brain-barrier
BOLD	blood oxygen level–dependent
CD163	cluster of differentiation 163 (T-cell co-receptor)
CD3	cluster of differentiation 3 (T-cell co-receptor)
CIS	clinically isolated syndrome
CNS	central nervous system
CSF	cerebrospinal fluid
CTLA4	cytotoxic T-lymphocyte-associated protein 4
DIS	dissemination in space
DIT	dissemination in time
DMTs	disease modifying therapies
DWI	diffusion weighted imaging
EDSS	expanded disability status scale
EPI	echo planar imaging
FLAIR	fluid attenuation inversion recovery
FLAIR*	the product of T2*-weighted and FLAIR images

FLIRT	FMRIB's Linear Image Registration Tool
FMRIB	Oxford Centre for Functional MRI of the Brain
FSL	FMRIB Software Library
GWAS	genome-wide association studies
HLA	human leukocyte antigen
ICAM1	intercellular adhesion molecule 1
IFNB	β-interferon
IgG	immunoglobulin G
MHC	major histocompatibility complex
MPRAGE	magnetisation prepared rapid acquisition gradient echo
MRI	magnetic resonance imaging
MRS	magnetic resonance spectroscopy
MS	multiple sclerosis
MTI	magnetisation transfer imaging
MTR	magnetisation transfer ratio
MTT	mean transit time
NAA	N-acetylaspartate
NAWM	normal appearing white matter
NHS	National Health Service
NMO	neuromyelitis optica
OCB	oligoclonal bands
PPMS	primary progressive multiple sclerosis
RF	radiofrequency
RRMS	relapsing-remitting multiple sclerosis
sABC	StreptAvidin-Biotin Complex

SAR	specific absorption rate
SE	standard error
SENSE	SENSitivity Encoding, a parallel imaging technique
SH2D2A	SH2 domain containing 2A (a protein coding gene)
SNP	single-nucleotide polymorphism
SNR	signal to noise ratio
SPECTRIMS	Secondary Progressive Efficacy Clinical Trial of Recombinant Interferon-beta-1a in MS
SPMS	secondary progressive multiple sclerosis
SWI	susceptibility-weighted imaging
T2*	pronounced "T - Two star", T2* relaxation is the loss of signal seen with dephasing of individual magnetizations
TE	echo time
TFE	turbo-field echo
TI	inversion time
TR	repetition time
VEP	visual evoked potentials
WML	white matter lesions

Acknowledgments

The work presented in this thesis was performed in: the Department of Clinical Neurology, University of Nottingham; the Department of Histopathology, Queens Medical Centre, Nottingham University Hospitals NHS Trust; and the Sir Peter Mansfield Magnetic Resonance Centre, University of Nottingham.

I thank Professor Nikos Evangelou for obtaining funding for my time in research and for his tenure as my supervisor. I am also indebted to Professor Penny Gowland for her support and counsel, Dr Paul Morgan for his MRI physics insights, and to Dr Tim Jaspan for lending his neuroradiological expert opinion.

Much of my work was enabled by bespoke software tools that Dr Chris Tench added to his NeuRoi image analysis suite, always expeditiously upon my every request. I am also thankful to Dr Tench for his expert statistics advice at the inception of each project, and for his close guidance in application of statistical methods to the data.

I am grateful to my successors Dr Amal Samaraweera and Dr Rasha Abdel-Fahim for helping to recruit volunteers for scanning, and for performing any image analyses that (for the purposes of blinding) needed to be done by someone other than me.

The research team at the Sir Peter Mansfield Magnetic Resonance Centre optimised the MRI sequences fundamental to my work, and patiently answered my incessant questions about MRI physics whenever we were scanning volunteers.

Most of all I am grateful to the people with MS and healthy volunteers who gave their time willingly and travelled to the Sir Peter Mansfield Magnetic Resonance Centre in order to undergo research MRI scans.

Any reference to the work of others is cited in the text and listed among the references. The work presented in chapters 2 to 5 is original and this dissertation is not substantially the same as any that I have submitted for another degree, diploma or similar qualification at this or any other university.

This work was supported by the UK Multiple Sclerosis Society (grant number 919) and the Medical Research Council (grant number G0901321).

Chapter 1: Introduction

The study of multiple sclerosis (MS) began in earnest with the works of Jean-Martin Charcot at the Salpétrière in the late 19th century. His influence grew throughout the English-speaking world with the publication of the New Sydenham Society edition of his lectures, which consolidated his various monikers for the disease into the translation "disseminated sclerosis" (Charcot, 1881).

In the New Sydenham Society translation, Charcot opined that: "Usually, there is superadded a whole group of phenomena, which are generally known as cephalic symptoms, and whose starting point is a lesion of the cerebral or bulbar nerves, such as the optic nerves, for instance, or the motor nerves of the eye. In this relation, we can draw a parallel between progressive locomotor ataxia and the disease which I have proposed to call disseminated sclerosis. The latter, like the former, invades different points of the cerebro-spinal system simultaneously, and we have cause to discriminate, in the clinical description of both affections, between the spinal symptoms and the cephalic symptoms. Disseminated sclerosis, like locomotor ataxia, most usually pursues a doomed downward path. But the analogies cease there, and, in detailing the symptoms, we have only to mark differences which almost always enable us to make a diagnosis without difficulty" (Charcot, 1881).

Since then many advances have been made in the understanding and management of MS, but we still recognise the commonest form of the disease principally by its tendency to repeatedly provoke distinct episodes of symptoms and signs (i.e. relapses), which are disseminated in time and in space (affecting different points of the "cerebro-spinal system"). We still rely on this trait to secure or exclude a diagnosis of MS, though now with the assistance of laboratory, neurophysiological, and radiological investigations.

While relapses disseminated in time and in space are a striking early feature of most cases of MS, most individuals with relapsing-remitting MS (RRMS) eventually enter a phase of gradual but unrelenting disease progression: secondary progressive MS (SPMS). The mechanisms underlying this transition are not fully understood. A minority of people with MS experience unrelenting gradual disease progression from the outset, i.e. primary progressive MS (PPMS), sometimes in the absence of any relapses. Why this happens in the relative absence of relapses and how PPMS relates to RRMS and SPMS is also not fully understood.

My thesis will exploit magnetic resonance imaging (MRI) tools that might supplement existing diagnostic techniques for MS, and will also interrogate potential disease mechanisms underlying progressive forms of MS.

1.1 Epidemiology of MS

Incidence in the UK is estimated at 2,500 new diagnoses per year, resulting in prevalence of 100 to 120 cases per 100,000; MS affects twice as many women as men, and incidence peaks in the third decade of life (Compston and Confavreux, 2005).

Prevalence increases with distance from the equator, independent of genetic factors, so that prevalence is highest in northern Europe, southern Australia, and North America (Compston and Confavreux, 2005). This raises the possibility of environmental aetiological factors including infections (Lipton *et al.*, 2007) and vitamin D deficiency due to lack of sun exposure (VanAmerongen *et al.*, 2004). Migration modifies risk only among those who migrate early in life; those who migrate from low to high prevalence areas after adolescence retain their country of origin's lower risk of developing MS (Alter *et al.*, 1978).

While environmental and genetic factors are contributory, the aetiology of MS remains unknown.

1.2 Genetics of MS

Genetic factors exert a substantial influence: the concordance rate of MS in monozygotic twins is 30.8%, whereas in dizygotic twins it is 4.7% (Sadovnick *et al.*, 1993). A genome screen in MS revealed susceptibility loci on chromosomes 6p21 and 17q22 (Sawcer *et al.*, 1996), but there are many genes that seem to be associated with MS including human leucocyte antigen (HLA) classes I and II, T-cell receptor β, CTLA4, ICAM1, and SH2D2A (Dyment *et al.*, 2004).

Across the entire human genome, the major histocompatibility complex (MHC) on chromosome 6 makes the single largest known genetic contribution to MS risk (Patsopoulos *et al.*, 2013). The recent advent of high-throughput typing for single-nucleotide polymorphisms (SNP) has enabled the study of thousands of individuals, allowing substantial progress to be made in determining associations between MS and variation in the genes encoding HLAs contained within the MHC (Sawcer *et al.*, 2014). The greatest effect on risk is driven by the HLA-DRB1*15:01 allele, which exerts an odds ratio of 3.10 (Sawcer *et al.*, 2011).

Little progress was made in the identification of risk alleles outside the major histocompatibility complex before the advent of genome-wide association studies (GWAS). The largest of those confirmed 23 previously reported associations and identified an additional 34 new associated variants, implicating genes coding for cytokine pathways (CXCR5, IL2RA, IL7R, IL7, IL12RB1, IL22RA2, IL12A, IL12B, IRF8, TNFRSF1A, TNFRSF14, TNFSF14), co-stimulation (CD37, CD40, CD58, CD80, CD86, CLECL1) and signal transduction (CBLB, GPR65, MALT1, RGS1, STAT3, TAGAP, TYK2), as well as genes related to Vitamin D metabolism (CYP27B1, CYP24A1) (Sawcer *et al.*, 2011).

Fine mapping within the resolution of GWAS signals using the ImmunoChip custom genotyping array identified 48 new susceptibility variants, such that there are now 110 established multiple sclerosis risk variants at 103 discrete loci outside of the MHC (Beecham *et al.*, 2013).

Meta-analysis of extant GWAS data and use of neoteric methods such as the Exomechip will further expand the catalogue of associated variants in the near future.

1.3 Clinical features of MS

Most people with MS have RRMS: discrete episodes of neurological symptoms and disability, acute in onset, followed by a period of improvement. Because relapses may affect any part of the central nervous system (CNS), diverse symptoms may arise with each relapse.

As Charcot had observed, MS seems to have a predilection for certain areas within the CNS: the optic nerves, cerebellum, spinothalamic and pyramidal tracts are commonly involved; giving rise to common presenting features of MS such as optic neuritis, ataxia, and sensorimotor disturbances of various body parts (Weinshenker *et al.*, 1989).

There is wide inter-individual variability in the frequency and severity of relapses. However, 25 years after disease onset, 80% of people with RRMS will have transitioned into SPMS (usually accompanied by a reduction in relapse frequency) (Kremenchutzky *et al.*, 2006), and 10% to 15% of people with MS have PPMS (Thompson *et al.*, 1997; Kremenchutzky, 2003). Mean age of onset of PPMS is 38 years (Confavreux *et al.*, 1980; Weinshenker *et al.*, 1989; McDonnell and Hawkins, 1998; Andersson *et al.*, 1999; Stevenson *et al.*, 1999), similar to the age at which transition from RRMS to SPMS tends to occur (Confavreux *et al.*, 2000).

1.4 The pathological substrate of clinical disability in MS

Whilst the pathological hallmark of MS is the white matter plaque, axonal loss is the pathological process chiefly responsible for irreversible neurological disability in people with MS (Tallantyre, Bø, *et al.*, 2010).

The white matter plaque is typically a sharply demarcated ovoid lesion sometimes reaching several centimetres in diameter, histopathologically characterised by breakdown of the blood-brain-barrier (BBB) and inflammatory cell infiltration (predominantly macrophages, either derived from blood-borne monocytes, or stemming from resident microglia) effecting demyelination, astroglial scarring, and axonal loss (Gay and Esiri, 1991; Kwon and Prineas, 1994; Trapp *et al.*, 1998; Lassmann and Wekerle, 2005).

Axonal loss occurs from an early stage in the disease, and is not confined to white matter plaques (Trapp *et al.*, 1999; Rovaris *et al.*, 2005; Bjartmar *et al.*, 2001).

Magnetic resonance spectroscopy (MRS) studies confirm that axonal loss, even in the normal appearing white matter (NAWM), denoted by reduction in N-acetylaspartate (NAA) levels, is a better predictor of clinical disability than conventional MRI lesion load (i.e. white matter plaques) (De Stefano *et al.*, 1998; Fu *et al.*, 1998; Lee *et al.*, 2000).

1.5 Treatment of MS

Current therapies are either symptomatic (e.g. to control sensory disturbance, spasticity, sphincter dysfunction, fatigue and depression) or "disease modifying therapies" (DMTs). High doses of corticosteroids such as methylprednisolone can be used to hasten recovery from a disabling relapse, but they do not significantly alter the final extent of recovery (Beck and Cleary, 1993).

The Association of British Neurologists (ABN) first published guidelines on the use of licenced DMTs in 1999 (at the time licenced DMTs comprised just β-interferon or glatiramer acetate). Their guidelines have been periodically updated since, most recently in 2015 (Scolding *et al.,* 2015). There is a growing fashion to treat MS earlier and more aggressively in those perceived to have a worse outlook, but there is a relative lack of evidence for a long-term benefit from this approach (Scolding *et al.,* 2015). Nevertheless, DMTs clearly impact on relapses and relapse-related disability, so the ABN recommends initiating treatment as soon as possible in eligible individuals.

All of the licensed DMTs for MS (currently β-interferons, glatiramer acetate, fingolimod, teriflunomide, dimethyl fumarate, natalizumab, and alemtuzumab) variably reduce relapse rates and lesion accumulation (detected using serial MRI scans) in people with relapsing forms of MS (Rice, 2014). There are few "head-to-head" comparison trials and inter-trial comparison of drugs is fraught with difficulties. Nevertheless, the ABN guidelines divide the DMTs into two classes: those with "moderate efficacy" and those with "high efficacy".

Moderate efficacy drugs (β-interferons, glatiramer acetate, teriflunomide, dimethyl fumarate and fingolimod) reduce the average relapse rate by 30% to 50%. High efficacy drugs (alemtuzumab and natalizumab) reduce the average relapse rate by substantially more than 50%, but with higher risk of potentially serious side effects (Scolding *et al.,* 2015).

Current therapeutic strategies are employed in the hope that reducing relapse rate and MRI lesion accumulation might improve long-term prognosis. However, it is quite clear from natural history studies that relapse frequency has only a weak correlation with long-term disability (Confavreux *et al.,* 2000; Scalfari A *et al.,* 2013).

Controlled trials have reported mixed results as to whether β-interferons reduce accumulation of disability over 2 to 3 years (The IFNB Multiple Sclerosis Study Group, 1993; Secondary Progressive Efficacy Clinical Trial of Recombinant Interferon-beta-1a in MS (SPECTRIMS) Study Group, 2001; The North American Study Group on Interferon beta-1b in Secondary Progressive MS, 2004). Much of the disability accumulated over a 2 or 3 year period may be directly attributable to the effects of relapses, rather than whatever mechanism effects genuine long-term disability progression.

There is no controlled trial data available that shows long-term benefit with DMTs; uncontrolled studies with follow-up up to 16 years (open-label retrospective analyses of cohorts that were originally in 2 or 3 year placebo-controlled β-interferon trials) have conflicting results, with some suggesting reduced long-term disability (Bermel *et al.*, 2010), while others do not (Ebers *et al.*, 2010; Greenberg BM *et al.*, 2013). It is unclear whether high efficacy drugs affect long-term (i.e. mean follow-up 6 years) disability (Willis *et al.*, 2015).

It is not clear that any of the currently available DMTs significantly modify progressively increasing disability unrelated to relapses, or long-term accumulation of disability, or transition from RRMS to SPMS; consequently none of the current DMTs are recommended in non-relapsing SPMS or PPMS (Scolding *et al.*, 2015).

1.6 The role of MRI in diagnosis of MS

Strategies to diagnose MS have necessarily evolved to include the valuable information provided by investigational techniques as they have become available. T2-weighted MRI has long been known to have excellent sensitivity for the detection of brain white-matter lesions (Young *et al.*, 1981). MRI, cerebrospinal fluid (CSF) analysis for oligoclonal bands, and visual and somatosensory

evoked potential testing are often invaluable when a diagnosis of MS cannot be achieved based on clinical features alone. Even in cases of MS that can be confidently diagnosed on clinical grounds, it would now be highly unusual for brain MRI to be omitted in modern Neurological practice. For relapsing-remitting MS, when history and examination fail to satisfy diagnostic criteria of separation of disease activity in (anatomical) space and time, MRI evidence fulfilling those criteria is accepted (Polman *et al.*, 2011).

Positive MRI findings, with or without CSF evidence (on the background of one year of disease progression) are formally established as a prerequisite for a diagnosis of primary progressive MS (Polman *et al.*, 2011).

Despite their usefulness, none of the above investigations in isolation can claim to demonstrate a pathognomonic feature of MS that proves or excludes the diagnosis. Although MRI sequences can return signal in brain areas that correlate with areas of inflammation or demyelinated plaques, MRI cannot expressly visualise myelin or demyelination. MRI T1 and T2 relaxation times are used to generate "scans" showing where (water) proton concentration and physico-chemical environments vary. Such changes on MRI scans are not specific for MS, which is why the skill of the neurologist will remain in the appropriate clinical evaluation, investigation, and interpretation of results according to the prevailing diagnostic criteria, in order to accurately diagnose MS.

1.7 Evolution of diagnostic criteria

In 1983 Poser *et al.* recommended MS diagnostic criteria based on a gold standard of two or more attacks with clinical (with or without supportive "laboratory") evidence that disease was disseminated in space and time. Where clinical evidence was lacking or there was only one attack, imaging, neurophysiological findings or oligoclonal bands were allowed to support the diagnosis.

By this method Poser stratified diagnoses of MS into one of five groups: 1) clinically definite MS; 2) clinically probable MS; 3) laboratory supported definite MS; 4) laboratory supported probable MS; 5) not MS. These criteria included no formal synthesis on use of MRI changes in MS (Poser *et al.*, 1983).

Poser's criteria did not allow for easy evaluation of people with progressive rather than RRMS. Thompson *et al.* addressed this issue in 2000 by proposing criteria that included findings from MRI, CSF, and evoked potentials. For a definite diagnosis of primary progressive MS, they required at least one year of clinical progression of disease, along with oligoclonal bands and either definite MRI abnormality, or equivocal MRI abnormality plus abnormal evoked potentials. Definite MRI abnormality was stipulated as nine or more brain lesions, or two or more spinal cord lesions, or one spinal cord lesion plus four to eight brain lesions (Thompson *et al.*, 2000).

In 2001 an international panel led by McDonald devised criteria which specified MRI features that would be accepted as demonstration of separation of MS disease activity in space and/or time (McDonald *et al.*, 2001). The advantage of this was that earlier secure diagnosis of MS could be facilitated by early MRI evidence for separation of MS disease activity in space and/or time, if this evidence was lacking clinically. Earlier diagnosis carries with it therapeutic implications and potential advantages, since the advent of DMTs.

Under the 2001 international panel "McDonald criteria" for MS:

- Two or more clinical attacks and objective clinical evidence of two or more anatomically separate CNS lesions requires no additional data to confer a diagnosis of MS.
- With two or more clinical attacks but objective clinical evidence of only one lesion, the additional data to diagnose MS can be dissemination in space (DIS) demonstrated by

MRI, or at least two MRI lesions consistent with MS plus CSF oligoclonal bands, or to await a subsequent attack of MS that implicates a different site for the new lesion.

- With only one attack but objective clinical evidence of two or more lesions, the additional data to diagnose MS can be dissemination in time (DIT) demonstrated by MRI, or a second clinical attack.
- With only one attack and objective clinical evidence of only one lesion, such as in a clinically isolated syndrome (CIS), the additional data to diagnose MS can be DIS demonstrated by MRI, or at least two MRI detected lesions consistent with MS plus CSF oligoclonal bands plus DIT demonstrated by MRI, or a second clinical attack.
- When neurological progression is suggestive of MS but proceeds insidiously, diagnosis of (progressive) MS requires positive CSF oligoclonal bands with either:
    - DIS demonstrated by 1) nine or more brain T2 lesions, or 2) two or more lesions in the spinal cord, or 3) four to eight brain lesions plus one spinal cord lesion

      or,
    - Abnormal visual evoked potentials (VEP), either with four to eight brain lesions, or less than four brain lesions plus one spinal cord lesion on MRI, and
    - DIT demonstrated by MRI

      or,
    - Continued progression for one year

- Meeting three of the following requirements satisfied McDonald *et al*'s 2001 MRI evidence criteria for DIS (based on Barkhof's criteria (Barkhof *et al.*, 1997) modified by Tintoré (Tintore *et al.*, 2000)):
    - One or more gadolinium enhancing lesions, or nine or more T2 hyperintense lesions in the absence of gadolinium enhancing lesions
    - One or more infratentorial lesions

- One or more juxtacortical lesions
- Three or more periventricular lesions

- The 2001 criteria laid out two scenarios for establishing MRI evidence for DIT:

1. If the initial MRI was three months or more after the clinical attack, then the presence of a single gadolinium enhancing lesion alone is enough evidence for DIT (unless it is at the same anatomical site implicated by the initial clinical attack). If there was no enhancing lesion on the original scan, then a follow-up scan is required. McDonald *et al.* recommended that this should probably be done three months after the initial scan. On the follow-up scan, a new gadolinium enhancing, or T2 lesion is then accepted as sufficient evidence that there was DIT.
2. If the initial MRI was less than three months after the clinical attack, a follow-up scan is required. This should be done after a delay of at least 3 months from the first scan. If the second scan shows a new gadolinium enhancing lesion then that is sufficient evidence for DIT. If not, then a third scan is required after another delay of at least three months. If the third scan shows either a new T2 or gadolinium enhancing lesion then DIT is considered evident.

In 2005 the international panel reconvened, led by Polman, and applied revisions to the 2001 "McDonald criteria" (Polman *et al.*, 2005). The main changes were that:

- New T2 lesions were now allowed as early evidence for DIT, when there was only a single clinical event.
- Individual spinal cord lesions could now contribute along with individual brain lesions to reach the required number of T2 lesions, for DIS.
- Positive CSF oligoclonal bands were no longer a prerequisite for the diagnosis of primary progressive MS.

In 2010 the international panel again reconvened, to produce the latest iteration of their diagnostic criteria (Polman *et al.*, 2011). The use of MRI for demonstration of dissemination of CNS lesions in space and time was simplified, and it became possible for DIS and DIT to be established by a single scan:

- Using these latest 2010 "McDonald Criteria" for Diagnosis of MS, if a patient experiences two or more "attacks" (i.e. relapses), and has objective clinical evidence of two or more lesions or objective clinical evidence of 1 lesion with reasonable historical evidence of a prior attack, no additional data is needed for MS diagnosis.
- If a patient experiences two or more attacks, with objective clinical evidence of one lesion, additional data needed for MS diagnosis is proof of DIS, demonstrated by:
    - One or more T2 lesions in at least 2 of 4 "MS-typical regions" of the CNS (i.e. periventricular, juxtacortical, infratentorial, or spinal cord)

      Or,
    - By awaiting a further clinical attack implicating a different CNS site
- If a patient experiences one attack, with objective clinical evidence of two or more lesions, additional data needed for MS diagnosis is proof of DIT, demonstrated by:
    - Simultaneous presence of asymptomatic gadolinium-enhancing and non-enhancing lesions at any time

      Or,
    - A new T2 and/or gadolinium-enhancing lesion(s) on follow-up MRI, irrespective of its timing with reference to a baseline scan

      Or,
    - By awaiting a second clinical attack.
- If a patient experiences one attack, with objective clinical evidence of one lesion (i.e. CIS), additional data needed for MS diagnosis is proof of DIS and DIT, demonstrated by:

- (For DIS):
  - One or more T2 lesion(s) in at least 2 of 4 MS-typical regions of the CNS (periventricular, juxtacortical, infratentorial, or spinal cord)

    Or,
  - Await a second clinical attack implicating a different CNS site
- And (for DIT):
  - Simultaneous presence of asymptomatic gadolinium-enhancing and non-enhancing lesions at any time

    Or,
  - A new T2 and/or gadolinium-enhancing lesion(s) on follow-up MRI, irrespective of its timing with reference to a baseline scan

    Or,
  - Await a second clinical attack

- If a patient experiences insidious neurological progression suggestive of primary progressive MS, additional data needed for MS diagnosis is:
  - 1 year of disease progression (retrospectively or prospectively determined) plus 2 out of 3 of the following criteria:
    1. Evidence for DIS in the brain based on one or more T2 lesions in the MS-characteristic (periventricular, juxtacortical, or infratentorial) regions
    2. Evidence for DIS in the spinal cord based on two or more T2 lesions in the cord
    3. Positive CSF (isoelectric focusing evidence of oligoclonal bands and/or elevated IgG index)

The international panel outlined that these latest revisions "simplify the criteria, preserve their diagnostic sensitivity and specificity, address their applicability across populations, and may allow earlier diagnosis and more uniform and widespread use" (Polman *et al.*, 2011).

1.8 Features distinguishing MS from small vessel ischaemic MRI lesions

Since the inception of MRI as a tool for MS investigation, it has emphasised MS lesions' predilection for the posterior fossa, brainstem, corpus callosum, centrum semiovale, periventricular white matter, juxtacortical white matter (subcortical U-fibres) and spinal cord, as well as the optic nerves (Ormerod *et al.*, 1987).

The periventricular white matter most frequently involved is adjacent to the trigones and bodies of the lateral ventricles (in 96% of clinically definite MS patients' MRI studies), followed by the white matter around the occipital horns (83%), frontal horns (73%), floor of the fourth ventricle (60%), and adjacent to the third ventricle (34%) (Ormerod *et al.*, 1987). Infratentorial lesions are more commonly in the brainstem (68%) than in the cerebellum (49%) (Ormerod *et al.*, 1987).

From pathology studies it is known that MS plaques frequently involve cortical grey matter (Bø *et al.*, 2003), but the sensitivity of MRI in demonstrating these still lags far behind white-matter lesion detection sensitivity (Geurts *et al.*, 2005, 2008).

From history and examination it is usually possible to distinguish MS from its commonest neuroradiological differential diagnosis, which is cerebral vascular disease giving rise to small vessel ischaemic MRI lesions. When there is clinical doubt, morphological differences in MRI findings are all the more important. In cerebral vascular disease, areas of MRI signal change can vary between large areas attributable to the territory of a major cerebral artery, or small lacunes

served by smaller perforating arteries. Changes corresponding to territories of major cerebral arteries and peripheral wedge-shaped lesions logically pertain to ischaemic or infarcted tissue. Periventricular lesions on MRI due to cerebral vascular disease are typically smooth in outline, whereas MS periventricular lesions are typically irregular in outline (Ormerod *et al.*, 1987), appearing as finger-like extension of lesions: "Dawson's fingers" (Dawson, 1916).

In 1965 Fog reported detailed post mortem pathological findings in two people who had MS. He showed that out of 43 analysed plaques, 39 followed one or two veins during their course through the white matter (Fog, 1965); this suggests that one of the reasons ischaemic lesions differ morphologically is because they do not follow the course of a vein, rather they arise at the territory supplied by a diseased artery/arteriole.

The predilection for spinal cord involvement in MS is in contrast with ischaemic changes, which rarely affect the cord (Kidd *et al.*, 1993; Thorpe *et al.*, 1993). Fog also demonstrated that spinal cord MS plaques follow the path of radicular veins in the cord's white matter tracts, though this does not necessarily determine the eventual form of the plaque in the cord (Fog, 1950).

Certain MRI techniques can be useful in distinguishing MS and ischaemia, irrespective of lesion topography and morphology. Gadolinium is used as a contrast agent because the gadolinium moiety has several unpaired electrons, which has the effect of markedly reducing T1 relaxation times for neighbouring water protons, thus generating T1-hyperintensity wherever gadolinium enters tissues. Gadolinium transudes only from vessels that have developed a leaky blood-brain-barrier, usually due to inflammation as found in active MS plaques; enhancement typically lasts 4 to 6 weeks (Miller *et al.*, 1988). Although gadolinium contrast-enhancing lesions are less frequent than T2 or FLAIR hyperintensities in MS, they can distinguish MS from ischaemic lesions, which do not enhance. The caveat is that other processes such as malignancy and granulomatous disease can also

enhance. Contrast enhancing lesions and juxtacortical lesions are highly predictive that monosymptomatic disease will progress to MS (Barkhof *et al.*, 1997).

Chronic T2-hyperintense lesions in MS are more likely to show T1-hypointensity ("black holes") when compared with T2-hyperintensities caused by other pathologies such as small vessel ischaemic change. Chronically T1-hypointense lesions are associated with worse axonal loss than T1-isointense (but T2-hyperintense) lesions. Not all T1-hypointensities are chronic; they can be a transient finding (resolving over several months) in gadolinium enhancing lesions (Uhlenbrock and Sehlen, 1989).

Diffusion weighted imaging (DWI) typically shows "restricted diffusion", i.e. reduced apparent diffusion coefficient (ADC) values in acute infarcts (though its utility in distinguishing old infarcts is poor). In MS plaques there is typically an increase in ADC value, and the diffusion change when compared to NAWM is more marked than changes in T2 signal intensity (Larsson *et al.*, 1992). However, it has also been reported that new contrast-enhancing MS lesions can initially show reduced ADC which subsequently converts to increased ADC, coinciding with the development of the peripheral vasogenic oedema seen as hyperintensity on T2-weighted images (Balashov *et al.*, 2011). Diffusion tensor imaging has shown value in detection and also quantification of tissue damage, both inside and outside of T2-intense MS lesions (Rovaris and Filippi, 2007).

Perfusion-weighted MRI mean transit time (MTT) values are more prolonged in acute and chronic stroke lesions and their surrounding NAWM, when compared to acute and chronic MS plaques (Zivadinov *et al.*, 2008).

Magnetisation transfer imaging (MTI) unveils the relative concentration of immobile protons closely associated with macromolecules such as myelin. In the CNS, reduction in magnetisation

transfer ratio (MTR) indicates relative reduction of macromolecular structure i.e. axons and their myelin, or an increase in the availability of mobile water protons e.g. due to inflammation and oedema (Mac Innes and Arnold, 2004). MTR is significantly different in MS plaques and cerebral ischaemic infarcts, and has been shown to distinguish between the two; however reduced MTR is not specific to MS plaques, and does not distinguish vasogenic oedema from subacute cerebral ischaemic infarcts (Reidel *et al.*, 2003).

Although MRS has had numerous reported applications in MS (and shows great promise as an advanced outcome measure), its diagnostic utility in distinguishing MS from ischaemic lesions requires further study (Gonzalez-Toledo *et al.*, 2006).

In summary, morphological and topographical indicators are currently the core features in assessing whether MRI lesions represent plaques of demyelination, or whether they are not demyelination (typically ischaemic areas). Advanced MRI techniques show some promise, but none as yet can be considered to show a feature pathognomonic for MS.

1.9 Ultra-high field MRI

By using ultra-high magnetic field strengths such as 7T, MRI systems can achieve a higher signal to noise ratio (SNR), because SNR increases linearly with the magnitude of the main magnetic field (B_0) (Uğurbil *et al.*, 2003; Duyn, 2012). This increase in SNR may be used to attain increased spatial resolution, or more rapid image acquisition (or some intermediate combination of the two).

Ultra-high magnetic fields also afford enhanced contrast mechanisms: improved imaging of non-proton nuclei such as sodium and phosphorus; greater spectral separation of metabolites in MRS;

and increased blood oxygen level–dependent (BOLD) contrast for higher resolution functional MRI (Balchandani and Naidich, 2014).

The improvement in BOLD contrast comes from augmented T2* dephasing around deoxygenated blood (Sanchez-Panchuelo *et al.*, 2012). Correspondingly, MRI sensitivity to susceptibility effects scales with field strength, improving the visibility of venous microvasculature (as well as microbleeds, and iron or calcium deposits) using susceptibility-weighted imaging (SWI) (Haacke *et al.*, 2009).

There are technical and physical limitations to the use of ultra-high field MRI. These include inhomogeneity of both B_0 and the applied radiofrequency (RF) field (B_1), errors in chemical shift localisation, and increased deposition of RF power within the patient (measured as the specific absorption rate (SAR), which increases as the square of B_0) (Balchandani and Naidich, 2014).

B_0 inhomogeneity directly scales with field strength, and as the B_0 field increases to 7T, the requisite RF wavelength becomes comparable with the diameter of the human head, resulting in a reduction of B_1 strength in the brain periphery compared with the centre, causing signal drop-out and unexpected changes in contrast (Vaughan *et al.*, 2001). These limitations cause image artefacts, limit section number and spatial coverage, and complicate the use of MRI and MRS at 7T.

Notwithstanding these limitations, advantages inherent to ultra-high field MRI ought to be exploited in order to improve understanding and management of neurological disease. If one looks through a different lens, one gets a different view. For diseases that are incompletely understood, a different view may be a boon.

Chapter 2: Ultra-High Field MRI Provides A Pathologically Specific Diagnostic Biomarker For Inflammatory Demyelination In The Brain

2.1 Introduction

Diagnosis of multiple sclerosis (MS) is based on demonstrating dissemination of central nervous system (CNS) lesions in space and time using a combination of clinical and investigative methods. At present, there is no single test that is diagnostic for multiple sclerosis, including magnetic resonance imaging (MRI). Brain white matter lesions are readily detected with MRI; however, most MRI techniques lack histopathological specificity. As a result, other conditions can produce MRI appearances which mimic those of MS (Rolak and Fleming, 2007). White matter lesions caused by small-vessel ischaemic changes related to ageing, cerebrovascular disease or migraine can cause diagnostic difficulties (Pretorius and Quaghebeur, 2003). Fortunately, the clinical history and the anatomical location and shape of the white matter lesions usually allow differentiation of MS from other conditions (Fazekas *et al.*, 1999). In the right clinical scenario, MRI can demonstrate dissemination in space (DIS) and dissemination in time (DIT) and permit an MS diagnosis according to the 2010 revisions to the criteria of the International Panel on Diagnosis of MS (Polman *et al.*, 2011). Clinical assessment and other paraclinical tests incorporated in the criteria counteract the inherent lack of specificity with which MRI depicts MS lesions.

In a significant minority of cases however, diagnosing MS can be challenging, especially in the early stages, in late-onset disease, and in the absence of typical history. This is a problem mainly encountered in MS referral centres. The International Panel stipulates that their criteria for MS diagnosis should be applied only when patients have experienced a typical clinically isolated syndrome (CIS) (or progressive paraparesis, cerebellar, or cognitive syndrome in the case of suspected primary progressive MS (PPMS)), thereby reinforcing specificity by improving "pre-test" probability of eventual MS. The presence of cerebrospinal fluid (CSF) oligoclonal bands (OCB) at

the time of initial presentation cannot always be relied upon; study results vary widely, but only 46% to 75% of newly presenting patients have OCBs (Tintoré *et al.*, 2008), and OCBs can be present in conditions other than MS (Rolak and Fleming, 2007). If MRI could have enhanced histopathological specificity for white matter lesions, future diagnostic criteria for MS could be simplified.

Many neurologists consider early treatment of MS, and even following a CIS, to be beneficial (Jacobs *et al.*, 2000; Comi *et al.*, 2001; Kappos *et al.*, 2007). Despite this, initial misdiagnosis, long referral delays, and long diagnostic delays are widespread (Levin *et al.*, 2003; Kingwell *et al.*, 2010).

The histopathological precedent that most MS lesions are centred on a vein was elegantly demonstrated long ago (Fog, 1964), and is consistent with the hypothesis that auto-reactive T-cells enter brain parenchyma from the systemic circulation and induce local destruction of myelin. Of all pathological features that define CNS demyelinating diseases and distinguish them from other predominantly white matter diseases, the perivenous demyelination identified by microscopy is the most specific (Greenfield, 2008). Standard T2-weighted 1.5T brain MRI in conjunction with additional susceptibility weighted imaging (SWI) MR venography has previously been used to show the relationship between MS lesions and blood vessels (Tan *et al.*, 2000). While this technique can demonstrate a MS lesion and a blood vessel in close proximity, its failure to demonstrate them simultaneously using a single image acquisition makes exact spatial relationships difficult to determine.

Ultra-high field in vivo MRI can be used to provide enhanced spatial resolution and strong T2* contrast (due to the paramagnetic properties of deoxyhaemoglobin, veins become especially hypointense in T2*-weighted images). Ultra-high field strength, i.e. 7T T2*-weighted MRI has

previously been used to demonstrate central veins in the majority of lesions in people known to have MS (Tallantyre *et al.*, 2008), and is superior to SWI for demonstrating relevant sizes of veins in varying orientations (Dixon *et al.*, 2011). Applying the same 7T MRI technique has been shown to accurately distinguish people known to have MS (in whom >40% lesions appeared to have central veins) from people known to have ischaemic (i.e. microangiopathic) incidental white matter MRI hyperintensities (in whom <40% lesions appeared to have central veins) (Tallantyre *et al.*, 2011).

The real usefulness of a diagnostic biomarker depends on its accuracy at the time of the patient's initial presentation, rather than its ability to distinguish established cases of MS from established cases without MS. The present study aimed to prospectively assess the value of a single 7T T2*-weighted MRI brain scan for predicting an eventual diagnosis of MS in patients in whom the question of inflammatory demyelination has been raised, but diagnosis could not initially be reached despite experienced clinical and radiological assessment.

2.2 Patients and methods

2.2.1 Study design

This was a longitudinal cohort study comparing the diagnostic utility of an index test (performed at baseline) against the reference standard after follow-up.

The index test was based on a single T2*-weighted 7T MRI brain scan performed and analysed in advance of any further investigations arranged by the treating neurologists.

The reference standard was the eventual diagnosis arrived at by treating neurologists (Dr Evangelou and his consultant colleagues) with specialist interest in MS blinded to results from the 7T MRI

analysis. The diagnosis, as is standard practice, was reached by using the clinical history and examination and paraclinical tests in accordance with the criteria of the International Panel on Diagnosis of MS available at the time.

2.2.2 Participants

Patients referred to the Neurology department of Nottingham University Hospitals NHS Trust were considered for enrolment in this study if a neurologist specialising in MS was unable to diagnose MS or not MS without further paraclinical testing and/or clinical follow-up. Participants prior to enrolment had at least one clinical brain MRI of satisfactory diagnostic quality, interpreted by an experienced neuroradiologist with whom the treating neurologist had discussed the clinical details. Patients were recruited by Dr Evangelou.

Recruited patients comprised two groups. The first group were those who had experienced a typical CIS (or sustained deterioration consistent with progressive MS), but had MRI findings inconsistent with or insufficient to support a diagnosis of MS. The second group comprised people with neurological presentations not conforming to typical CIS (or sustained deterioration consistent with progressive MS), in whom subsequent MRI appearances raised neuroradiological suspicions of demyelinating disease. The study population was a consecutive series of participants defined by the inclusion and exclusion criteria prospectively enrolled before the index test (7T MRI scan) was performed. After the index test, patients were followed-up prospectively to allow for the reference standard of clinical diagnosis to be achieved, by the accrual of further clinical events and/or additional clinical investigations.

Potential participants were excluded if they did not wish to undergo an additional research MRI scan. All subjects gave informed consent and the study had been approved by the local research ethics committee.

2.2.3 Image acquisition

Images were acquired using a Philips Achieva 7T system (Philips Medical Systems, Best, The Netherlands) equipped with whole-body gradients, a 16-channel head-only parallel imaging SENSE receive coil and a head-only volume transmit coil (Nova Medical, Inc., Wilmington MA, USA). The scanner console was operated by Dr Dixon, with Dr Mistry present in all cases. A 3-dimensional gradient echo sequence was acquired using 200 transverse slices acquired in 4 stacks, each stack overlapping by 10 slices (192 X 164 X 85 mm3 field of view, 0.5 mm isotropic voxels, echo time = 20 ms, repetition time = 150 ms, and flip angle 14°). A parallel imaging SENSE factor of 2 (right–left direction) and an EPI factor of 3 were employed; acquisition time was 8.8 minutes.

2.2.4 Data analysis

Dr Mistry analysed the anonymised MRI data, blinded to all clinical information and guided by an experienced neuroradiologist (Dr Jaspan).

Analysis was restricted to the supratentorial brain volume because at the time of this study, the 7T receive coil array yielded suboptimal SNR infratentorially. Lesions were classed as perivenous if they appeared to have one or more central veins. On 7T images a central vein was considered to be present if its hypointensity appeared at the centre of the surrounding hyperintense lesion in at least two out of three orthogonal planes.

A perivenous lesion percentage "cut-off" of 40% was chosen to predict a diagnosis of MS (>40%) or non-MS (<40%) based on the findings of previous work (Tallantyre *et al.*, 2011).

2.2.5 Statistical methods

Dr Tench devised the statistical methodology which was applied by Dr Mistry. Fisher's exact test was used to compare the proportion of perivenous lesions and the occurrence rate of specific vein-lesion morphologies in the MS vs. the non-MS groups. We estimated accuracy of the index test by calculating the proportion of agreement with the reference standard.

Although data was anonymised there was potential for un-blinding according to whether lesions had an anatomical distribution characteristic for MS. To assess lesion vein classification reproducibility and determine whether lesion classification had been influenced by such un-blinding, tightly cropped images of randomly selected lesions (without anatomical context or orientation information) were classified according to perivenous status by a second observer (Dr Abdel-Fahim) who was blinded to the original results. This was done for 20 lesions seen in three orthogonal planes. Cohen kappa coefficient of agreement between the two observers was calculated by Dr Mistry.

2.3 Results

2.3.1 Participants

Twenty nine patients were recruited between 13 May 2009 and 10 February 2012; comprising 21 females and 8 males, whose median age was 50.7 years (range 30.6 to 74.5). Each individual's demographic data is listed in table 2.1. All participants underwent the index test. Seven have not yet received a clinical diagnosis from their neurologist. This is summarised in figure 2.1. The

median follow-up period (since the index test) was 26 months (range 4 to 37 months). None of the patients received disease modification therapies during the study period. All those eventually diagnosed with MS had minimal or no disability.

2.3.2 Test results

Of the 22 participants with a clinical diagnosis, 13 were diagnosed with MS and 9 were diagnosed with microangiopathic white matter lesions. All 13 patients with an eventual diagnosis of MS had central veins visible in >40% of brain lesions (median 97%, range 70% to 100%). All 9 patients with an eventual non-MS diagnosis had central veins visible in <40% of lesions (median 25%, range 9% to 33%; figure 2.2). This difference between the proportion of perivenous lesions in the MS versus non-MS group was highly significant ($p<0.0001$). Example lesions from each group are shown in figure 2.3. Lesions in MS diagnosed patients often had characteristic morphology when seen using 7T T2*-weighted MRI, as shown in figure 2.4. Cross-tabulation of the 7T index test results vs. clinical MRI findings and paraclinical test data at the time of recruitment is shown in table 2.1.

One subject's 7T brain scan was of poor quality due to movement artefact which obscured the visibility of small veins, rendering the scan uninterpretable.

In the MS group the total lesion count was 181 (of which 159 were perivenous) and median lesion volume was 36.0mm^3 (range 1.9mm^3 to 5500.5mm^3).The MS group had a median of 10 lesions per scan (range 5 to 32). In the non-MS group the total lesion count was 165 (of which 35 were perivenous) and median lesion volume was 10.8mm^3 (range 0.3mm^3 to 807.7mm^3). The non-MS group had a median of 16 lesions per scan (range 10 to 35).

There were no adverse events associated with the index test and none documented pertaining to the reference standard.

For 7T lesion vein classification, inter-rater agreement was perfect (Cohen kappa coefficient = 1.000, SE of kappa = 0.000), suggesting excellent reproducibility and that un-blinding based on perceived anatomical pattern of lesions had not influenced the primary observer's classification.

2.4 Discussion

In this prospective study we found that a single 7T T2*-weighted MRI scan can be used to accurately diagnose inflammatory demyelination and predict MS at follow up. The number of individuals enrolled in this study was small, and further follow-up of this preliminary study's cohort will be required to corroborate eventual diagnoses, due to the limitations of the reference standard. In reality, the definite diagnosis is sometimes only established after years, and currently only expert histopathological examination can be truly definitive. If confirmed in a large prospective cohort using 3T clinical scanners in multiple centres, the diagnosis of inflammatory demyelination and MS could be simplified.

The conventional MRI characteristics of MS lesions are non-specific. For this reason, the International Panel's 2010 MS diagnostic criteria only apply in cases with typical CIS (or a year of sustained progression for PPMS) and cannot be used for white matter lesions found incidentally, when the MRI was performed for another indication. Even in the context of a typical CIS, existing diagnostic MRI criteria for dissemination in space are imperfect (sensitivity of 71.9% and a specificity of 77.2%) (Díaz-Sánchez *et al.*, 2010). In cases without a typical CIS history, or with non-typical MRI findings, diagnostic dilemma and delay can impact on patients' emotional wellbeing, as well as diverting further resources into additional tests and clinical assessments.

Patients commonly find lumbar puncture to be an unpleasant experience, and it is often diagnostically unhelpful. CNS tissue biopsy has been the only specific way to identify demyelinating plaques in vivo. T2*-weighted MRI enables simultaneous visualisation of hyperintense MS lesions and their central veins, which appear contrastingly hypointense due to the paramagnetic properties of deoxyhaemoglobin. Along with visual evoked potential testing (VEP), this could form the basis for another non-invasive pathologically specific single in vivo test for detecting inflammatory demyelinating CNS plaques, which (in common with VEP) seems able to distinguish MS from neuromyelitis optica (NMO) (Kister *et al.*, 2013; Neto *et al.*, 2013). Even so, it has not been tested for distinguishing MS from other rarer causes of inflammatory demyelination; therefore clinical acumen and appropriate paraclinical testing would still be required in order to distinguish other causes (such as acute disseminated encephalomyelitis) from MS.

In our cohort, using 7T T2*-weighted MRI analysis to dichotomise patients (according to whether more or less than 40% of their lesions were perivenous) was a reliable way to predict eventual clinical diagnosis, with 100% positive and negative predictive value for MS.

This cohort's median age of almost 51 years differs from the usual presentation of MS: typically a patient in her 20s (Coles, 2009). This difference seems a product of the inclusion criteria, suggesting that in our centre difficult to diagnose patients were more likely to be older (perhaps due to greater likelihood of coincidental small-vessel ischaemic lesions). This raises issues regarding the generalisability of our findings. Limiting inclusion to younger patients could have limited this study's generalisability to older patients who may be referred to clinic with diagnostic difficulty. Seven of the patients included in this study were in their 30s, of whom 6 received a clinical diagnosis. Reassuringly, in all 6 of those cases the index test's positive and negative predictive value for MS was maintained (table 2.1). However, future larger studies with analysis subdivided by age will be required to prove whether the predictive value really persists across age groups.

The visibility of small veins is impaired if the image signal to noise ratio is poor, for example when movement artefact degrades image quality. Interpretation of images degraded by movement could result in false negatives. In this study, only one attempt was made to acquire a T2*-weighted scan for each participant. Were such a technique to be used clinically in the future, image acquisition could be reattempted in the event of poor initial scan quality.

To conclude, for the current cohort of patients in whom conventional methods left initial diagnostic doubt, a single early T2*-weighted 7T MRI had 100% positive and negative predictive value for MS.

Figures and tables

Figure 2.1 Flow diagram summarising 7T study design

All participants underwent the index test which was a single 7T MRI brain scan. The 7T MRI result was positive if >40% of visible brain lesions appeared perivenous, and negative if <40% of visible brain lesions appeared perivenous. The reference standard was clinical diagnosis, *i.e.* the eventual diagnosis arrived at by the treating neurologist with specialist interest in MS. In one participant the 7T brain scan could not be interpreted as it was degraded by movement artefact. The reference standard has so far been inconclusive in 7 of the participants, who remain under clinical follow-up.

CIS = clinically isolated syndrome; 7T = 7 Tesla; MRI = magnetic resonance imaging; MS = multiple sclerosis.

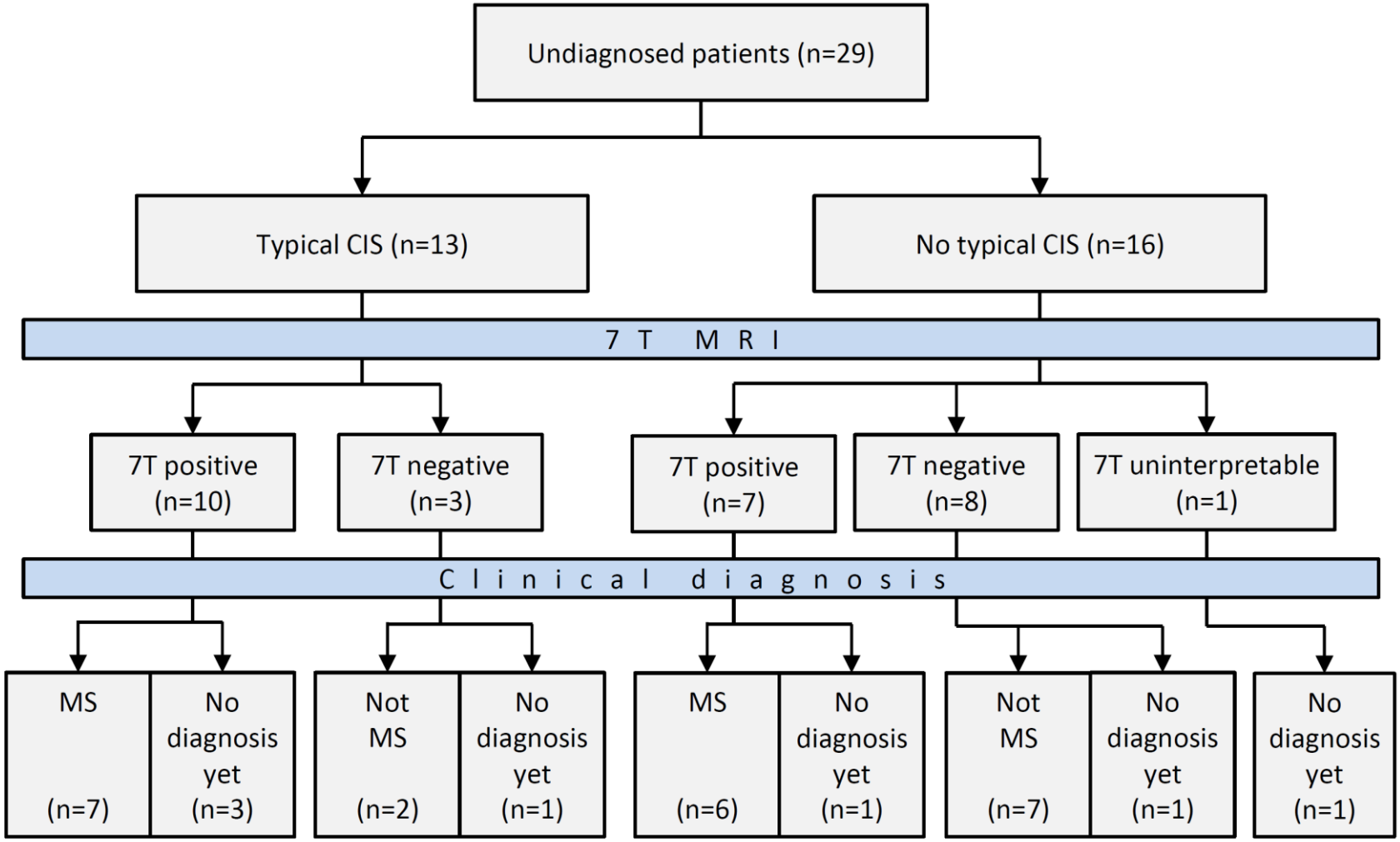
Undiagnosed patients (n=29)
Typical CIS (n=13)
No typical CIS (n=16)
7 T M R I
7T positive (n=10)
7T negative (n=3)
7T positive (n=7)
7T negative (n=8)
7T uninterpretable (n=1)
C l i n i c a l d i a g n o s i s
MS (n=7)
No diagnosis yet (n=3)
Not MS (n=2)
No diagnosis yet (n=1)
MS (n=6)
No diagnosis yet (n=1)
Not MS (n=7)
No diagnosis yet (n=1)
No diagnosis yet (n=1)

Figure 2.2 Distribution of 7T MRI index test results according to reference standard

Eventual diagnosis could be dichotomised into MS or not, according to whether the percentage of perivenous lesions was above or below 40%.

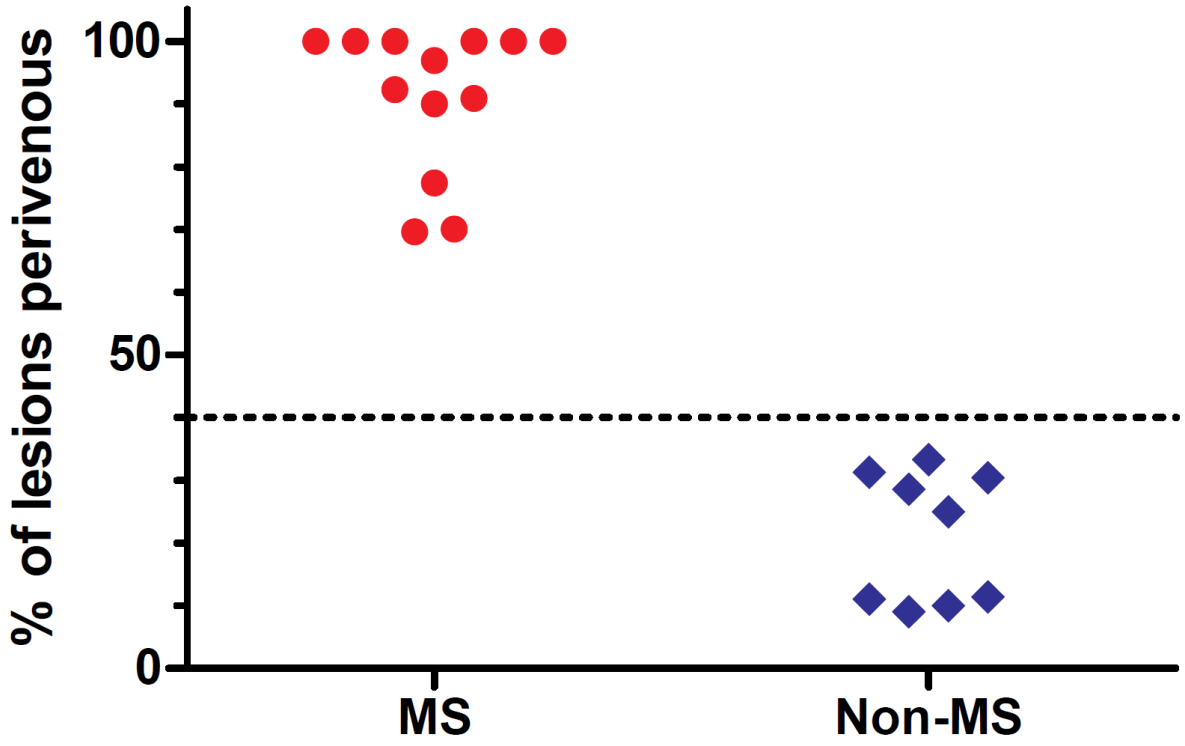

Figure 2.3 Examples of lesions detected using 7T MRI

7T T2*-weighted MRI. Panel A shows a lesion from a patient diagnosed with MS, which appears to have a vein coursing through it. Panel B shows a microangiopathic lesion from a patient diagnosed as not having MS; contrastingly this lesion does not have a vein passing through its centre.

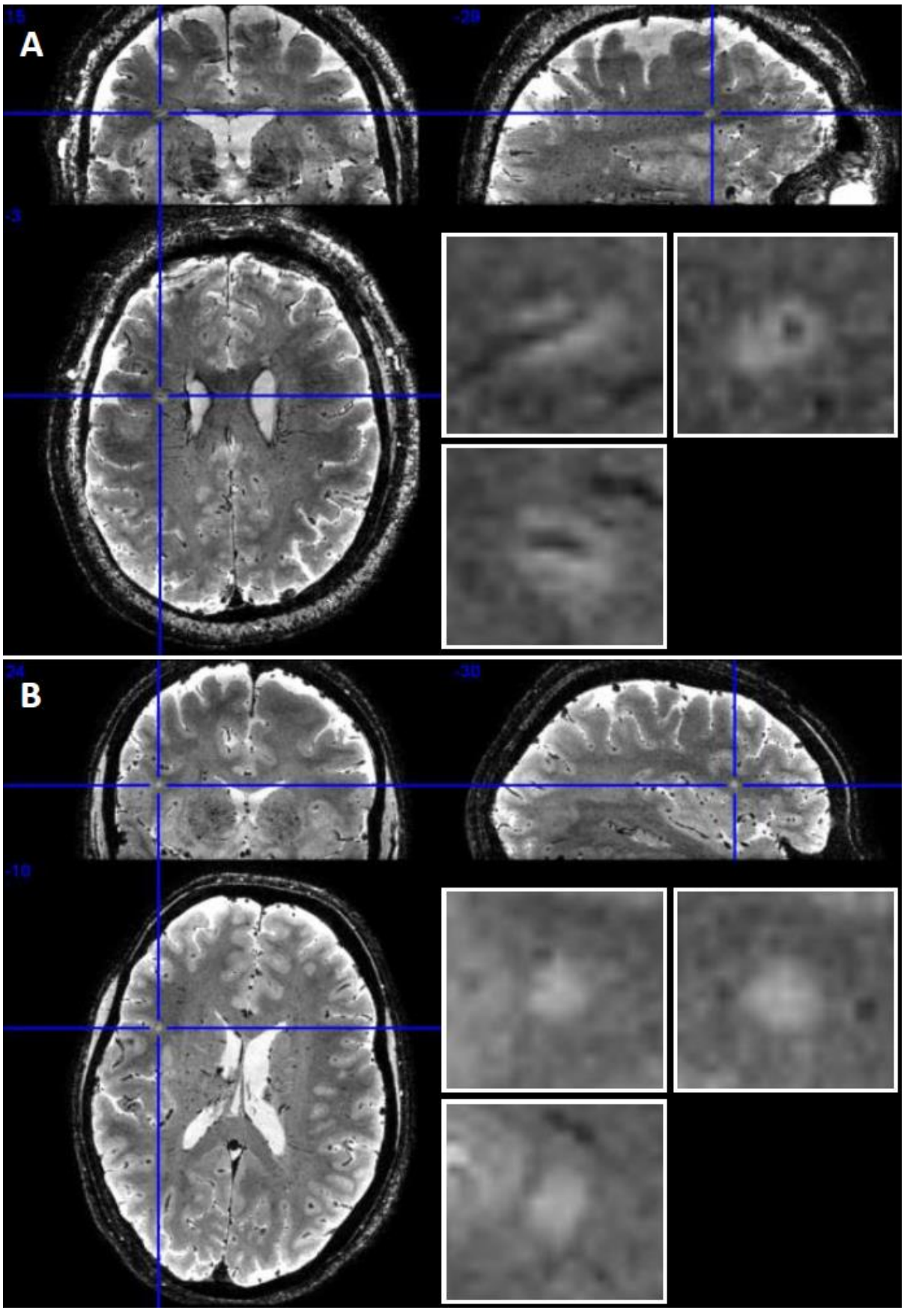
A
B

Figure 2.4 Characteristic 7T MRI MS lesion morphologies

7T T2*-weighted MRI. Panel A shows a sagittal view of a periventricular lesion with a "Dawson's finger" appearance. Deep white matter lesions are shown in panels B (axial view) and C (coronal view), with a "donut" appearance in B, and a "coffee bean" appearance in C.

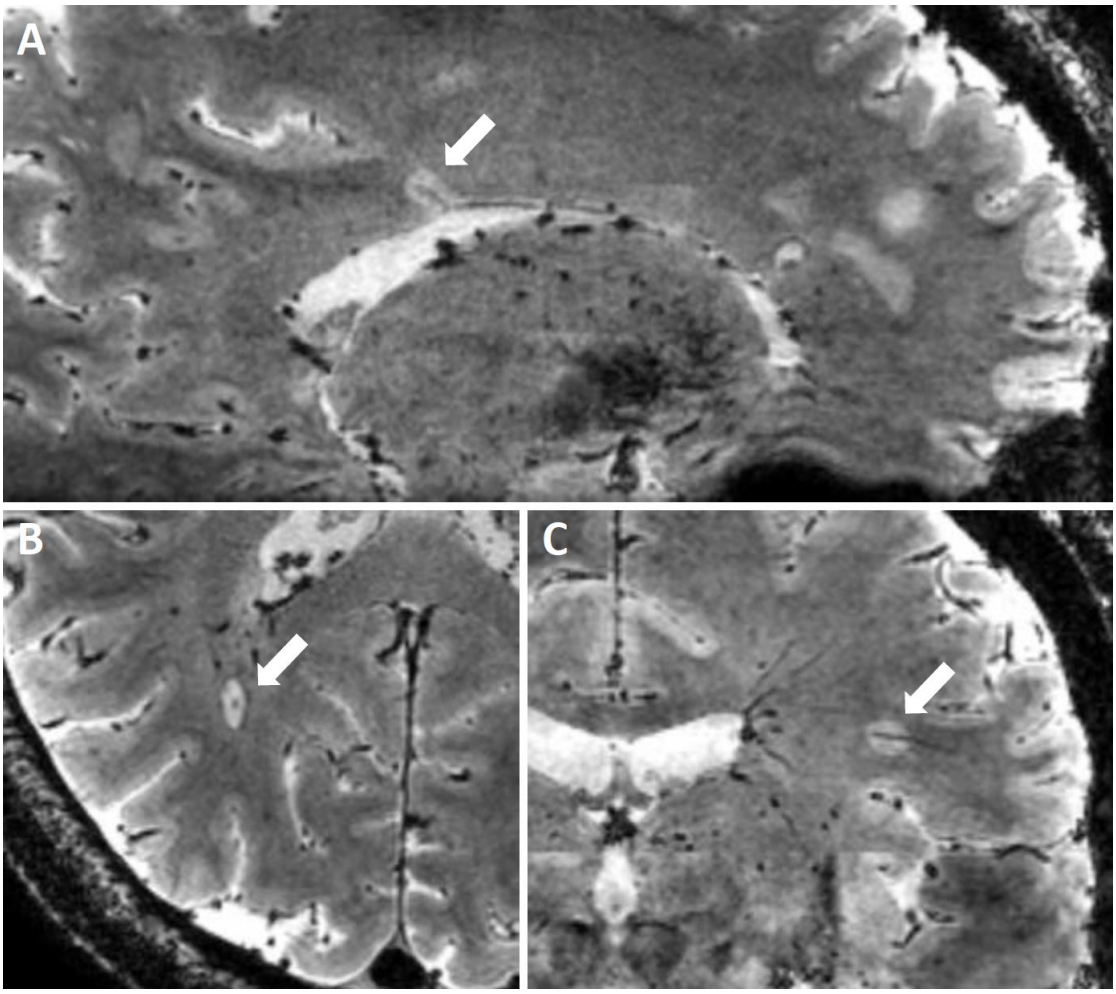

Table 2.1 Cross tabulation of results from 7T index test and reference standard with summary of clinical MRI scans available at the time of inclusion in the 7T MRI study

The 7T MRI index test was considered positive if >40% of lesions were perivenous. All patients with an eventual diagnosis of MS had a high percentage of perivenous lesions on 7T MRI, and vice-versa. The clinical FLAIR and T2-weighted spin-echo MRI images available at baseline were assessed for dissemination in space (DIS) and dissemination in time (DIT) of visible white matter lesions according to the 2010 diagnostic criteria for MS. It must be noted that those diagnostic criteria are not to be used in the absence of a typical clinically isolated syndrome (CIS) (*or one year of progressive paraparesis, cerebellar, or cognitive syndrome in the case of suspected primary progressive MS); therefore DIS and DIT assessments listed in absence of CIS have the caveat that they could not have been used diagnostically. For those with a non-MS diagnosis, risk factors for small vessel ischemic lesions are given in brackets.

I.T. = index test; R.S. = reference standard; M.S.A. = multiple system atrophy; F.M.F. = familial Mediterranean fever; N/A = not available.

Perivenous lesions % (Index test)	Eventual Diagnosis (Reference Standard)	Age (years)	Sex	I.T. to R.S. Interval (years)	Current follow-up (months)	Oligoclonal Bands	Evoked potentials	Clinical head MRIs	Clinical spine MRIs	Gadolinium contrast	DIS	DIT	Typical CIS*
100	Multiple sclerosis	54.8	F	0.13	29.59	Positive	Positive	1	1	NO	NO	NO	YES
100	Multiple sclerosis	36.7	F	0.42	24.93	N/A	N/A	1	1	NO	YES	NO	YES
100	Multiple sclerosis	36.3	F	0.27	33.05	Positive	Positive	1	1	NO	NO	NO	NO
100	Multiple sclerosis	30.8	F	0.32	30.09	Positive	N/A	N/A	N/A	N/A	N/A	N/A	NO
100	Multiple sclerosis	41.4	M	0.06	24.96	Positive	N/A	2	2	YES	NO	NO	NO
100	Multiple sclerosis	30.6	F	1.11	31.57	Positive	N/A	4	1	YES	YES	YES	YES
97	Multiple sclerosis	63.4	M	0.02	38.54	Negative	N/A	1	1	NO	YES	NO	NO
92	Multiple sclerosis	45.1	M	0.12	38.34	N/A	N/A	N/A	N/A	N/A	N/A	N/A	NO
92	No diagnosis yet	52.5	M	2.29	27.46	Negative	N/A	2	1	NO	YES	NO	YES
91	Multiple sclerosis	59.0	F	0.33	22.66	N/A	N/A	2	0	NO	YES	NO	YES
90	Multiple sclerosis	61.3	F	1.04	36.93	Positive	Positive	2	3	YES	NO	YES	YES
85	No diagnosis yet	69.1	F	1.95	23.39	Negative	N/A	1	1	NO	YES	NO	YES
84	No diagnosis yet	67.6	M	0.46	5.57	Negative	N/A	1	1	NO	NO	NO	YES
82	No diagnosis yet	48.0	F	2.99	35.84	Negative	N/A	N/A	N/A	N/A	N/A	N/A	NO
77	Multiple sclerosis	59.6	F	0.3	33.31	Positive	N/A	1	0	NO	NO	NO	NO
70	Multiple sclerosis	74.5	M	0.16	23.55	Negative	N/A	1	1	NO	YES	NO	YES
70	Multiple sclerosis	53.8	F	0.11	27.46	Positive	N/A	2	1	YES	YES	YES	YES
33	Migraine	50.4	F	0.32	23.39	Negative	Negative	2	3	NO	YES	NO	NO
31	M.S.A. (smoker)	72.4	F	0.95	23.16	N/A	N/A	3	0	YES	YES	NO	NO
30	Antiphospholipid syndrome	60.8	F	0.41	11.18	Positive	N/A	N/A	N/A	N/A	N/A	N/A	NO
30	No diagnosis yet	38.6	F	0.46	5.57	N/A	N/A	1	1	NO	NO	NO	YES
29	Functional disorder (migraineur)	40.5	F	0.33	27.49	Negative	Negative	1	1	NO	YES	NO	NO
25	Stroke (smoker, hypertension)	50.7	M	0.17	35.32	Negative	N/A	2	0	NO	YES	NO	YES
19	No diagnosis yet	46.1	F	1.96	23.55	Negative	N/A	1	0	NO	YES	NO	NO
11	Migraine	31.6	F	1.31	33.05	N/A	N/A	2	1	NO	NO	NO	NO
11	Glioma (hypercholersterolaemia)	64.4	F	0.22	7.7	Positive	N/A	1	0	YES	NO	NO	NO
10	Stroke (smoker)	41.0	F	0.82	35.32	Negative	Negative	1	0	NO	NO	NO	YES
9	F.M.F. (smoker)	36.5	F	0.91	36.93	Negative	N/A	N/A	N/A	N/A	N/A	N/A	NO
Uninterpretable	No diagnosis yet	55.7	M	2.47	29.59	N/A	N/A	1	0	NO	YES	NO	NO

Chapter 3: Central Veins In Brain Lesions Visualized With 3 Tesla Magnetic Resonance Imaging: A Clinically Applicable Diagnostic Biomarker For Inflammatory Demyelination In The Brain

3.1 Introduction

Using current diagnostic criteria, confirming a diagnosis of MS is relatively straightforward in most cases. However, in a significant minority of patients posing diagnostic difficulties, pathologically specific imaging of brain lesions could expedite accurate diagnosis, reduce the anxiety of non-diagnosis, and facilitate earlier intervention using current or emerging treatments, when appropriate.

Ultra-high field strength 7T T2*-weighted magnetic resonance imaging (MRI) has been used to demonstrate central veins in the majority of white matter lesions in people known to have MS (Tallantyre *et al.*, 2008). The same 7T MRI technique can reliably distinguish people known to have MS from those known to have small vessel ischaemia (Tallantyre *et al.*, 2011), and can accurately predict which patients who have brain white matter lesions but diagnostic uncertainty will develop MS (Mistry *et al.*, 2013).

The relevance of this diagnostic approach depends on its translation to clinically available MRI scanners. Although the perivenous distribution of MS lesions has been shown by many groups using 7T MRI (Tallantyre *et al.*, 2008; Kollia *et al.*, 2009), 3T MRI studies investigating whether perivenous visualisation of lesions characterises MS have given conflicting results (Lummel *et al.*, 2011; Tallantyre, Morgan, *et al.*, 2009). However, optimised 3T T2*-weighted MRI techniques have yielded encouraging initial results (Dixon *et al.*, 2011). We aimed to assess the effectiveness of a single 3T T2*-weighted MRI brain scan in distinguishing between people known to have MS, and people known to have microangiopathic brain lesions.

3.2 Patients and methods

3.2.1 Study design

This was a cross-sectional study comparing the index test, which was based on a single T2*-weighted 3T MRI brain scan, against the reference standard, which was the diagnosis already established by the patient's neurologist.

3.2.2 Participants

Dr Evangelou, Dr Mistry and Dr Samaraweera recruited patients from the Neurology outpatients department of Nottingham University Hospitals NHS Trust. For inclusion in the study, MS patients had to have a diagnosis of MS already established or confirmed by a tertiary centre neurologist specialising in MS, in conjunction with expert neuroradiological interpretation of pre-existing MRI scans, in accordance with the current criteria from the International Panel on MS Diagnosis. Disability was assessed in clinic by the patient's treating physician using EDSS (Kurtzke, 1983). Control subjects had to have brain white matter lesions on pre-existing MRI scans, diagnosed by neurologist and neuroradiologist in consensus as due to small vessel ischaemia. All subjects gave informed consent and the study had been approved by the local research ethics committee. The first 20 patients formed a test cohort. A further 20 patients were recruited and scanned to form a validation cohort.

3.2.3 Image acquisition

Each participant underwent a T2*-weighted 3T MRI brain scan using an Achieva 3T system (Philips Medical Systems, Best, The Netherlands) with a 32-channel parallel imaging head receive coil. Dr Dixon operated the scanner console with Dr Mistry or Dr Samaraweera present in all cases.

A 3-dimensional gradient echo sequence was acquired using 96 transverse slices acquired in 4 interleaved axial stacks, each stack overlapping by 3 slices (220 x 186 x 95.2 mm^3 field of view, voxel dimensions 0.55 x 0.55 x 1.05 mm^3, angulation to B_0 = 0°, echo time = 25 ms, repetition time = 150 ms, flip angle = 14°, parallel imaging factor of 2 (right-left direction), EPI factor of 3); acquisition time was 8.6 minutes.

3.2.4 Data analysis

Dr Mistry analysed the anonymised MRI data, blinded to all clinical information guided by an experienced neuroradiologist (Dr Jaspan). Each white matter lesion visible on the T2*-weighted image was assessed for the presence or absence of a central vein. A central vein was considered to be present if its hypointensity appeared at the centre of the surrounding hyperintense lesion. Confluent lesions were included; each was counted as a single lesion for the purpose of this study. Confluent lesions are more likely to straddle a vein (regardless of aetiology), and large ones may contain several veins, especially in periventricular white matter; they were classed as perivenous if there was a central vein (e.g. in a lesion with 3 vessels, as long as one was "central", it was classed as perivenous).

As Virchow-Robin spaces could be seen as linear hyperintense streaks, sometimes up to 4 voxels in thickness (i.e. approximately 2mm), hyperintensities were not considered "lesions" unless they exceeded 4 voxels in their shortest dimension, in order to avoid false positives. Every white matter lesion exceeding 4 voxels in its shortest dimension was included in the study and evaluated for the presence of a vessel in the test cohort.

3.2.5 Diagnostic rules and validation

Clinical application of this technique requires a method which is practical; calculating the proportion of perivenous lesions based on the total lesion load is laborious and time consuming. However, within the test cohort, small perivenous MS lesions centred on a single vein were frequently seen to exhibit stereotypical morphology: when the MRI slice was along the vein's axis, lesions assumed a "coffee bean" appearance (or a "Dawson's finger" appearance if the vein projected perpendicularly from the ventricular border), and when the MRI slice was more perpendicular to the vein they had a ring or "donut" appearance (figures 3.1 and 3.2). Using these features Dr Mistry devised simple rules, so that an observer could rapidly allocate 3T T2*-weighted scans into the correct disease category. These rules are:

1. If there are 6 or more morphologically characteristic lesions the diagnosis is inflammatory demyelination.
2. If there are fewer than 6 morphologically characteristic lesions, but morphologically characteristic lesions outnumber non-perivenous lesions, the diagnosis is inflammatory demyelination.
3. If neither of these conditions is met, inflammatory demyelination should not be diagnosed.

These diagnostic rules were used on the validation cohort by Dr Mistry.

3.2.6 Statistical methods

Dr Tench devised the statistical methodology which was applied by Dr Mistry. Fisher's exact test was used to compare the proportion of perivenous lesions and the occurrence rate of specific vein-lesion morphologies in the MS vs. the non-MS groups. We estimated accuracy of the index test by calculating the proportion of agreement with the reference standard.

Although data was anonymised there was potential for un-blinding according to whether lesions had an anatomical distribution characteristic for MS. To assess the reproducibility of identifying veins

and determine whether results had been influenced by such un-blinding, tightly cropped images of randomly selected lesions (without anatomical context or orientation information) were classified according to perivenous status by a second observer (Dr Abdel-Fahim) who was blinded to the original results. This was done for 20 lesions and a Cohen kappa coefficient of agreement between the two observers was calculated by Dr Mistry.

3.3 Results

3.3.1 Participants

For the test cohort, 20 patients were recruited: 10 of them had MS (comprising 4 females and 6 males, median age 50 years (range 35 to 66)). Their median EDSS was 3.5 (range 0 to 7.5), 7 of them had relapsing-remitting MS, 2 had secondary progressive MS, and 1 had primary progressive MS. Their median disease duration was 10 years (range 2 to 22). The other 10 patients (5 females and 5 males, median age 58 years (range 43 to 76)) were known to have microangiopathic white matter lesions related to small-vessel ischaemic disease (in 7 cases) or migraine (in 3 cases).

For the validation cohort, 20 patients were recruited: 13 of them had MS (comprising 6 females and 7 males, median age 42 years (range 25 to 62)). Their median EDSS was 4.0 (range 0 to 6.0); 11 of them had relapsing-remitting MS, 2 had secondary progressive MS, and none had primary progressive MS. Their median disease duration was 10 years (range 2 to 21). The other 7 patients (5 females and 2 males, median age 53 years (range 46 to 61)), were known to have microangiopathic white matter lesions related to hypertension associated small-vessel ischaemic disease (in 4 cases) or migraine (in 3 cases).

3.3.2 Test results

Lesion characteristics on 3T scans for the test cohort are summarised in table 3.1, and example lesions are shown in figure 3.3. The MS group had a significantly higher proportion of lesions with perivenous appearance compared to the non-MS group ($p<0.0001$). All MS patients had central veins visible in >45% of brain lesions (median 72%, range 56% to 100%). All non-MS patients had central veins visible in <45% of lesions (median 8%, range 0% to 37%; figure 3.4). "Dawson's finger", "coffee bean", and "donut" morphologically characteristic lesions were significantly more frequent in the MS group than in the non-MS group ($p<0.0001$). Total lesion numbers, perivenous lesion percentages, number of morphologically characteristic lesions, and patients' diagnoses are shown in table 3.2.

3.3.3 Estimates

For the test cohort, agreement of 3T index test (i.e. whether proportion of perivenous lesions was above or below 45%) with the reference standard was 100% (lower bound of the one-sided 95% confidence interval is 86%).

Inter-rater agreement on 3T lesion vein classification was very good (Cohen kappa coefficient = 0.886, SE of kappa = 0.110), suggesting excellent reproducibility and that un-blinding based on perceived anatomical pattern of lesions had not influenced the primary observer's classification.

3.3.4 Validation of diagnostic rules

By applying rules based on morphologically characteristic lesion counts the blinded observer (Dr Mistry) correctly categorised 20 out of the 20 subsequent scans. This took less than two minutes per scan.

3.4 Discussion

T2*-weighted MRI enabled simultaneous visualisation of hyperintense MS lesions and their central veins, which appeared contrastingly hypointense due to the paramagnetic properties of deoxyhaemoglobin. Employing optimised T2*-weighted MRI in a standard 3T clinical scanner suggests that perivenous demyelination, as a pathologic hallmark of MS, could be relied upon as the primary MRI diagnostic feature. If confirmed in a large prospective cohort (including people presenting with CIS, with fewer lesions) using clinical scanners in multiple centres, the diagnosis of brain MRI lesions in cases of clinical uncertainty could be simplified.

Diagnosis of MS currently relies on demonstrating dissemination of CNS lesions in space and time using a combination of clinical and investigative methods (Polman *et al.*, 2011). At present, there is no single test that is diagnostic for multiple sclerosis, including MRI (Rudick and Miller, 2012). Brain white matter lesions are readily detected with MRI; however, most MRI techniques lack histopathological specificity. As a result, other conditions can produce MRI appearances which mimic those of MS (Rolak and Fleming, 2007). The lesions that most often cause diagnostic difficulty are incidental small-vessel ischaemic changes related to ageing, cerebrovascular disease or migraine (Pretorius and Quaghebeur, 2003). Fortunately, the clinical history and the anatomical pattern of MRI signal abnormalities usually allow differentiation of MS from other conditions (Fazekas *et al.*, 1999).

Among people referred to MS treatment centres with a possible diagnosis of MS, fewer than 50% are found to have MS, indicating that diagnosing MS in a significant minority of cases can be challenging (Carmosino MJ *et al.*, 2005; Kelly *et al.*, 2012). Often patients with other neurological presentations not conforming to a typical clinically isolated syndrome (CIS) (e.g. headache), undergo brain MRI that raises radiological suspicions of demyelinating disease. Late-onset neurological symptoms associated with white matter brain lesions can also be diagnostically

challenging as those patients tend to have more coexistent vascular risk factors. The International Panel on the Diagnosis of MS make it clear that their criteria should be applied only when people have experienced a typical CIS or features of primary progressive MS (PPMS), thereby reinforcing specificity by ensuring a high "pre-test" probability of MS. In cases without typical CIS, or with contradictory conventional MRI findings, diagnostic dilemma and delay can impact on patients' emotional wellbeing, as well as diverting further resources into additional tests and clinical assessments. The presence of cerebrospinal fluid oligoclonal bands (OCBs) at the time of initial presentation cannot always be relied upon; study results vary widely, but only 46% to 75% of newly presenting patients have OCBs (Tintoré *et al.*, 2008), and OCBs can be present in conditions other than MS (Rolak and Fleming, 2007). Increased MRI specificity for demyelinating lesions could strengthen future diagnostic criteria.

Furthermore, some neurologists consider that treatment early in the course of MS following a CIS, or even after the diagnosis of radiological isolated syndrome, is possibly beneficial (Jacobs *et al.*, 2000; Comi *et al.*, 2001; Kappos *et al.*, 2007; Okuda and Vrenken, 2013).

In the previous chapter a "cut-off" of 40% was used for the 7T MRI data, because that had been established by prior work using the same 7T MRI sequence in patients with known MS or non-MS brain lesions (Tallantyre *et al.*, 2011). In the present 3T MRI study, a slightly different threshold of 45% appeared more appropriate based on the results shown in figure 3.4. The fact that there is a difference is perhaps unsurprising, considering the differences between the 7T and 3T studies, including the strength of the susceptibility effect and image slice thickness. These factors influence the rate of true positive/negative and false positive/negative classification of perivenous lesions, which in turn will have an effect on the ideal threshold.

In the test cohort every single visible lesion was classified by Dr Mistry according to its perivenous status. Certainly there are small lesions that have not been identified using our protocol, as there is no sequence at 3T that can identify all white matter demyelinating lesions. Furthermore, in clinical practice, classifying every visible lesion in individuals with high lesion loads would be impractical. There are at least two potential ways to address this problem. One is a statistical approach: as advised by Dr Tench, Dr Mistry applied binomial distribution theory to calculate the accuracy with which diagnosis could be predicted if perivenous classification was applied to only 10 randomly selected lesions (in scans with more than 10 lesions). If 10 lesions are randomly selected from a patient's 3T T2*-weighted scan, 98.2% of MS patients and 1.2% of non-MS patients would have 4 or more vein-positive lesions. Using binomial distribution theory and only analysing a sample of 10 randomly selected lesions (in patients with >10 lesions) had accuracy comparable to analysing all the lesions, however, this is reliant on a sample of lesions being selected without bias. This may be difficult to achieve in clinical practice, as the first lesions noted are likely to be the largest or most obvious ones, rather than a random selection from the total population of lesions. Unbiased random selection of lesions may also be difficult to achieve if experienced clinicians and radiologists already favour a particular diagnosis based on clinical workup and conventional MRI findings. An alternative that overcomes these problems is a pattern-recognition based approach closer to neuroradiologists' usual modus operandi. This leaves the onus with reporting neuroradiologists to appreciate the frequency of morphologically characteristic lesion appearances such as "coffee beans", "donuts", and "Dawson's fingers" to enrich the specificity of data available to them, especially when conventional MRI appearances are equivocal or atypical. Incorporating this approach into a diagnostic "rule of six" proved to be sensitive, specific and time efficient when applied in our validation cohort.

MS patients with few lesions in total have few morphologically characteristic lesions (for example, the MS patient with 4 morphologically characteristic lesions only had 6 visible lesions in total, and

they were all perivenous; table 3.2). The chance co-localisation of a non-MS lesion and a vein could mimic the appearance of a morphologically characteristic lesion, but the vast majority of accompanying non-MS lesions will not (for example, the non-MS patient with 5 morphologically characteristic lesions had 68 lesions in total, of which only 13% were perivenous; table 3.2).

Susceptibility weighted images and also FLAIR* images (the product of T2*-weighted and FLAIR images), can be used to demonstrate the perivenous distribution of MS lesions with 3T and 7T MRI (Lummel *et al.*, 2011; Sati *et al.*, 2012; Kilsdonk *et al.*, 2014). Further study is required to test the utility of FLAIR* in distinguishing between people with MS and those with microangiopathic brain lesions. Whilst FLAIR is more sensitive than T2*-weighted MRI for lesion detection, the purpose of our work is to augment the specificity of MRI for demyelinating lesions: future work could also compare the performance of FLAIR* and the T2*-weighted sequence we used for distinguishing the two pathologies. Although, for this study we have used anisotropic voxels, since the publication by Sati *et al.* we are employing their optimised 3D T2*-weighted sequence, that offers even easier identification of perivenous lesions in MS with very fast coverage of the whole brain volume, including the posterior fossa (Sati *et al.*, 2014). We anticipate that the search for the optimal sequence as well as image analysis or clinical reporting methodology will continue.

In order to avoid false-positives, hyperintensities were not considered "lesions" unless they exceeded 4 voxels in their shortest dimension, so genuine lesions thinner than this were excluded from our analysis. Additionally, assessment of whether such small MS lesions have a central vessel was not attempted because of the limits of resolution (when using voxels with dimensions of $0.55mm^2$ in-plane).

There are many causes of white matter lesions in non-MS patients. In the most common of those diseases we would not expect to be able to detect perivenous demyelination and hence we believe

there is a value of the central vein sign. Our non-MS group included patients with many risk factors and certainly does not include sufficient numbers of all potential white matter diseases to be able to draw firm conclusions about the identification of central veins in other pathologies apart from MS. Although the clinical heterogeneity of the non-MS group should be noted with caution, it is reassuring though that in our study, the MS and non-MS patients were clearly separated in terms of the presence of central veins, suggesting that in clinical practice the detection of central vein at 3T could be useful. Future studies will no doubt study the presence of the central vein sign using clinical scanners in other more uniform groups of non-MS patients with white matter disease as already has been done for Susac's syndrome and NMO using 7T MRI (Sinnecker *et al.*, 2012; Wuerfel *et al.*, 2012; Kister *et al.*, 2013). In our MS cohort we did not fully quantify how many had all the possible vascular comorbidities for white matter lesions, such as high blood pressure, tobacco use, and migraine. This would be an important factor to include in future studies, since a large group of MS patients with such comorbidities could influence how well our proposed technique performs (i.e. it could lead to a "false-negative" diagnosis if an MS patient has fewer than 6 demyelinating lesions with a visible central vein, that are outnumbered by comorbid non-perivenous lesions).

To conclude, our findings suggest optimised 3T T2*-weighted MRI can be used to differentiate between individuals with MS and those with microangiopathic brain lesions. If validated in a large prospective cohort, this technique could complement existing diagnostic algorithms by improving the specificity with which MRI demonstrates inflammatory demyelinating brain lesions. It could also expedite diagnosis and avoid the further (often invasive) paraclinical tests and protracted uncertainty experienced by many people suspected to have MS.

Figures and tables

Figure 3.1 3T T2* MRI characteristic lesion morphologies in people with MS

3T T2*-weighted MRI. The top row shows periventricular lesions with a “Dawson’s finger” appearance. White matter lesions are shown with a “coffee bean” appearance in the middle row and a “donut” appearance in the bottom row.

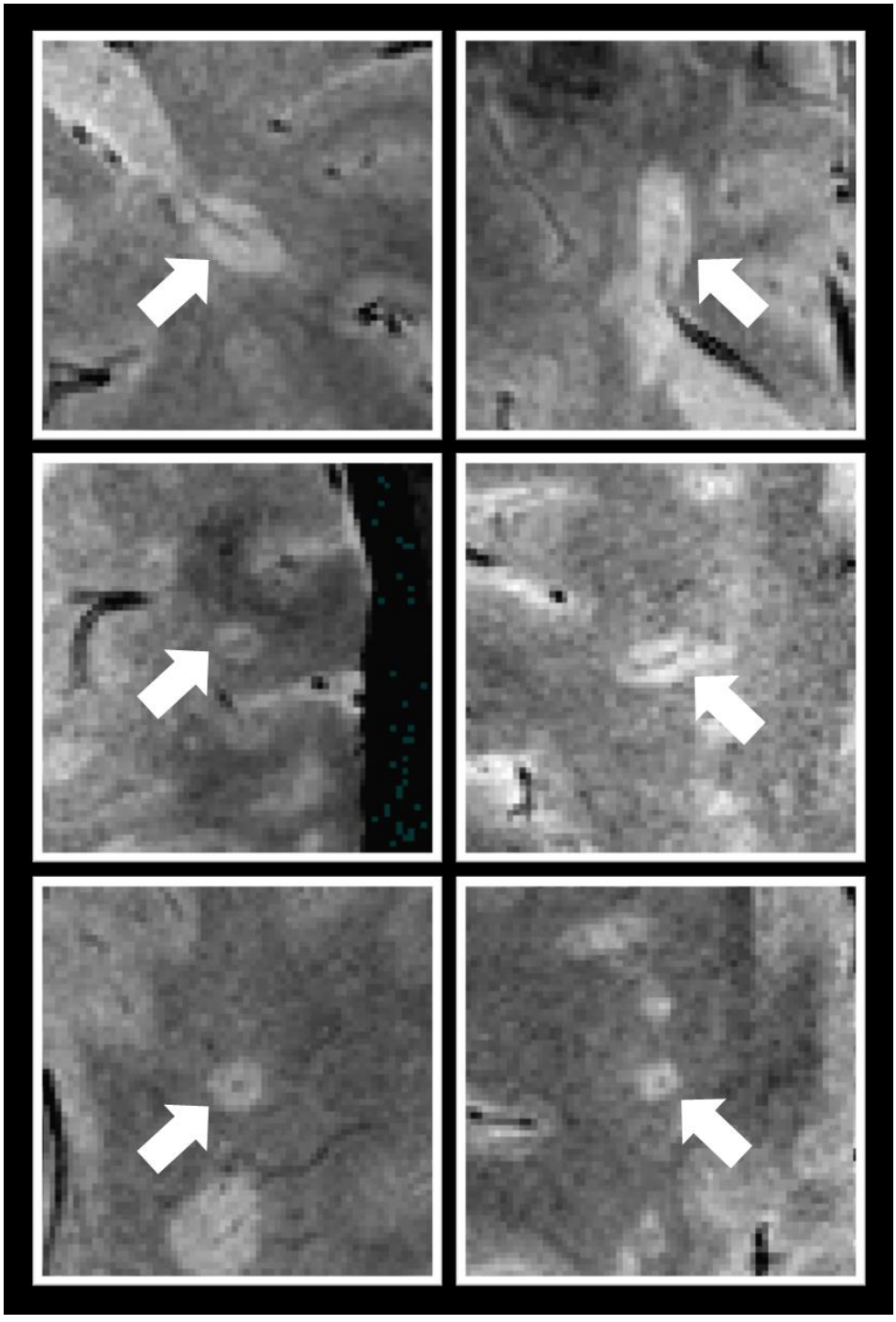

Figure 3.2 Examples of perivenous lesion morphology according to vein orientation

3T T2*-weighted MRI. The left image shows a “coffee bean” lesion where a central vein remains within the plane of the image slice for the entirety of its course through the lesion, bisecting the lesion. The right image shows a “donut” lesion, where the central vein is perpendicular to the plane of the image slice, showing the central venous hypointensity as a circular dot. The middle image shows a perivenous lesion in which the central vein passes diagonally through the plane of the image slice; this still gives a “coffee bean” appearance, because the central dot becomes elongated, but the vein does not bisect the lesion edge-to-edge.

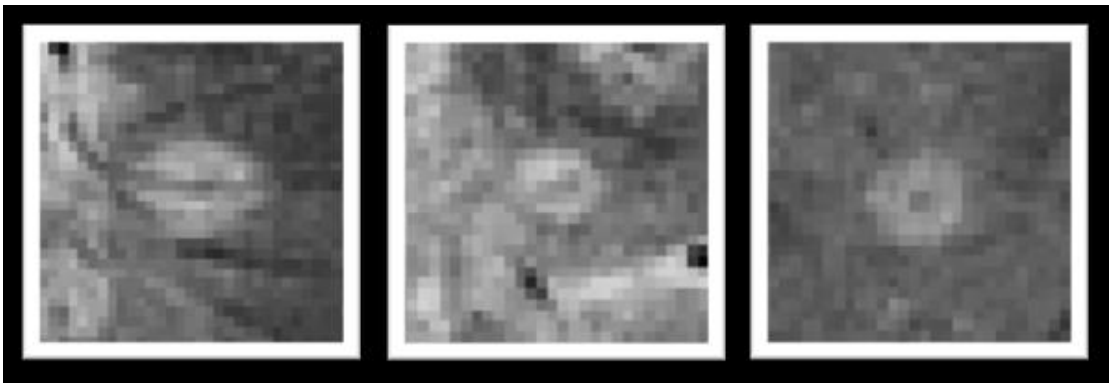

Figure 3.3 Examples of lesions detected using optimised 3T T2*-weighted MRI

3T T2*-weighted MRI. These T2*-weighted images (with insets showing white matter lesions) were acquired using a standard 3T MRI system. The top row shows examples of lesions from people with MS. The top left image's inset shows an MS lesion apparently formed by the coalescence of three neighbouring lesions, each with its own central vein, resulting in a lesion with multiple central veins. The other MS lesions shown have a single central vein, appearing as a line or a dot of hypointensity through their centre. Contrastingly the lesion examples from non-MS patients shown in the middle row do not appear to contain veins. The bottom row shows examples of "false positive" lesions from non-MS patients that do appear to contain a vein.

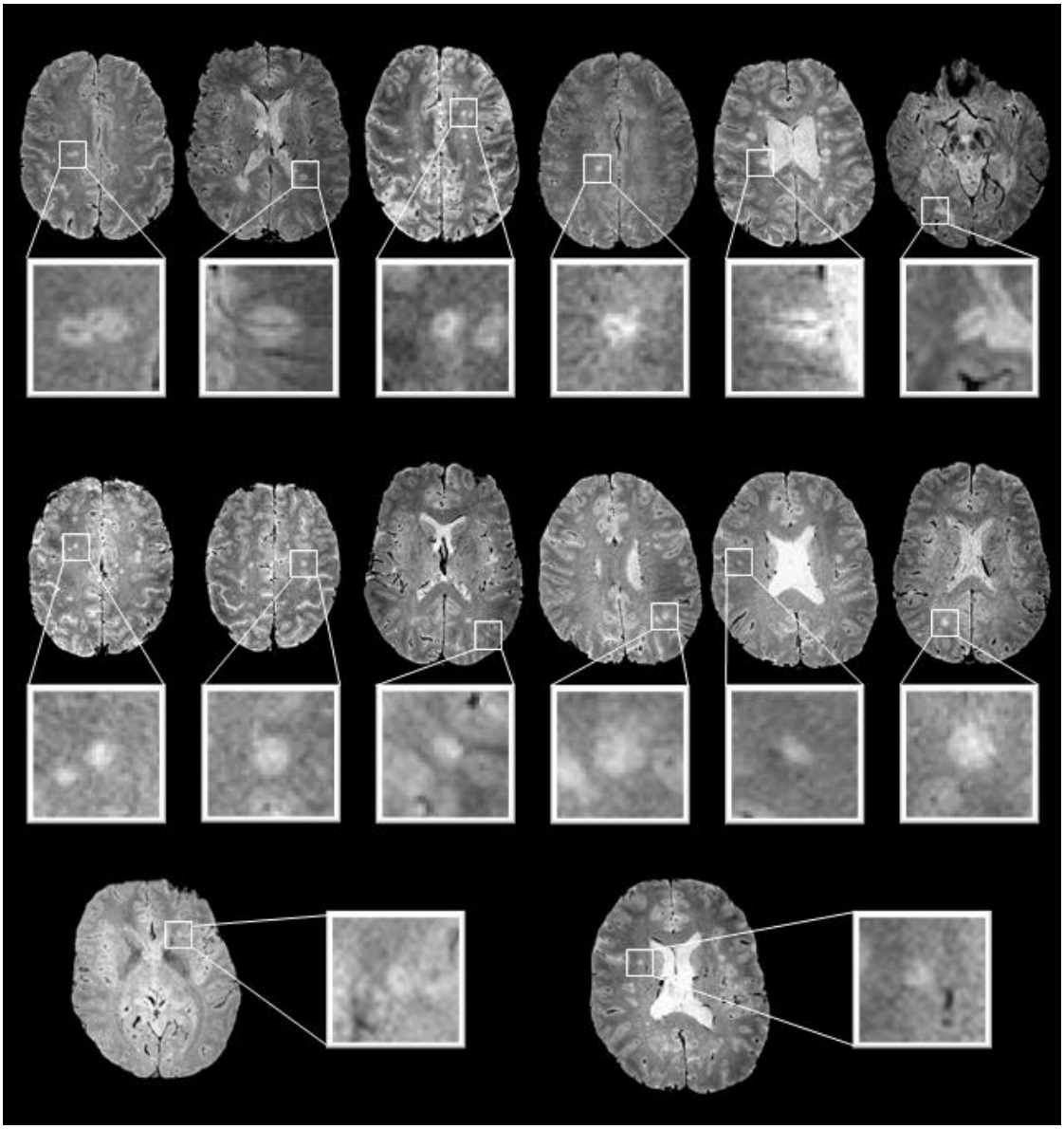

Figure 3.4 Distribution of 3T MRI results according to patients' diagnoses in the test cohort

Perivenous lesion percentages for 10 people known to have MS and 10 people known to have microangiopathic brain white matter lesions (test cohort) are shown in this plot. Each patient could be categorised into the correct disease group according to whether the percentage of perivenous lesions was above or below 45%.

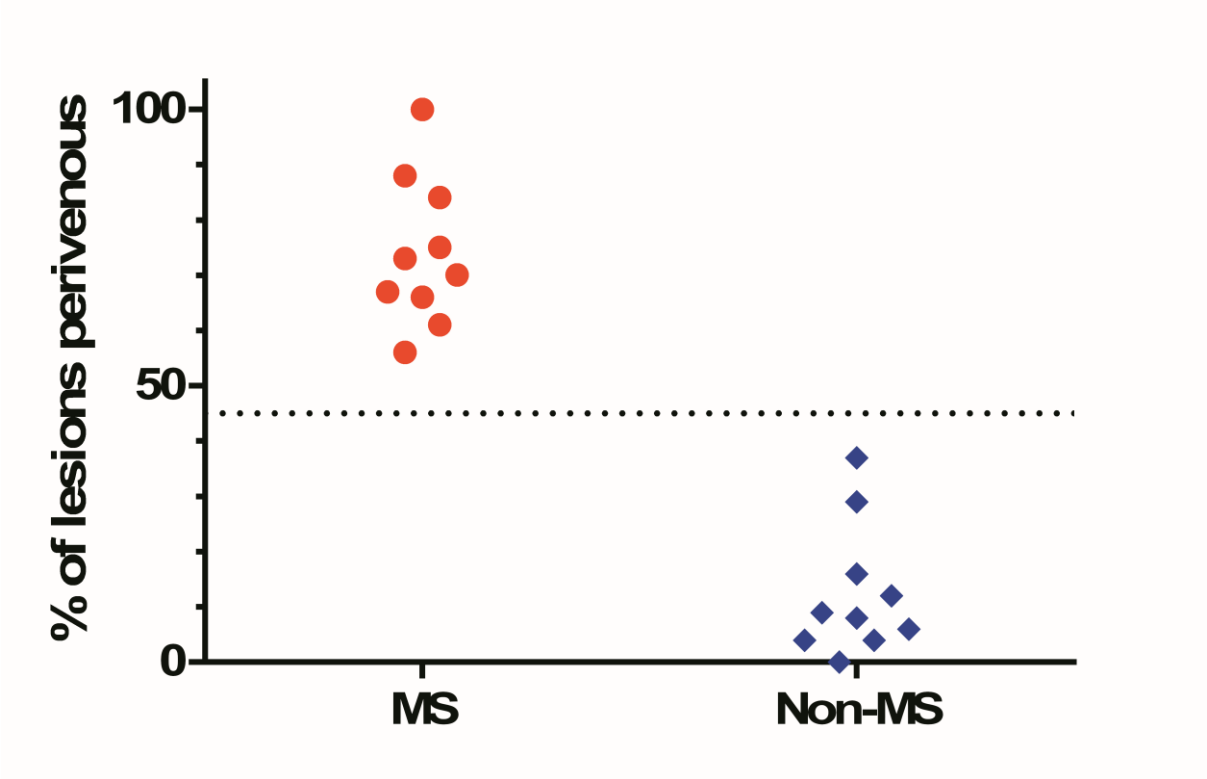

Table 3.1 Summary of lesion characteristics in the test cohort, including percentage of lesions in each anatomical category

3T cross-sectional study	MS group	Non-MS group
No. of subjects	10	10
Total lesion count	436	489
Median lesions per subject (range)	35 (6 – 142)	50 (7 – 107)
Median lesion volume (range) (mm3)	51.1 (4.4 – 14339.5)	22.6 (1.6 – 7459.9)
PV %	24.1	3.3
DW %	48.4	79.1
JC %	27.5	17.6

PV = periventricular; DW = deep white matter; JC = juxtacortical

Table 3.2 Cross-tabulation of 3T test MRI findings and patients' diagnoses

The non-MS patient category included those who had microangiopathic brain white matter lesions due either to migraine or small vessel ischaemic disease. MCLs = morphologically characteristic lesions. * People with a clinical diagnosis of migraine.

Total lesions	Perivenous %	Total MCLs	Actual diagnosis
142	56	32	MS
57	61	12	MS
41	66	13	MS
12	67	5	MS
30	70	11	MS
71	73	37	MS
8	75	6	MS
45	84	18	MS
24	88	12	MS
6	100	4	MS
46	4	1	Small vessel ischaemia*
64	6	1	Small vessel ischaemia*
22	9	0	Small vessel ischaemia*
11	0	0	Small vessel ischaemia
107	4	0	Small vessel ischaemia
79	8	3	Small vessel ischaemia
68	13	5	Small vessel ischaemia
55	16	2	Small vessel ischaemia
7	29	1	Small vessel ischaemia
30	37	2	Small vessel ischaemia

Chapter 4: Focal Multiple Sclerosis Lesions Abound In "Normal Appearing White Matter"

4.1 Introduction

Quantitative MR techniques have enabled in vivo demonstration of alterations in MS "normal appearing white matter" (NAWM). The aetiology and pathological substrate of processes affecting NAWM remain unclear but three main explanations exist (figure 4.1) (Filippi, Tortorella, *et al.*, 1999).

Macroscopic white matter lesions are known to exert effects on functionally connected NAWM via Wallerian degeneration (Evangelou *et al.*, 2000), and trans-synaptically (Evangelou *et al.*, 2001). However, this fails to explain fully why marked NAWM abnormalities are also observed in primary progressive MS (Davie *et al.*, 1997; Filippi, Iannucci, *et al.*, 1999), in which imaging typically reveals relatively few visible white matter lesions. Cytokines have been implicated in mediating MS symptoms without intermediary acute inflammatory plaque formation (Moreau *et al.*, 1996), and up-regulation of both pro-inflammatory and anti-inflammatory genes has been shown in NAWM in MS (Zeis *et al.*, 2008). T2-weighted MRI sequences such as fluid attenuation inversion recovery (FLAIR) are accepted as having excellent sensitivity to MS white matter lesions (Moraal *et al.*, 2008); they are therefore commonly used to segment-out areas of visible white matter abnormality and thus to define NAWM. Use of high field and ultra-high field MRI has already uncovered small MS lesions undetected using 1.5T MRI (Keiper *et al.*, 1998; Kollia *et al.*, 2009). In clinical settings 3T MRI employing a highly sensitive sequence such as FLAIR is regarded as the investigation of choice to detect demyelinating lesions. No prior studies have examined whether small discrete white matter lesions exist within areas classified as normal using 3T FLAIR MRI. This might have diagnostic implications in a few individuals and would also contribute to a better understanding of NAWM pathology.

In previous studies comparing MRI lesion detection sensitivity against histopathology, white matter lesions were missed with imaging. However those studies were performed using low field strength MRI scanners (Newcombe *et al.*, 1991). Subsequent use of 4.0T MRI systems detected many brain MS lesions in vivo that were missed using 1.5T MRI (Keiper *et al.*, 1998); consequently high-field T2-weighted MRI has generally been regarded as having exquisite sensitivity for MS WML. In the spinal cord 4.7T MRI seems able to demonstrate virtually all MS lesions detectable histopathologically (Nijeholt *et al.*, 2001; Gilmore *et al.*, 2009). However, it is not clear whether there are still histopathologically detectable brain WML that are missed using modern high-field or ultra-high-field MRI. Much recent historadiological correlation work has instead focused on MRI's sensitivity for cortical lesions, but from those data it may still be possible to comment on MRI's sensitivity to WML by considering detection rates of leucocortical (i.e. mixed, or "type 1") lesions. While MRI sensitivity for purely intracortical lesions remains disappointingly low regardless of field-strength or sequence used (Kilsdonk *et al.*, 2016), nearly all leucocortical lesions are reliably detected c.f. histopathology when using 1.5T and 4.7T MRI (Geurts *et al.*, 2008). Using 7T MRI apparently all histopathologically defined lesions are detected (Kilsdonk *et al.*, 2016). However, as formalin fixation reduces T1 and T2 relaxation times, any correlations between fixed tissue and in vivo data are complicated (Schmierer *et al.*, 2008). Additionally (unlike in vivo MRI), scanning of post mortem tissue is not constrained by the limitations of SAR, scan duration and patient movement.

Post mortem histopathological confirmation of additional lesions (c.f. FLAIR) found using in vivo MRI sequences was beyond the scope of this study. Instead we sought histopathological equivalents of our in vivo MRI findings, using pre-existing post mortem tissue obtained from other people with MS.

Currently 7T MRI remains a research tool and is not used in clinical practice. The increase in field strength leads to an increase in SNR, allowing a combination of improvement in spatial resolution and shorter acquisition times. Ultra-high field imaging in MS has shown promise in the detailed characterisation of cortical lesions (Kangarlu *et al.*, 2007; Kollia *et al.*, 2009; Mainero *et al.*, 2009; Schmierer *et al.*, 2010), and also white matter lesions in MS (Tallantyre *et al.*, 2008). However there are also technical challenges, and optimisation of inversion recovery spin echo sequences such as FLAIR remains challenging at 7T, principally due to inhomogeneities in the RF pulse flip angle across the head. While RF inhomogeneities also affect other pulse sequences, in our experience 3D magnetisation prepared rapid acquisition gradient echo (MPRAGE) at 7T does not reflect this inhomogeneity as dramatically, has the advantage of providing good contrast between lesions and the adjacent white matter, and offers rapid acquisition times with good anatomical coverage and high resolution isotropic voxels. Hence we elected to compare standard clinical 3T FLAIR and MPRAGE sequences with the 7T MPRAGE.

The objective of this study was to investigate whether high field and ultra-high field T1-weighted MPRAGE MRI enables detection of MS white matter lesions in areas defined as NAWM using high field T2-weighted FLAIR MRI; i.e. to ascertain whether undetected lesions are likely contributors to the burden of abnormality in similarly defined NAWM.

4.2 Patients and methods

4.2.1 Participants

Patients known to have clinically definite MS were recruited from the Neurology outpatients department at Nottingham University Hospitals NHS Trust, UK by Dr Evangelou. Patients who had received corticosteroid treatment within six months prior to this study were excluded. On the day of the MRI scan, disability was assessed in clinic by the patient's treating physician using EDSS

(Kurtzke, 1983). Healthy volunteers were recruited by local advertisement. Each participant provided prior written informed consent. This study was approved by Nottingham Local Research Ethics Committee.

4.2.2 Image acquisition

For each patient 3T and 7T scans were obtained on the same day. The healthy volunteers had 7T scans only. 7T images were acquired using a Philips Achieva system (Philips Medical Systems, Best, The Netherlands) equipped with whole-body gradients, a 16-channel head-only parallel imaging SENSE receive coil and a head-only volume transmit coil (Nova Medical, Inc., Wilmington MA). Dr Dixon operated the scanner console, with Dr Mistry or Dr Tallantyre present in all cases. Images were acquired using a 3D T1-weighted MPRAGE sequence (192 x 164 x 100 mm^3 field of view; 0.5-mm isotropic voxels; TE = 6.5 ms; TR = 14 ms; TI = 1033 ms; inter-shot interval = 3000 ms; flip angle = 8^o; acquisition time 11.9 minutes) and a 3D gradient-echo sequence with strong T2*-weighting (200 transverse slices in 4 overlapping stacks, interleaved to decrease imaging time, giving a field of view of 192 x 164 x 85 mm^3; 0.5-mm isotropic voxels; TE = 20 ms; TR = 150 ms; flip angle = 14^o; parallel imaging factor 2 (RL direction); EPI factor 3; acquisition time 8.8 minutes).

3T images were acquired using a Philips Achieva system (Philips Medical Systems, Best, The Netherlands) equipped with whole-body gradients, an 8-channel head-only parallel imaging SENSE receive coil and a whole-body transmit coil. Dr Dixon operated the scanner console, with Dr Mistry or Dr Tallantyre present in all cases. Images were acquired using a 3D T1-weighted MPRAGE sequence (164 x 164 x 118 mm^3 field of view; 0.8-mm isotropic voxels; TE = 2.3 ms; TR = 7.6 ms; TI = 960 ms; inter-shot interval = 3000 ms; flip angle = 8^o; acquisition time 9.4 minutes) and a 2D multi-slice FLAIR sequence (256 x 204 x 140 mm^3 field of view, 1 x 1 x 2.5 mm^3 voxels; echo

train length 27; 120^{o} refocusing pulse; TE = 125 ms; TR = 11 s; TI = 2800 ms; acquisition time 6 minutes). No interpolation was performed at acquisition for any of the sequences.

4.2.3 Data analysis

Dr Tallantyre identified all visible white matter lesions on 3T FLAIR images. Dr Mistry (blinded to FLAIR data) independently identified all visible white matter lesions on 3T MPRAGE and 7T MPRAGE images. Comparisons were then performed by Dr Mistry to ascertain if each individual lesion was identified prospectively on 3T FLAIR, 3T MPRAGE, or 7T MPRAGE. Ascertaining whether each individual lesion was detected on each sequence is more representative of lesion detection. Drawing conclusions based on simple lesion counts is fraught with difficulties since lesion appearances differ between sequences (which can impact on the lesion counts) as illustrated in figure 4.2. Additional (i.e. not seen on FLAIR) abnormalities found on 3T and 7T MPRAGE were reviewed by an experienced Neuroradiologist (Dr Jaspan); thus consensus was reached with the Neuroradiologist that additional abnormalities identified using high field MPRAGE were consistent with MS lesions. These additional abnormalities seen on MPRAGE were also cross-checked against 7T T2*-weighted images (and against 3T FLAIR) by Dr Mistry; this allowed exclusion of MPRAGE "false positives" caused by misinterpretation of hypointensities due to blood vessels or Virchow-Robin (or other CSF) spaces.

Dr Mougin registered all of the acquired images to the same space using FLIRT in FSL (www.fmrib.ox.ac.uk/fsl/) (Jenkinson *et al.*, 2002). Dr Mistry drew "regions of interest" around visible abnormalities (using a semi-automatic intensity threshold seeding technique), and then calculated lesion map overlaps using an in-house software package (https://www.nottingham.ac.uk/research/groups/clinicalneurology/neuroi.aspx). Analysis was restricted to supratentorial volumes because the existing 7T receive coil yielded poor SNR

infratentorially. All lesions without overlapping counterparts in the other sequences were visually checked by Dr Mistry to eliminate potential errors in the event of imperfect co-registration of the images. The volume of each lesion detected on MPRAGE images was calculated by Dr Mistry using the lesion maps.

If a lesion was not identified on one or two of the three (3T FLAIR, 3T MPRAGE, 7T MPRAGE) sequences, its anatomical location was categorised by Dr Mistry. The location categories were: periventricular (lesion edge touching or within 2mm of ventricular border), subcortical (lesion edge within 2mm of cortex, but not touching cortex) or juxtacortical (white matter lesion which touches cortex), deep white matter (white matter lesions not encroaching within 2mm of cortex or ventricle), and deep grey matter.

4.2.4 Statistical methods

Dr Tench devised the statistical methodology which was applied by Dr Mistry. The "GenStat" software package (http://www.vsni.co.uk/software/genstat/) was used for statistical analysis. A paired sample t-test was applied to the null hypothesis that the difference between the numbers of additional lesions found for each patient on 7T MPRAGE compared to the numbers of additional lesions found on 3T MPRAGE is equal to 0. To test whether the volume of the lesions seen on both FLAIR and MPRAGE is different from the volume of lesions seen only on MPRAGE, we applied a two sample t-test with the null hypothesis that there is no significant difference between the volumes of lesions that were also seen on 3T FLAIR vs. those that were not.

4.3 Results

4.3.1 Participants

Fourteen patients were recruited for the study. All of them had clinically definite MS. Their mean age was 41 years (range 24 – 60), mean disease duration was 12.0 years (range 1.2 – 25.0), and median EDSS was 2.5 (range 0 – 6.5). Disease course was as follows: 11 had relapsing–remitting MS, 2 had secondary progressive MS and 1 had primary progressive MS. Nine of them were receiving disease modification treatment (1 on azathioprine, 5 on beta interferon and 3 on glatiramer acetate). None had received corticosteroid treatment within six months prior to this study. Three healthy volunteers (one man aged 45, and two women of age 29 and 30) were also recruited.

4.3.1 Test results

Total lesion counts according to the sequence used were: 7T MPRAGE, 1075 lesions; 3T MPRAGE, 967 lesions; 3T FLAIR, 812 lesions. However, these totals misrepresent lesion detection using FLAIR imaging for the reasons discussed in data analysis methods above, and as depicted in figure 4.2. Examples of lesions found on MPRAGE and not on FLAIR are shown in figure 4.3.

Although the majority of lesions were detected both on FLAIR and MPRAGE images, a substantial proportion were only detected using 3T MPRAGE (186 lesions, i.e. 19% of the total number of lesions detected) and 7T MPRAGE (231 lesions*, i.e. 22% of the total number of lesions detected). Of those additional (i.e. not found on 3T FLAIR) lesions detected using 3T and 7T MPRAGE, over half were juxtacortical or subcortical (see figure 4.4). Significantly more additional lesions were detected using 7T MPRAGE compared to 3T MPRAGE ($p=0.012$) as shown in figure 4.5. Direct comparison of lesion detection using 3T MPRAGE vs. 7T MPRAGE is shown in figure 4.6. In the lower half of the brain the SNR of the 7T images started to become suboptimal; this at least partly explains why some lesions were missed on 7T MPRAGE cf. 3T FLAIR/MPRAGE (see discussion).
*(of which 94 were also detected using 3T MPRAGE)

In two of the three healthy volunteers no lesions were seen on 7T MPRAGE images. The 29 year old female healthy volunteer had three small discrete white matter lesions, not accounted for by veins, Virchow-Robin spaces or other CSF spaces when checked against T2*-weighted and FLAIR imaging.

Considering lesion volumes calculated from 3T MPRAGE and 7T MPRAGE lesion maps, those lesions not found using FLAIR were significantly smaller than those that were ($p < 0.001$). Volume data is summarised in table 4.1.

4.4 Discussion

There is a growing body of evidence that the radiologically observed changes in NAWM are clinically relevant in MS (Ruiz-Peña *et al.*, 2004; Sastre-Garriga *et al.*, 2005; Khaleeli *et al.*, 2007). Studies using MR techniques including magnetisation transfer, T1 relaxation time mapping, spectroscopy and diffusion tensor imaging continue to uncover abnormalities in NAWM in people with MS (Filippi, Tortorella, *et al.*, 1999; Griffin *et al.*, 2002; Castriota-Scanderbeg *et al.*, 2004; De Stefano and Filippi, 2007; Filippi and Agosta, 2007; Rovaris and Filippi, 2007; Neema *et al.*, 2009; Sajja *et al.*, 2009).

In this study, we used 3T and 7T MPRAGE MRI to identify lesions in areas of white matter that were defined as NAWM using 3T FLAIR. It follows that discrete lesions such as these are likely to contribute to the radiological changes that have been reported in NAWM. The total volume of the additional lesions found using MPRAGE was relatively small, but their contribution to NAWM abnormality should not be assumed to be proportionately small. There are two reasons for this: firstly, it is known that pathological effects of focal MS lesions project beyond the lesion and into

surrounding NAWM (Evangelou *et al.*, 2000, 2001); secondly, it is probable that there are yet more focal lesions (perhaps even smaller) which were undetected in our study.

FLAIR MRI is used routinely in clinical practice (alongside other T2-weighted spin echo sequences) to detect MS lesions on account of its high sensitivity (Moraal *et al.*, 2008), aided by its combination of strong T2-weighting and CSF signal suppression. Currently, acquiring high quality FLAIR images at 7T is challenging, preventing us from performing a direct comparison of 7T FLAIR vs. 3T FLAIR during the period over which this study was performed. Three-dimensional MPRAGE was more practical to implement at both field strengths whilst also maintaining good contrast between lesions and adjacent white matter, relatively short acquisition times, and (especially at ultra-high field) high spatial resolution.

The focus of this study was not to examine "which sequence is best for overall lesion detection"; indeed many lesions were detected using 3T FLAIR which were not identified on MPRAGE images. Table 4.2 shows counts of lesions (per patient) detected on 3T FLAIR that were missed on 7T MPRAGE, according to whether they were located in the bottom or top half of the supratentorial volume. A paired t-test was applied to the differences in numbers of lesions detected in the bottom (group one) vs. top (group two) halves of the supratentorial volume. Significantly more lesions were missed on 7T MPRAGE in the bottom half of the supratentorial volume compared to the top half ($p=0.0172$). The mean of Group One minus Group Two equals 3.00, and the 95% confidence interval of this difference was 0.62 to 5.38.

Instead we have focused on trying to determine whether additional small demyelinating lesions exist which could account for some of the NAWM abnormality. In our study, image slice thickness was greatest for 3T FLAIR, intermediate for 3T MPRAGE and smallest for 7T MPRAGE. It is known that reduction in slice thickness enables visualisation of greater numbers of smaller lesions

(Molyneux *et al.*, 1998). However, it is unlikely that slice thickness alone accounts for all the additional lesions detected using MPRAGE images. As can be seen in table 4.1, there was some variance in the size of additional lesions detected using both 3T and 7T MPRAGE (i.e. though smaller on average, lesions undetected on FLAIR were not uniformly small). We postulate a combination of slice thickness/resolution, increased SNR (at least near the cranial vertex, using the existing 7T receive coil) afforded by ultra-high field strength, and differing contrast mechanisms of MPRAGE vs. FLAIR offered complementary information contributing to the detection of additional lesions on MPRAGE images.

A disadvantage of MPRAGE is that MS lesions, veins and CSF are all hypointense: necessitating the additional steps of cross-checking MPRAGE findings with T2*-weighted and FLAIR images. On MPRAGE images veins in cross-section can be similar in appearance to small lesions, both appearing as small circular hypointensities, if viewed on a single slice in isolation. Veins can usually be distinguished from small spherical or ovoid lesions, because veins are comparatively longitudinally extensive through adjacent slices. Another limitation of this study is that the MRI sample size was small. Larger studies would be required to characterise differences in lesion counts between different MS clinical course types and levels of disability, e.g. to measure correlation between subcortical lesion load and cognitive impairment.

A strength of this study was that we avoided drawing conclusions based on simple lesion counts. Though time-consuming, ascertaining whether each individual lesion was detected on each sequence is more representative of lesion detection performance.

In our study, more than half the additional lesions detected using 3T and 7T MPRAGE were subcortical or juxtacortical. This is despite the fact that detection of subcortical lesions has been regarded as a specific strength of FLAIR imaging (Boggild *et al.*, 1996; Kates *et al.*, 1996; Bastianello *et al.*, 1997; Filippi *et al.*, 1998). MS subcortical white matter lesions are more likely to

cause significant cognitive impairment than comparable lesion loads in other locations (Damian *et al.*, 1994). A 1.5T MRI study found fast-FLAIR to be superior to conventional spin echo in identifying juxtacortical MS lesions, and presence of these lesions correlated with impaired performance in verbal memory tasks (Moriarty *et al.*, 1999). Lesion load in U-fibres has been associated with impaired memory and executive function, using conventional T2-weighted MRI (Miki *et al.*, 1998).

In conclusion, we have demonstrated that MRI with 3T and 7T MPRAGE enables detection of MS lesions in areas defined as NAWM using standard clinical 3T FLAIR. Focal MS lesions contribute to the abnormalities known to exist in what has previously been classified as the NAWM. In future, inclusion of 7T MPRAGE-visible lesion maps may refine segmentation of NAWM. Improved segmentation of NAWM should augment accuracy of analyses involving NAWM metrics. Thus, future studies using (e.g. diffusion or MT) maps of NAWM could be better placed to improve our knowledge about the other possible mechanisms leading to damage beyond discrete lesions.

Figures and tables

Figure 4.1 Proposed explanations for the abnormalities known to exist in NAWM

Whilst there is evidence supporting hypotheses that diffuse factors and damage to axons traversing lesions contribute to the abnormalities in NAWM, until now evidence has been lacking that NAWM contains substantial numbers of small focal lesions undetected using high field imaging (i.e. 3T FLAIR).

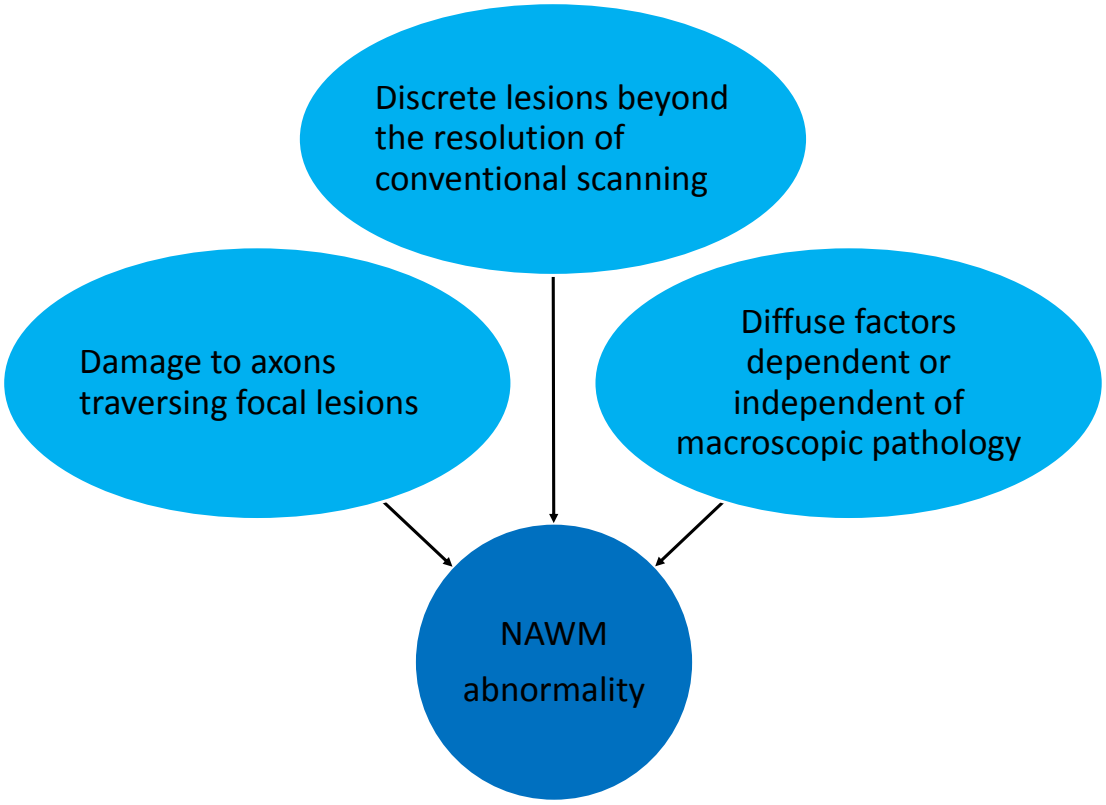

Figure 4.2 Differences in lesion counting when using MPRAGE and FLAIR images

Left image: 3T FLAIR MRI; right image: 7T MPRAGE MRI. On FLAIR images neighbouring lesions appeared as confluent hyperintense regions. On MPRAGE images the corresponding lesions appeared as more numerous discrete hypointensities.

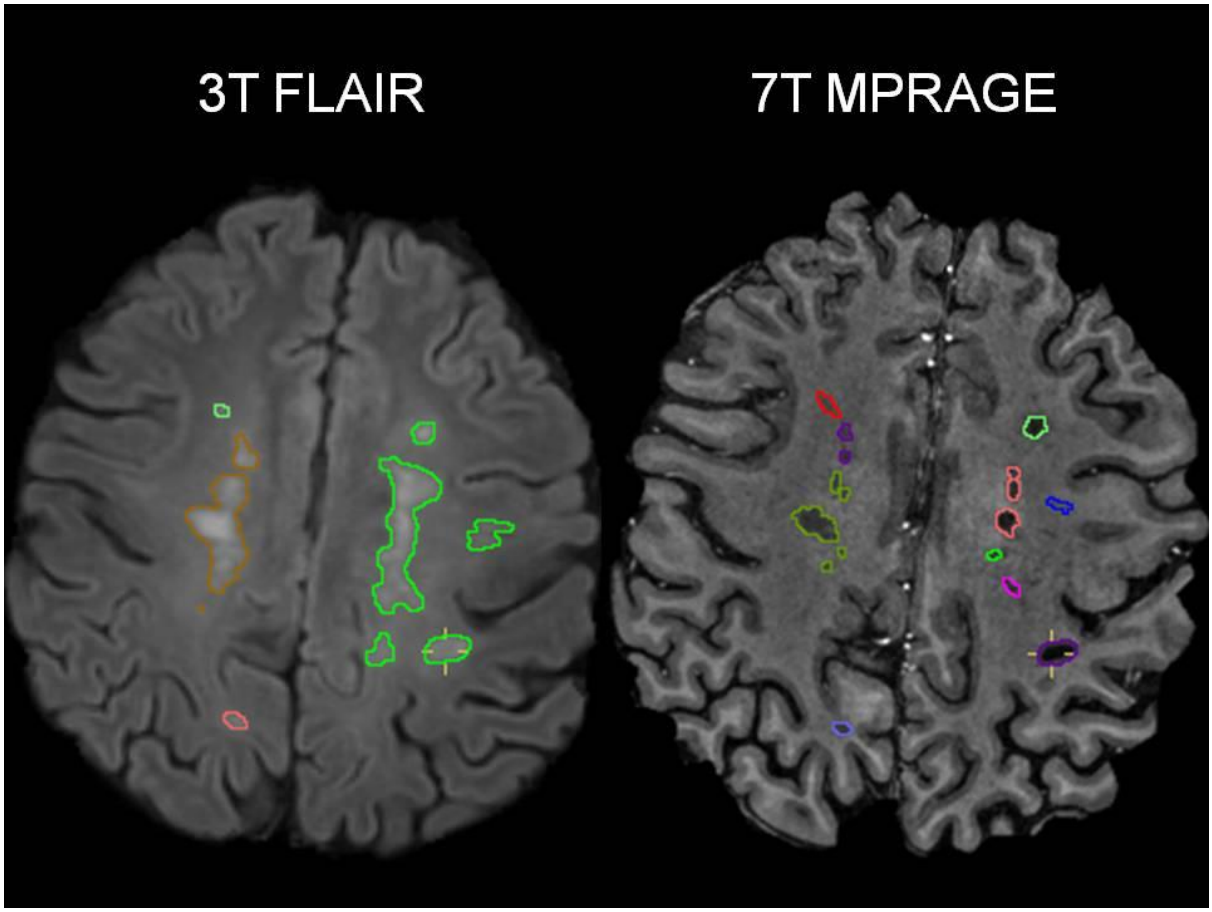

Figure 4.3 Examples of lesions prospectively identified on MPRAGE images and not on 3T FLAIR

Left column: 3T FLAIR MRI; middle column: 3T MPRAGE MRI; right column 7T MPRAGE MRI. Examples of typical lesions detected by the observer using MPRAGE but not by the observer using 3T FLAIR images. The example in the third row was detected using 3T MPRAGE and 7T MPRAGE. The other examples were only detected using 7T MPRAGE.

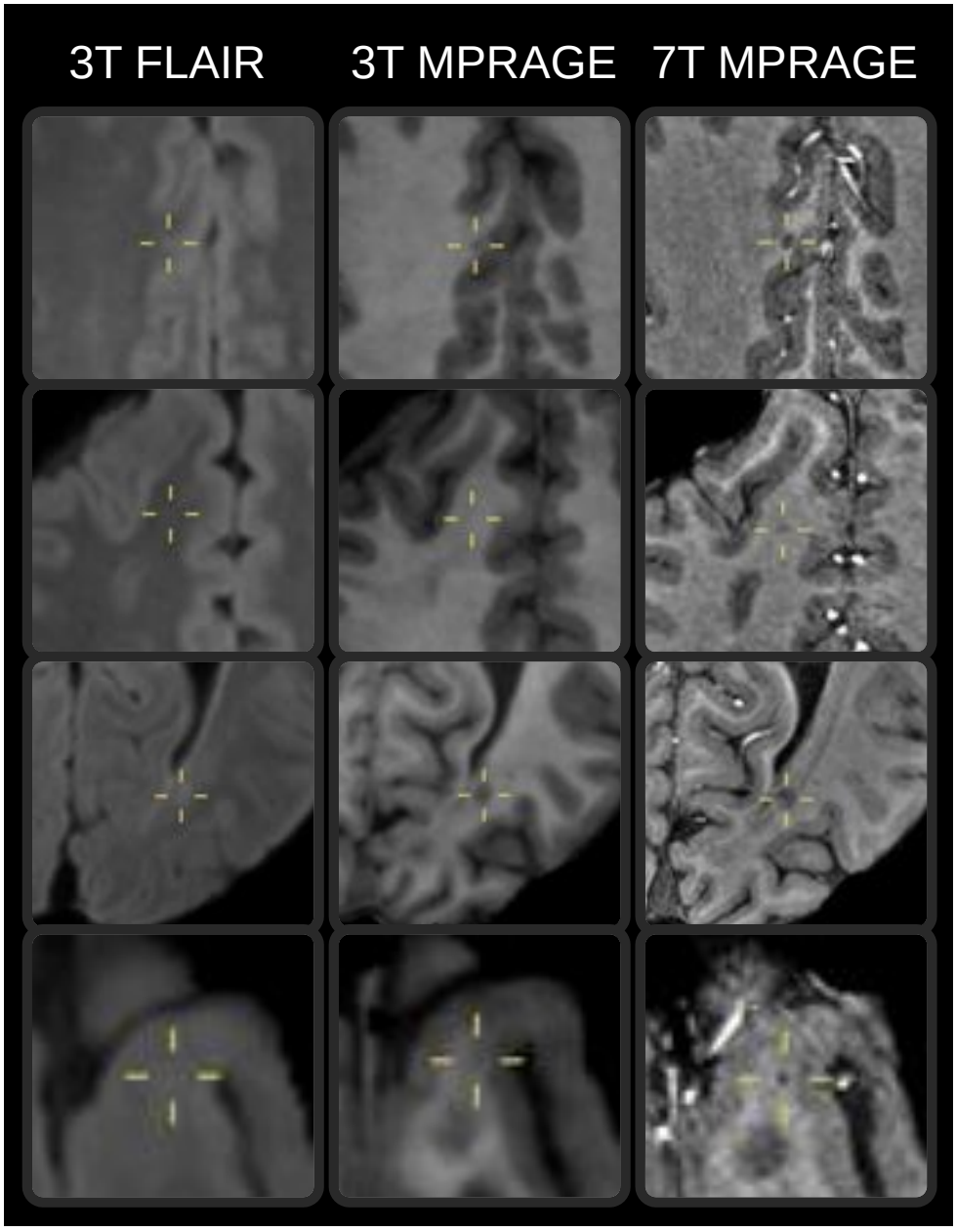

Figure 4.4 Anatomical distribution of additional lesions detected using MPRAGE

Pie chart labels: JC = Juxtacortical, SC = Subcortical, DW = Deep white matter, PV = Periventricular, DG = Deep grey matter

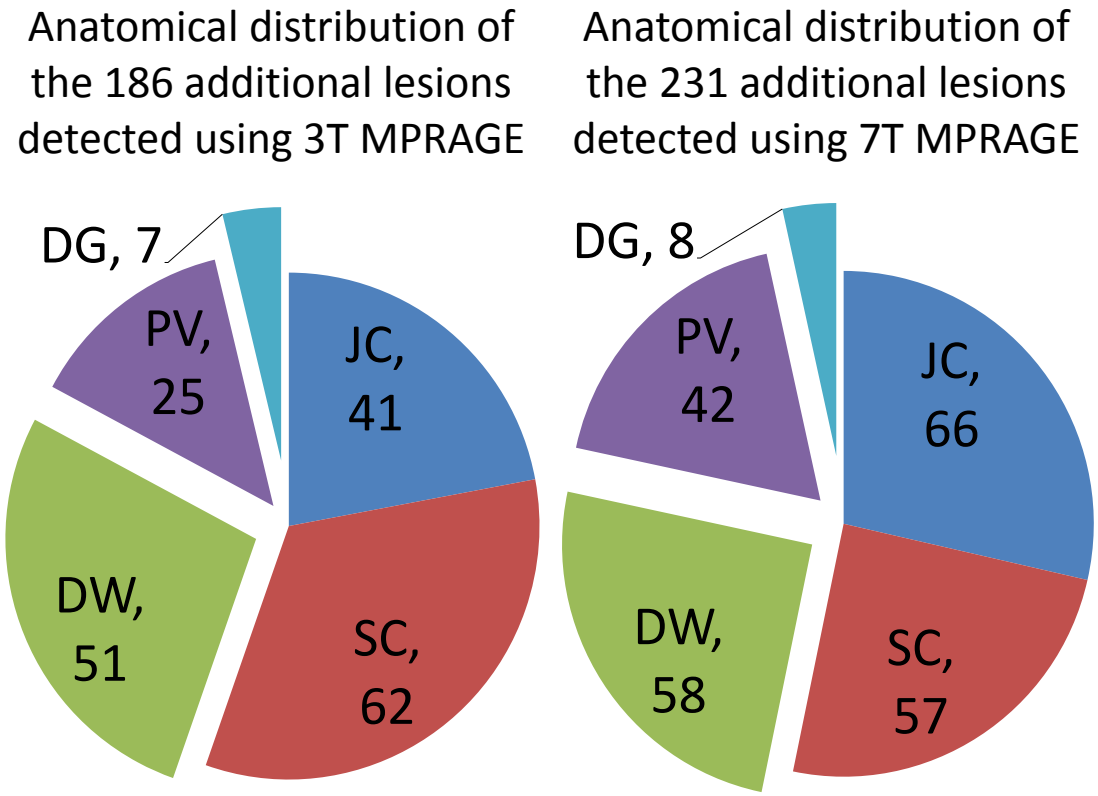

Figure 4.5 Significantly more extra lesions were found using 7T MPRAGE than using 3T MPRAGE

Number of additional (i.e. not detected using FLAIR) lesions detected using 7T and 3T MPRAGE for each patient.

PP = primary progressive, RR = relapsing remitting, SP = secondary progressive

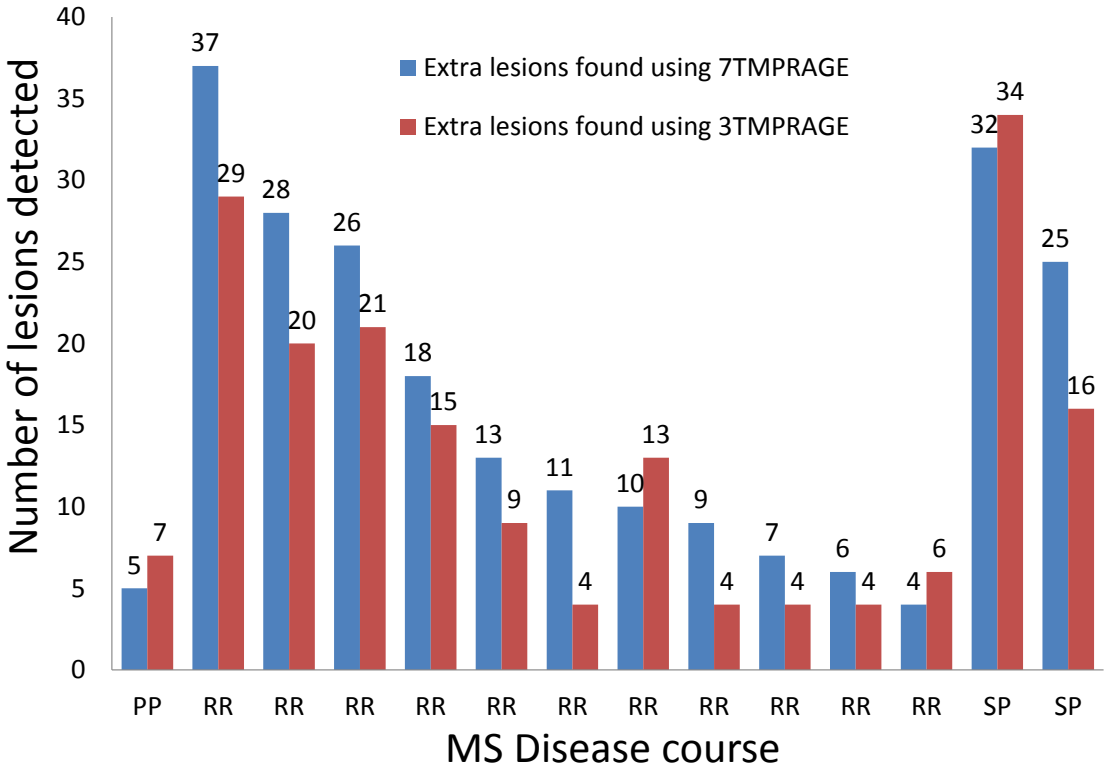

Figure 4.6 Comparison of lesion detection using 3T MPRAGE vs. 7T MPRAGE

The majority of lesions were common to both 3T and 7T MPRAGE. More lesions were seen on 7T MPRAGE only than on 3T MPRAGE only.

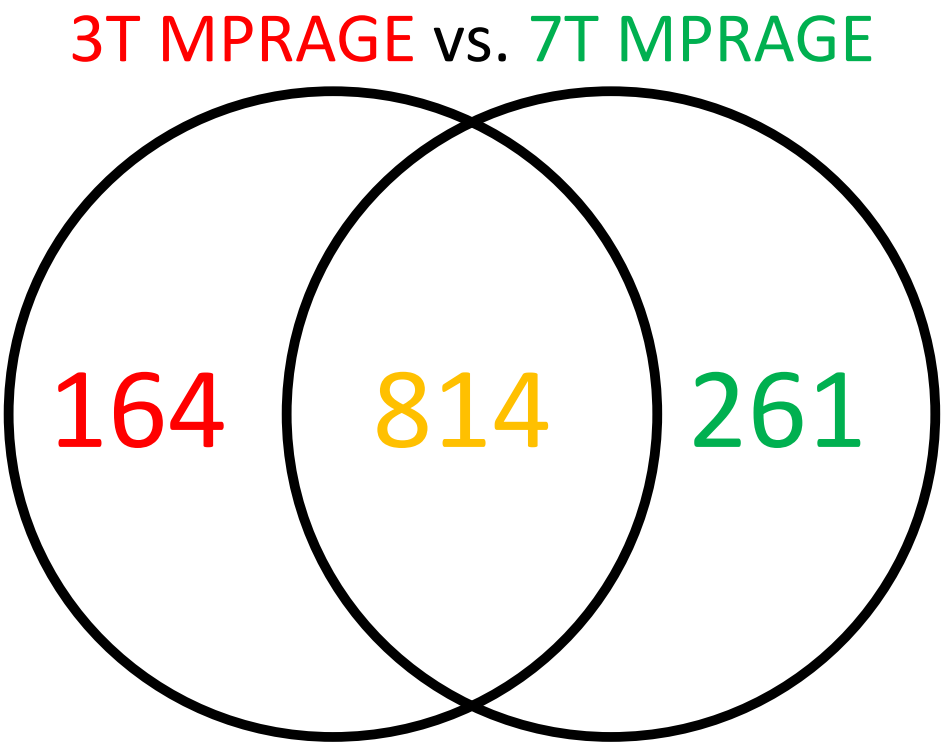

Table 4.1 MPRAGE lesion volume comparison

7T MPRAGE lesion volumes (mm^3)			3T MPRAGE lesion volumes (mm^3)		
Lesion type	Mean	S.D.	Lesion type	Mean	S.D.
Not seen on FLAIR	11.2	15.2	Not seen on FLAIR	13.5	29.6
Also seen on FLAIR	96.6	334.3	Also seen on FLAIR	103.5	518.0

Table 4.2 Counts of lesions (per patient) detected on 3T FLAIR that were missed on 7T MPRAGE

Patient	1	2	3	4	5	6	7	8	9	10	11	12	13	14	**total**
7T missed FLAIR lesions bottom half of supratentorial volume	4	3	15	13	20	9	10	7	2	12	7	7	3	3	**115**
7T missed FLAIR lesions top half of supratentorial volume	6	1	4	16	11	5	10	4	4	7	3	0	1	1	**73**

Chapter 5: A Corticocentric Model For MS Pathogenesis

5.1 Introduction

Demyelinating white matter lesions (WML) and clinical relapses are two of the most striking features of multiple sclerosis (MS); understandably they have been central to traditional pathogenetic and therapeutic precepts about MS. Despite their prominence, MS relapses are not directly related to long-term disability progression (Confavreux *et al.*, 2000, 2003; Kremenchutzky *et al.*, 2006). Accordingly, MRI-visible focal WML load in the brain or spinal cord fails to fully explain disability and progression in MS (Thompson *et al.*, 1990; Kidd *et al.*, 1993; Barkhof, 2002).

Normal appearing white matter (NAWM) axon loss (rather than focal demyelination in WML) is the pathological substrate underlying chronic, irreversible disability in MS (Tallantyre, Bø, *et al.*, 2010). Changes in MR metrics reflecting interlinked demyelination and axon loss in the NAWM (and normal appearing grey matter) correlate well with disability in MS (De Stefano *et al.*, 1998; Traboulsee *et al.*, 2003; Ruiz-Peña *et al.*, 2004; Sastre-Garriga *et al.*, 2005). This involvement of the normal appearing brain tissues occurs early in the course of MS (De Stefano *et al.*, 2002, 2003), and is only partly related to WML (Filippi and Rocca, 2005).

The spastic paraparesis that typifies disabling MS is underpinned by axon loss in the corticospinal tract (Ganter *et al.*, 1999; Bjartmar *et al.*, 2000; Wilson *et al.*, 2003). Post mortem cerebral WML burden does not correlate with axon loss in the corticospinal tracts on histopathology (DeLuca *et al.*, 2006). Several studies have found that in vivo cerebral or spinal cord WML burden on MRI does not correlate with quantitative MR estimates of axon loss in the corticospinal tracts, or the whole NAWM (using magnetisation transfer ratio (MTR), and other measures) (Rovaris *et al.*, 2000; Griffin *et al.*, 2002; Filippi *et al.*, 2003; Wilson *et al.*, 2003; Filippi and Rocca, 2007; Bellmann-Strobl *et al.*, 2009). In another MTR study which used tissue diffusion characteristics to

segment white and grey matter of the brain, all MTR histogram derived metrics for NAWM and normal appearing grey matter were significantly lower in people with MS vs. healthy controls; furthermore moderate correlation was found between T2 WML volumes and the peak height of the normal appearing grey matter MTR histogram (Cercignani *et al.*, 2001). However, caution must be applied in the interpretation of correlations with "normal appearing grey matter" as defined using any existing MRI technique, as it is likely riddled with occult focal lesions (Kilsdonk *et al.*, 2016).

Whilst it is evident that axon loss and disability are at least partly independent of WML, the true mechanism of disease has remained uncertain. Cortical lesions are functionally connected to remote NAWM just as WML are. Many studies have tested the relationship between macroscopic WML and diffuse NAWM disease. The same cannot be said for cortical lesions. Previous work has shown that 7T magnetisation-prepared-rapid-acquisition-gradient-echo (MPRAGE) MRI performs favourably for cortical lesion detection (Tallantyre, Morgan, *et al.*, 2010). The objective of this study was to assess correlation between cortical lesion load on 7T MRI, and the MTR of the NAWM, in order to test the hypothesis that cortical lesions cause NAWM axon loss.

5.2 Patients and methods

5.2.1 Participants

People with clinically definite MS were recruited from Neurology outpatients at Nottingham University Hospitals NHS Trust by Dr Evangelou, Dr Mistry and Dr Abdel-Fahim. All participants gave prior informed consent and the study had received ethical approval from the local research ethics committee. Disease duration data was obtained from hospital records, and disability was assessed in clinic by the patient's treating physician using EDSS (Kurtzke, 1983).

5.2.2 Image acquisition

All images were acquired using a Philips Achieva 7T MRI system, equipped with whole-body gradient coils, a head-only quadrature transmit RF coil, and a NOVA 32 channel SENSE receive coil. Dr Mougin operated the scanner console, with Dr Mistry or Dr Abdel-Fahim present in all cases.

MPRAGE images were acquired using a tailored inversion pulse to reduce effects of B1 inhomogeneity (Hurley *et al.*, 2010). Acquisition parameters were: TI 1070ms, flip angle 8˚, TE 7ms, TR 15ms, voxel size 0.5x0.5x0.5mm^3, field of view 205×215×140mm^3, acquisition time 10 minutes 11s.

Dr Mougin produced MTR maps from an acquisition giving two images (MT_{sat} and $MT_{no\text{-}sat}$). The sequence used a turbo-field echo (TFE) readout. The MT_{sat} was acquired by applying 20 off-resonance pulses (sinc pulses with bandwidth of 300 Hz and off-resonance by 1.0 kHz (-3.4ppm), 20ms between each pulse) before each TFE readout train. Acquisition parameters were: TR 12ms, TE 6.4ms, flip angle 8˚, voxel size 0.5×0.5×1mm^3, field of view 205×175×80mm^3, centre-out sampling, shot to shot interval 10s, acquisition time 8minutes 50s. High resolution MTR maps were calculated from $(MT_{noSat}\text{-}MT_{Sat})/MT_{noSat}$ on a pixel by pixel basis after registration of the two volumes of interest using FLIRT in FSL (http://www.fmrib.ox.ac.uk/fsl/).

Owing to the less extensive MTR field of view, and reducing MPRAGE signal-to-noise-ratio infratentorially, brainstem and posterior fossa structures were not included in any of the analysis.

5.2.3 Data analysis

5.2.3.1 Cortical lesion detection

All image data had been anonymised. So that apparent WML lesion load would not bias the observer segmenting cortical lesions (Dr Abdel-Fahim), only cortical ribbons were presented; with the white matter, cerebellum, and deep grey matter removed by Dr Mougin. Dr Mougin generated cortical ribbons by segmenting MPRAGE volumes using the Freesurfer image analysis suite (http://surfer.nmr.mgh.harvard.edu/), and he additionally manually edited the ribbons to remove any WML erroneously included by the automated segmentation.

Dr Abdel-Fahim manually drew cortical lesion maps on the cortical ribbons, on a slice-by-slice basis using the ImageJ analysis suite (http://rsb.info.nih.gov/ij/). Cortical lesion maps were used to calculate total cortical lesion volume as well as lesion counts for each subject.

Whilst the objective of cortical lesion segmentation was to ascertain cortical lesion load, currently no imaging modality is able to reliably demonstrate 100% of cortical lesions present. We could not validate our in vivo cortical lesion counts against the gold standard of histopathology. In order to verify whether MPRAGE cortical lesion counts reliably reflect underlying cortical lesion load, we used comparator cortical lesion counts obtained using an entirely independent contrast mechanism. The signal-to-noise and spatial resolution of 7T MRI allowed us to use MTR as an imaging modality (in addition to using it for measuring average tissue properties). Cortical ribbons were generated from MTR images by Dr Mougin (which had been registered to the MPRAGE images by Dr Mougin using FSL (www.fmrib.ox.ac.uk/fsl/)), by masking them with the MPRAGE cortical ribbons previously segmented. The observer who segmented lesions in the MPRAGE cortical ribbons (Dr Abdel-Fahim) did the same using MTR cortical ribbons, which had been randomised and anonymised, so they could not be matched with the corresponding MPRAGE. Correlation

between cortical lesion counts using the independent contrast mechanisms of MPRAGE and MTR was calculated by Dr Mistry; a tight correlation would suggest that each mechanism yielded counts proportional to the real cortical lesion load. Because inter-observer reproducibility would not show whether MTR or MPRAGE lesion counts related to true underlying lesion load, it was considered beyond the scope of the current study and not performed.

5.2.3.2 NAWM segmentation following WML detection

A second observer (Dr Mistry) independently identified WML in anonymised 7T MPRAGE images. For WML detection, 7T MPRAGE has sensitivity exceeding that of 3T FLAIR MRI (Mistry *et al.*, 2011). The previously generated cortical ribbons were subtracted from MPRAGE volumes prior to WML detection by Dr Mougin, so that apparent cortical abnormalities would not influence the observer looking for WML. Dr Mistry then drew WML maps semi-automatically on a lesion-by-lesion, slice-by-slice basis using an intensity-based flood-fill function in the NeuRoi image analysis program (http://www.nottingham.ac.uk/scs/divisions/clinicalneurology/software/neuroi.aspx). Previous work comparing lesion appearances on 7T MPRAGE and 3T FLAIR showed that FLAIR lesion hyperintensity extended beyond the edge of the lesion as depicted using 7T MPRAGE (Mistry *et al.*, 2011). WML maps were 3D-dilated by 5 voxels using a tool in NeuRoi (i.e. approximately 2.5mm dilatation from lesion surface), to encompass these beyond-edge effects in proximity to WML.

White matter volumes were produced by Dr Mistry in two steps using NeuRoi: 1) initial classification of white matter using automated template-based segmentation, 2) subtraction of previously generated cortical ribbons from white matter segments (to remove any cortical tissue erroneously retained by the template-based segmentation).

Dr Mistry produced NAWM masks by subtracting dilated WML maps from white matter volumes. These masks were applied to the MTR volumes (which had been registered to the MPRAGE by Dr Mougin), to calculate the average MTR of the NAWM for each subject. If non-dilated WML maps had been subtracted, the resulting "NAWM" would be polluted by the inclusion of WML edge-related signal, giving a false-positive correlation between WML load and NAWM MTR. NAWM segmentation is summarised in figure 5.1.

5.2.4 Statistical methods

Dr Tench devised the statistical methodology which was applied by Dr Mistry. Pearson correlation coefficients were calculated between mean MTR of the NAWM, cortical lesion counts and volumes, WML volumes, and clinical data; and also to assess correlation between MPRAGE and MTR cortical lesion counts. Multiple linear regression analysis was used to determine how strongly cortical lesion load predicted NAWM MTR, when controlling for potential confounders. The dependent variable was NAWM MTR; independent variables were cortical lesion volume, WML volume, EDSS, disease duration, and age.

5.3 Results

5.3.1 Participants

Nineteen people with MS were recruited: 12 were female; 16 relapsing remitting, 2 secondary progressive, and 1 primary progressive. Their median EDSS was 3.0 (range: 0-7.5); mean age 48 years (range: 32-65); and mean disease duration 7 years (range: 2-19).

5.3.2 Test results

Cortical lesion volumes and counts on MPRAGE and MTR images correlated significantly with NAWM MTR (shown in table 5.1). Scatter plots showing cortical lesion vs. NAWM MTR data are shown in figure 5.2. WML volumes did not correlate significantly with NAWM MTR. In our cohort none of the clinical data correlated significantly with NAWM MTR.

Cortical lesion counts obtained using the independent contrast mechanisms of MPRAGE and MTR correlated significantly with each other ($r = 0.842$, $p = 0.000003$; figure 5.3). Examples of cortical lesions detected using MPRAGE and MTR cortical ribbons are shown in figure 5.4.

Multiple linear regression analysis showed cortical lesion load was the only variable considered that made a significant contribution to the model, with NAWM MTR as the dependent variable, when also taking into account age, disease duration, EDSS, and WML volume. Results are summarised in table 5.2. ANOVA comparison of models with and without WML volume included as a variable (table 5.3) showed no significance ($p = 0.786$), implying little contribution from WML load.

5.4 Discussion

Our findings are consistent with the hypothesis that cortical lesions cause NAWM axon loss. These findings are in keeping with the histopathological precedent that diffuse injury of the NAWM and cortical demyelination exist in tandem, and are characteristic hallmarks of primary progressive MS (PPMS) and secondary progressive MS (SPMS); furthermore there is a significant correlation between the histopathological extent of cortical demyelination and diffuse changes in the NAWM (Kutzelnigg *et al.*, 2005).

In our cohort NAWM MTR did not correlate with disability measured using EDSS. This may be because our sample size was small and lacked the power to assess correlations beyond our stated

objective and because our cohort comprised mostly relapsing remitting MS (RRMS) patients with a low EDSS. In a slightly larger study cortical lesion load correlated strongly with physical and cognitive disability (Nielsen *et al.*, 2013). The significant correlation we have found between cortical lesion load and NAWM MTR does not prove causation, but future larger studies with longitudinal follow-up may clarify this.

There is evidence that focal WML load correlates with axon loss specifically within the corpus callosum, and that it correlates with grey matter atrophy in the cortex and deep grey matter nuclei (Evangelou *et al.*, 2000; Charil *et al.*, 2007; Sepulcre *et al.*, 2009, 2006; Mühlau *et al.*, 2013). However, a definite relationship between WML load and whole NAWM or corticospinal tract axon loss is evidently absent (Griffin *et al.*, 2002; DeLuca *et al.*, 2006). The presence of microscopic inflammation in the NAWM is often used to support the argument that diffuse inflammation causes NAWM deterioration. However, neuronal damage caused by other processes, such as Alzheimer's, or even following ischaemic stroke, has been shown to stimulate inflammation (DeGraba, 1998; Akiyama *et al.*, 2000). Since inflammation can arise secondarily to neuronal damage, microscopic NAWM inflammation does not exclude the possibility that cortical lesions cause NAWM axon loss.

Cortical lesions are less focally destructive than WML (Trapp *et al.*, 1998; Peterson *et al.*, 2001), but the remote effects could still be significant. Most central nervous system (CNS) neurons cannot divide mitotically and must therefore last a lifetime; this necessitates maintenance and repair. Most of the proteins, vesicles, and organelles (including all-important mitochondria) required for axon survival are synthesised in the cell body (housing the neuron's nucleus and ribosomes, figure 5.5), and are then transported along the axon as needed (Goldstein and Yang, 2000; Hollenbeck and Saxton, 2005). The majority of CNS neurons' cell bodies reside in the cortex. Even if an inflammatory demyelinating cortical lesion only modestly impairs activity within a neuronal cell body, this could still lead to the eventual demise of its axon, if the rate of maintenance falls below

that required. CNS neurons are among the most metabolically demanding cells in the body. The longest axons (e.g. corticospinal tract) maintain cellular processes up to a metre away from their cell bodies, and could be the worst affected if their cell bodies are perturbed by cortical lesions.

White matter plaque-centred explanations for the disparity between WML burden and NAWM changes remain prevalent. Greater loss of axons inside PPMS WML compared to SPMS WML has been interpreted as a cause for greater axon loss in PPMS NAWM despite low WML load (Tallantyre, Bø, *et al.*, 2009). However, greater loss of axons inside PPMS WML does not prove that inflammatory plaque-formation is more aggressive in PPMS, thereby causing worse NAWM pathology. The fact that PPMS WML are smaller on average, and that PPMS WML have a trend towards lower inflammatory scores suggest the opposite (Thompson *et al.*, 1990; Tallantyre, Bø, *et al.*, 2009). There are two logical possibilities for why intra-lesional axon loss should be worse in some cases: either the focal inflammatory insult is more potent, or the substrate (NAWM in this context) is frailer at the time of inflammatory injury. When interpreting post mortem "snapshots" it is important to remember the context when histopathological features arose. In histopathological studies of SPMS WML, most of those lesions exhausted their acute inflammatory phase while the subject had RRMS and a less diseased cortex.

A "two-hit" mechanism could better explain axon loss/damage inside WML (figure 5.6). A "cortical-hit" comprises cortical MS lesions, causing a "brittle" NAWM, less resilient to subsequent inflammation. An "axonal-hit" comprises acute inflammatory WML formation, in the white matter tracts functionally connected to the diseased cortex. An axon traversing an acute WML either survives and partially recovers, or transects and suffers Wallerian degeneration. The likely outcome may depend on whether that neuron had already suffered a cortical-hit. If the two-hit hypothesis is correct, newly occurring WML in progressive types of MS would sustain more axon loss than

newly occurring WML in RRMS. Longitudinal MTR MRI data from SPMS and RRMS patients already supports this (Rocca *et al.*, 1999).

Taken together, cortical lesions' potential influence on NAWM and a two-hit mechanism could explain the relationship between cortical lesions, NAWM, and WML. Overall, these mechanisms provide the basis for a corticocentric model of multiple sclerosis pathogenesis.

The present study is limited by the lack of any MRI measure that provides an entirely specific appraisal of either axonal density/loss or demyelination within NAWM or focal lesions. Owing to this lack of specificity, most MRI techniques can be confounded by intermixed heterogeneous pathological processes, including demyelination, axon loss, microglial activation and oedema; this is especially true for conventional T2-weighted imaging: an archetype for high sensitivity but low specificity. Whilst no existing in vivo technique can duplicate histopathology's specificity for measuring the degree of axonal density, quantitative MRI techniques including MTR go some way toward overcoming the limitations of conventional MRI. Furthermore even histopathological assessment of axonal density within brain tissue is not without associated difficulties, because (compared to study of the spinal cord) the fibre orientation is multidirectional. Post mortem historadiological comparisons show that MTR has a strong correlation with the degree of axonal loss within focal MS white matter lesions and also NAWM (van Waesberghe *et al.*, 1999). Subsequent quantitative histopathological measures of myelin content and axonal density also correlate strongly with MTR, whilst the extent of gliosis does not (Schmierer *et al.*, 2004). This is corroborated by experimental animal data showing reduction in MTR correlates strongly with histopathological findings of demyelination and axon loss within lysolecithin-induced brain plaques in primates (Dousset *et al.*, 1995). It is important to note that loss of axons and loss of myelin are different processes, between which MTR cannot reliably distinguish; however they are not entirely independent processes, indeed quantitative histopathology using post mortem brain slices shows

that myelin content and axonal count are strongly associated with each other (Schmierer *et al.*, 2008). Therefore even though MTR conflates demyelination and axon loss, it may still be of utility as an in vivo investigative tool if interpreted sensibly. While post mortem studies indicate that demyelination and loss of axons are the main substrates of MTR abnormality in MS, other pathological processes described in established MS, such as diffuse astrocytic hyperplasia, patchy oedema, and perivascular cellular infiltration are also likely to contribute to the observed reduction of MTR values (Rocca *et al.*, 2008). Although acute oedema is undoubtedly a significant contributor to the early reduction in MTR of newly-formed or gadolinium-enhancing white matter lesions, this potential confounder is less of an issue when considering NAWM, as in this chapter. Notwithstanding the complicating effects of axonal integrity, inflammation, changes in water content, and axonal neurofilament proteins, the large literature on magnetization transfer imaging indicates that MTR is a robust and sensitive measure of tissue damage (Moore and Laule, 2012).

Because of the limitations discussed above, the "two-hit" hypothesis arguably lacks credibility; meanwhile post mortem histopathological analysis (despite its specificity) cannot solve that conundrum since it has no facility for interval longitudinal assessment. Because the gold-standard of whole-brain histopathology is inapplicable to in vivo study, quantitative MRI correlates for axonal loss such as MTR at least provide a practicable approach for future longitudinal studies.

In conclusion, cortical lesion load determined using 7T MRI has a significant correlation with NAWM MTR. Although it does not prove causation, the correlation implicates cortical lesions in the pathogenesis of NAWM axon loss, which underlies progression and disability in MS. A corticocentric model for MS pathogenesis invites reconsideration of therapeutic strategies for MS, especially if cortical lesions arise by immunopathogenetic mechanisms different to those of WML (Choi *et al.*, 2012).

Figures and tables

Figure 5.1 NAWM segmentation

Top left: 7T MPRAGE MRI; bottom left: 7T MTR image. MPRAGE volumes (a) were automatically segmented to produce cortical ribbons (b) and white matter segments (d). Cortical ribbons were dilated to produce cortical masks (c), which were subtracted from MPRAGE images (a) prior to manual segmentation of WML (e). WML maps were 3D dilated by 5 voxel layers (f), to encompass beyond-edge-effects in proximity to lesions. White matter segment masks (d) were applied to the MTR volumes (g), which had been co-registered to the MPRAGE. The resultant MTR white matter volumes were pruned by subtracting dilated cortical masks (c) and dilated WML maps (f), yielding a NAWM MTR volume (h).

MPRAGE = magnetisation prepared rapid acquisition gradient echo; WML = white matter lesion; MTR = magnetisation transfer ratio; NAWM = normal appearing white matter

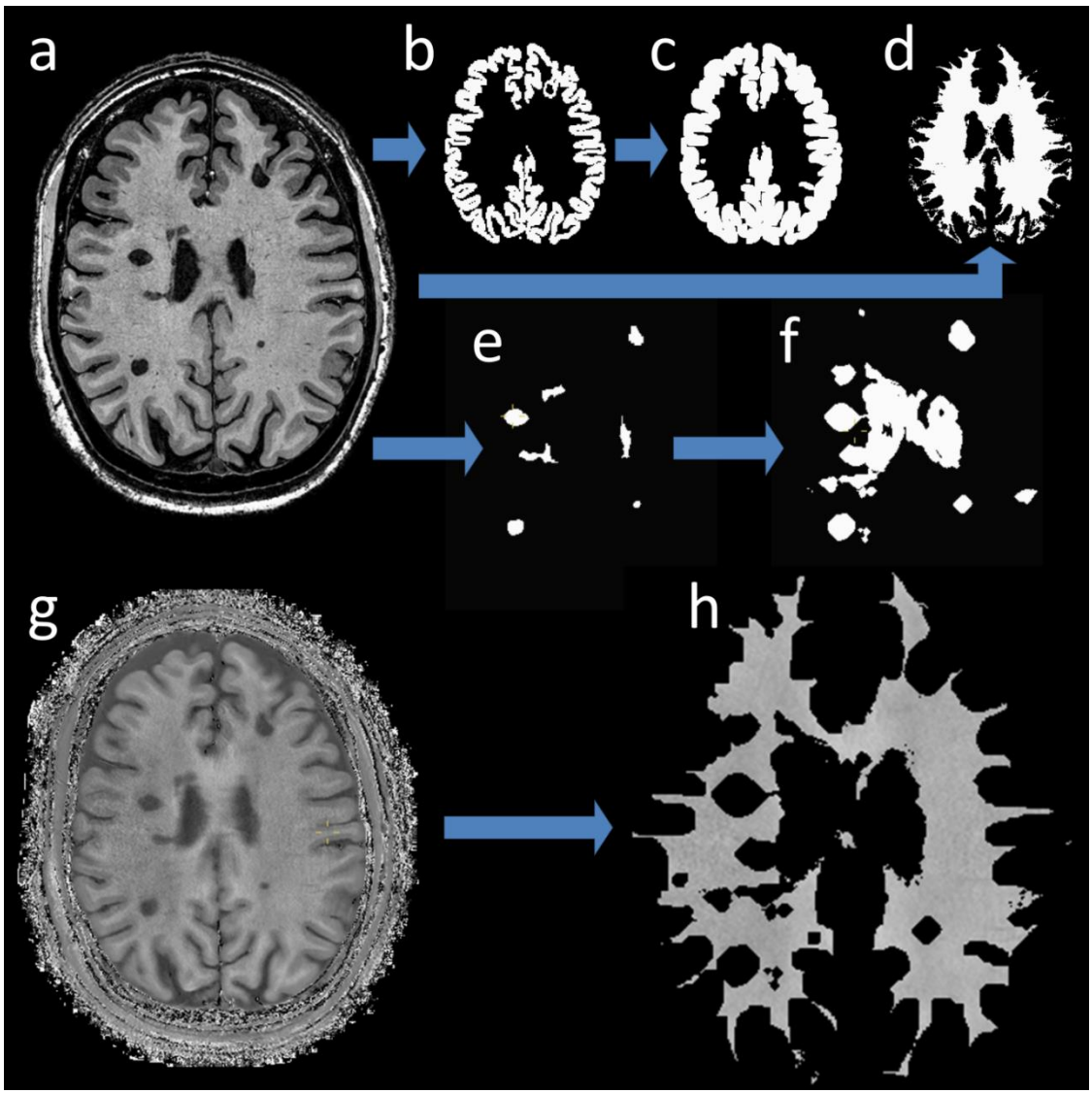
a
b
c
d
e
f
g
h

Figure 5.2 NAWM MTR vs. cortical lesion load

Scatter plots showing mean MTR of the NAWM vs. cortical lesion load. Cortical lesion load was measured using lesion counts and total cortical lesion volume. This was done using MTR images and MPRAGE images.

MTR = magnetisation transfer ratio; NAWM = normal appearing white matter; MPRAGE = magnetisation prepared rapid acquisition gradient echo

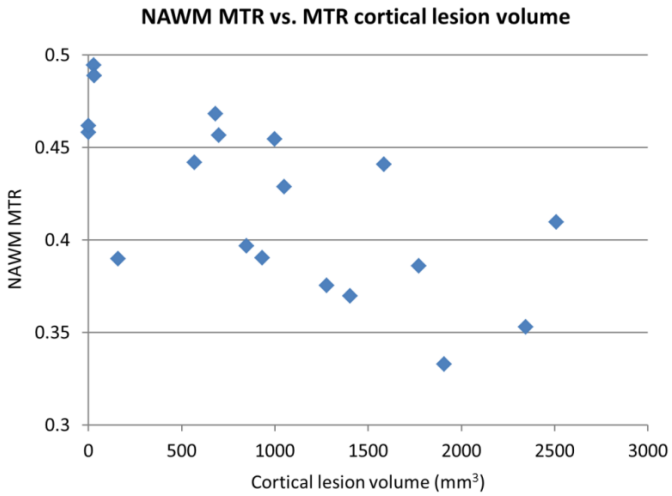
NAWM MTR vs. MTR cortical lesion volume
NAWM MTR
0.5
0.45
0.4
0.35
0.3
0
500
1000
1500
2000
2500
3000
Cortical lesion volume (mm³)

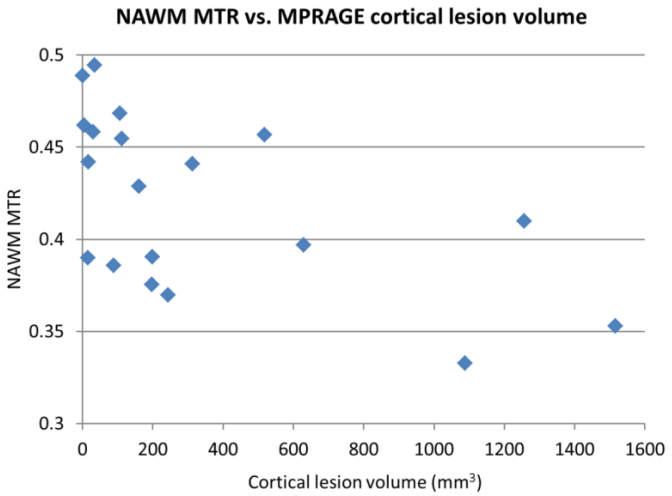
NAWM MTR vs. MPRAGE cortical lesion volume
NAWM MTR
0.5
0.45
0.4
0.35
0.3
0
200
400
600
800
1000
1200
1400
1600
Cortical lesion volume (mm³)

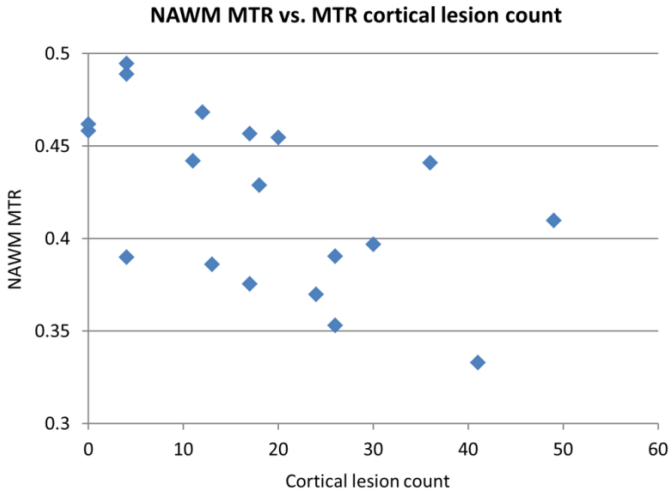
NAWM MTR vs. MTR cortical lesion count
NAWM MTR
0.5
0.45
0.4
0.35
0.3
0
10
20
30
40
50
60
Cortical lesion count

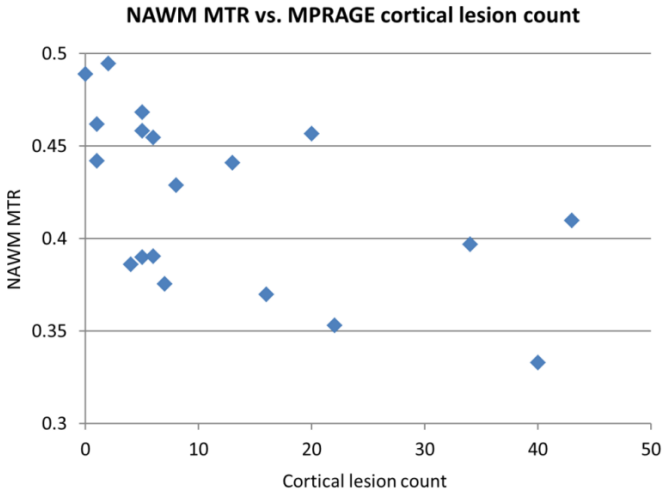
NAWM MTR vs. MPRAGE cortical lesion count
NAWM MTR
0.5
0.45
0.4
0.35
0.3
0
10
20
30
40
50
Cortical lesion count

Figure 5.3 MTR cortical lesion counts vs. MPRAGE cortical lesion counts

Often more cortical lesions were found using MTR than MPRAGE images. Whilst a difference in sensitivity is to be expected (since the contrast mechanisms of MTR and MPRAGE are independent), a plot of MTR vs. MPRAGE counts appears to intercept the origin. Therefore, though the sensitivity of MTR and MPRAGE for cortical lesions differs (and in neither case is likely to be 100%), they both yielded counts proportional to the true lesion load.

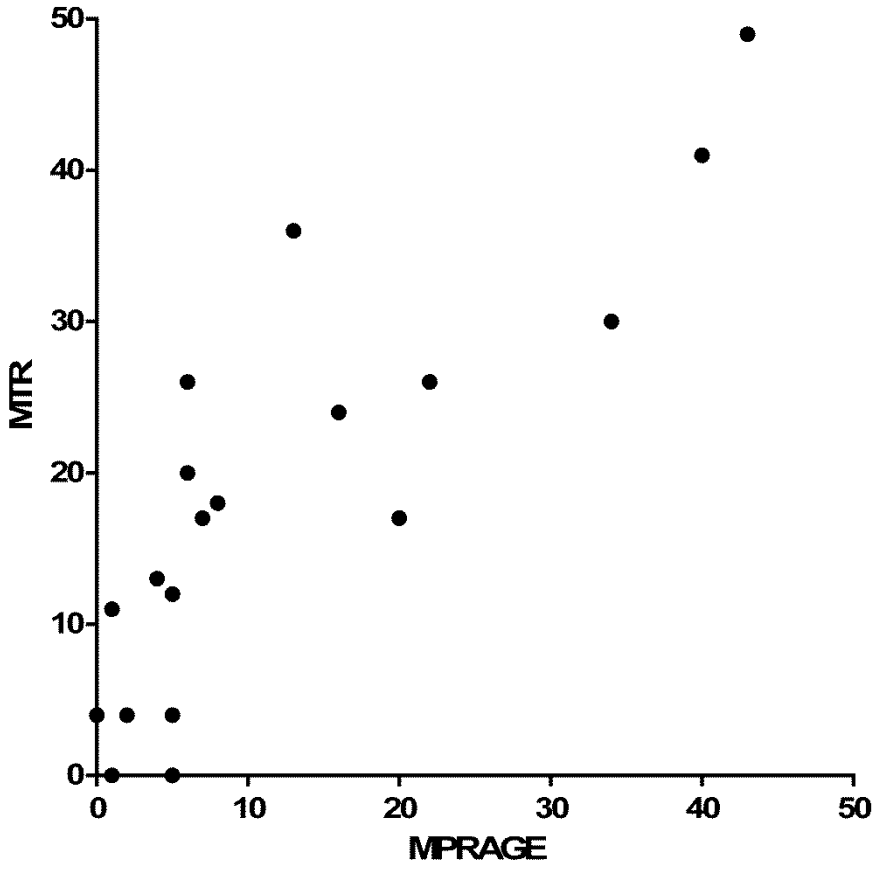

Figure 5.4 Examples of cortical lesions

Left column: 7T MPRAGE MRI; right column 7T MTR images. Two cortical lesions are shown, in each case using MPRAGE on the left, and MTR on the right.

MPRAGE = magnetisation prepared rapid acquisition gradient echo; MTR = magnetisation transfer ratio

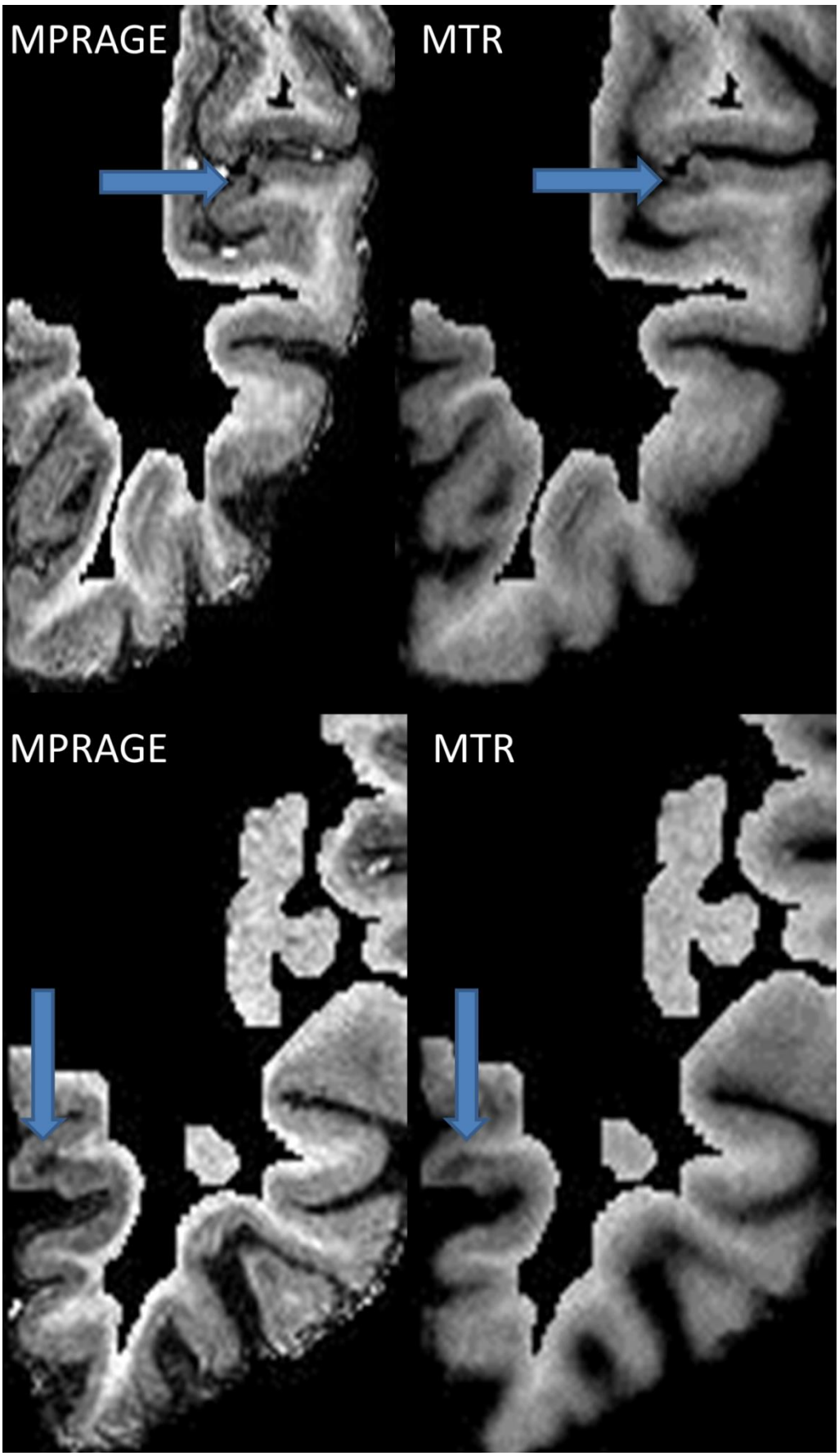
MPRAGE
MTR
MPRAGE
MTR

Figure 5.5 Effect of cortical lesion load

Most of the proteins, vesicles, and organelles (including all-important mitochondria) required for axon survival are synthesised in cell bodies (most of which reside in the cortex), and then transported along the axon as needed.

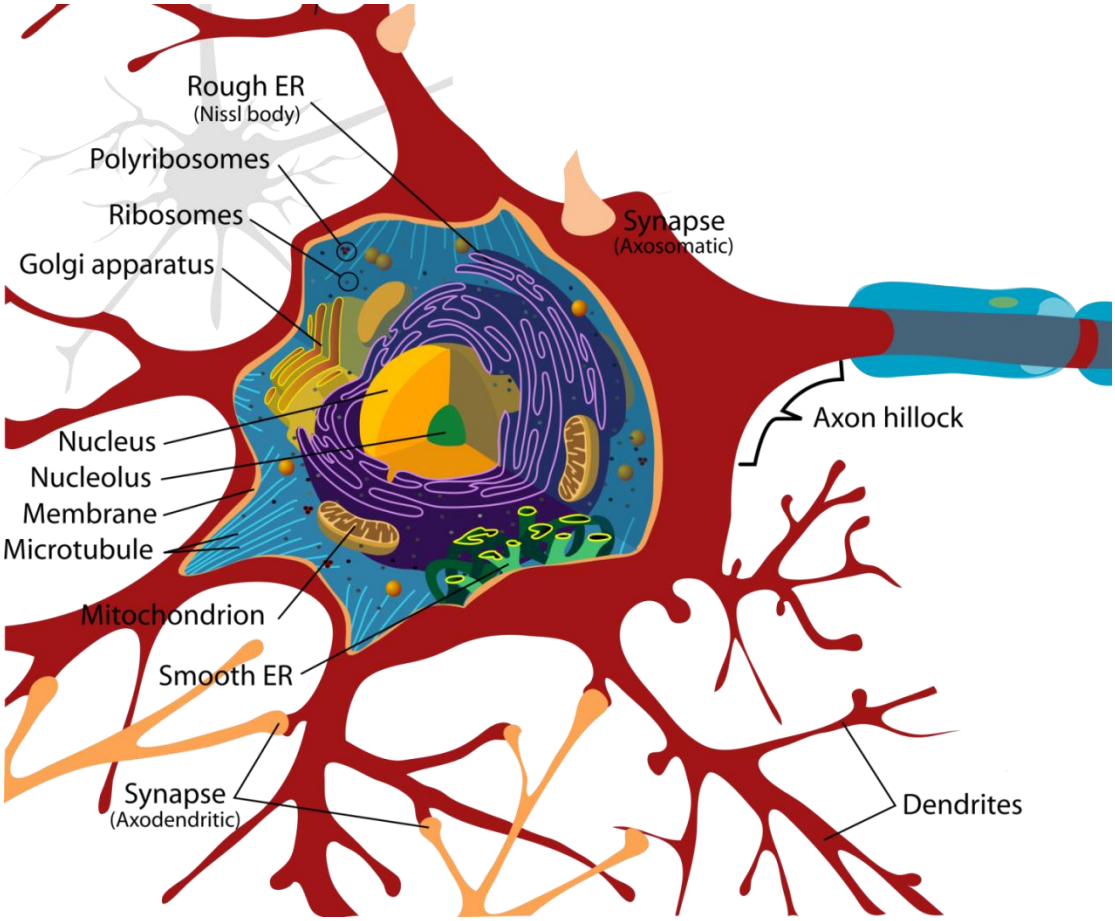

Image from Wikimedia Commons: the free media repository

Figure 5.6 A "two-hit" mechanism might better explain severity of white matter lesion axon loss

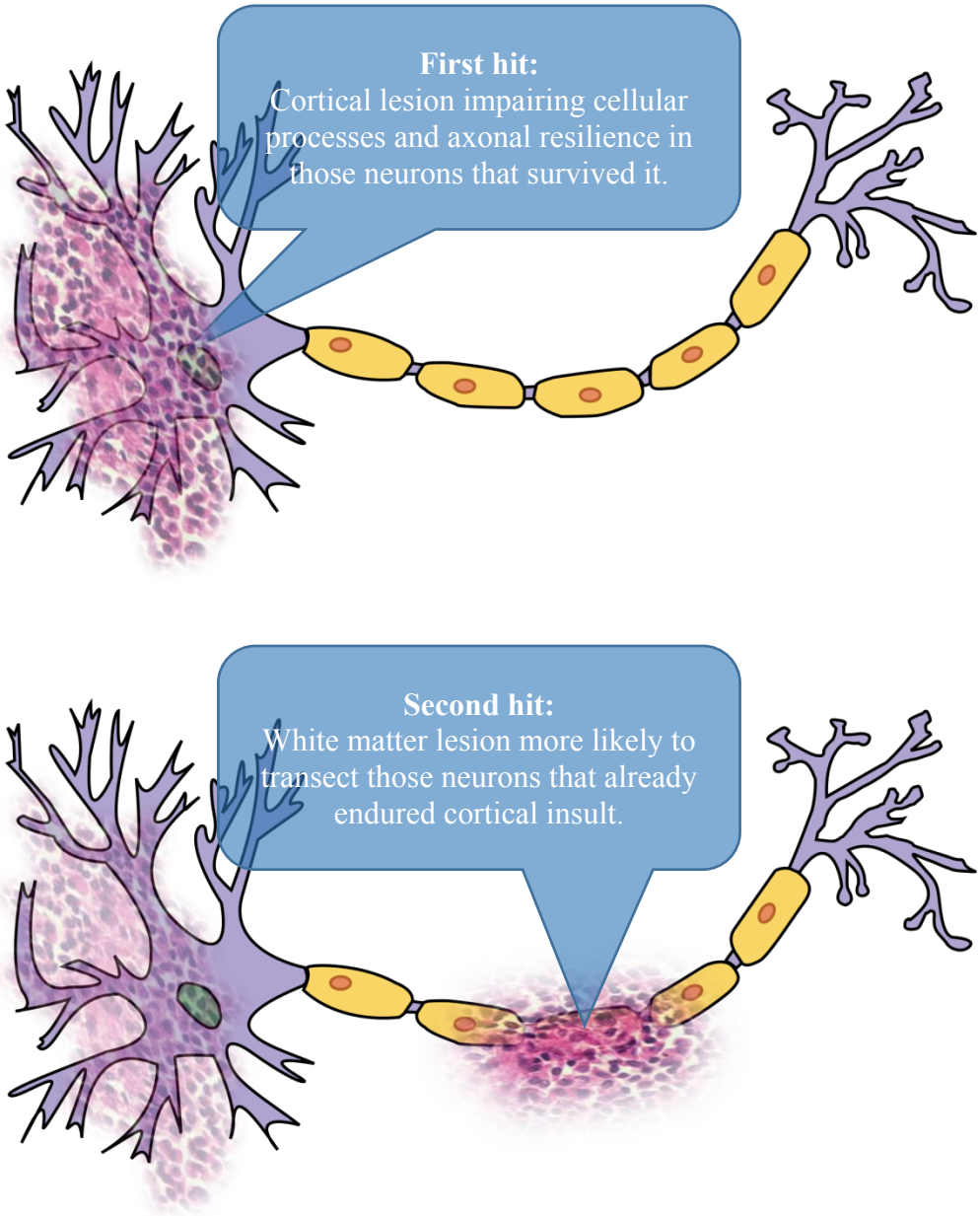

Table 5.1 Pearson correlations of NAWM mean MTR vs. other variables

Correlations of variables vs. NAWM mean MTR	MTR cortical lesion volume	MPRAGE cortical lesion volume	MTR cortical lesion count	MPRAGE cortical lesion count	WML volume	EDSS	Disease duration	Age
Pearson r	-0.6874	-0.5706	-0.5572	-0.5385	-0.08706	-0.02662	-0.3205	0.04699
95% confidence interval	-0.8700 to -0.3390	-0.8139 to -0.1570	-0.8072 to -0.1377	-0.7977 to -0.1115	-0.5208 to 0.3824	-0.4752 to 0.4329	-0.6763 to 0.1567	-0.4162 to 0.4908
p value	0.0006	0.0054	0.0066	0.0087	0.3615	0.4569	0.0905	0.4243
Significant? (alpha = 0.05)	Yes	Yes	Yes	Yes	No	No	No	No

Correlation with NAWM MTR was significant vs. all measures of cortical lesion load, and was strongest using cortical lesion volumes on MTR images. WML volume had no correlation with NAWM MTR.

NAWM = normal appearing white matter; MTR = magnetisation transfer ratio; WML = white matter lesion

Table 5.2 Multiple linear regression analysis (including WML volume)

With WML volume included as a variable	MTR cortical lesion volume	WML volume	EDSS	Disease duration	Age
t value	-3.221	0.277	0.372	-1.213	0.496
p value	0.007	0.786	0.716	0.247	0.628
Significant? (alpha = 0.05)	yes	no	no	no	no

Multiple linear regression analysis showed cortical lesion load was the only variable considered that made a significant contribution to the model (model summary: percentage variance accounted for = 54.8%, p = 0.044).

MTR = magnetisation transfer ratio; WML = white matter lesion

Table 5.3 Multiple linear regression analysis (excluding WML volume)

Without WML volume included as a variable	MTR cortical lesion volume	EDSS	Disease duration	Age
t value	-3.502	0.678	-1.484	0.467
p value	0.004	0.509	0.160	0.648
Significant? (alpha = 0.05)	yes	no	no	no

Removing WML volume from the model had little effect on cortical lesion load's influence on NAWM MTR (model summary: percentage variance accounted for = 54.5%, p = 0.019).

Summary

Owing to a lack of disease-specific tests, diagnosing MS can be protracted and sometimes requires multiple, possibly invasive, investigations. In a prospective study, we showed that visualization of central veins in brain lesions using 7T T2*-weighted MRI is a sensitive and specific method to predict an eventual diagnosis of MS. We studied 29 individuals with suspected MS who had brain lesions, and of the 13 individuals who were subsequently diagnosed with MS, all had central veins visible in the majority of their brain lesions as detected using 7T MRI. Conversely, the 9 individuals in whom a diagnosis of MS was subsequently excluded did not have visible central veins in the majority of their brain lesions.

In a cross-sectional study, visualisation of central veins in brain lesions using 3T T2*-weighted MRI differentiated 10 individuals with MS from 10 with microangiopathic brain lesions. Based on this technique, a “rule of six” was devised that quickly and accurately characterised MS cases in a further validation cohort of another 20 individuals with brain lesions (13 of them had MS, the other 7 were known to have microangiopathic WML related to hypertension associated small-vessel ischaemic disease (in 4 cases) or migraine (in 3 cases)). If validated in a large prospective cohort, this technique could complement existing diagnostic algorithms by improving the specificity with which MRI demonstrates inflammatory demyelinating brain lesions.

Using 7T MRI we found focal MS lesions that would contribute to the abnormalities in NAWM as defined using 3T FLAIR MRI. Truer segmentation of NAWM will increase accuracy of analyses that include NAWM metrics.

Cortical lesion load correlated with reduction in NAWM MTR in 19 patients with MS. The cortex contains so much critical cellular machinery that lesions in the cortex might eventually lead to loss

of axons in the white matter, which is the hallmark of progressive MS. Whilst correlation does not prove cause, future longitudinal studies may help determine causality.

References

Akiyama H, Barger S, Barnum S, Bradt B, Bauer J, Cole GM, et al. Inflammation and Alzheimer's disease. Neurobiol. Aging 2000; 21: 383–421.

Alter M, Kahana E, Loewenson R. Migration and risk of multiple sclerosis. Neurology 1978; 28: 1089–1089.

Andersson PB, Waubant E, Gee L, Goodkin DE. Multiple sclerosis that is progressive from the time of onset: clinical characteristics and progression of disability. Arch Neurol 1999; 56: 1138–42.

Balashov KE, Aung LL, Dhib-Jalbut S, Keller IA. Acute Multiple Sclerosis Lesion: Conversion of Restricted Diffusion Due to Vasogenic Edema. J. Neuroimaging 2011; 21: 202–204.

Balchandani P, Naidich TP. Ultra-High-Field MR Neuroimaging. AJNR Am. J. Neuroradiol. 2014

Barkhof F. The clinico-radiological paradox in multiple sclerosis revisited. Curr. Opin. Neurol. 2002; 15: 239–245.

Barkhof F, Filippi M, Miller DH, Scheltens P, Campi A, Polman CH, et al. Comparison of MRI criteria at first presentation to predict conversion to clinically definite multiple sclerosis. Brain 1997; 120: 2059–2069.

Bastianello S, Bozzao A, Paolillo A, Giugni E, Gasperini C, Koudriavtseva T, et al. Fast spin-echo and fast fluid-attenuated inversion-recovery versus conventional spin-echo sequences for MR quantification of multiple sclerosis lesions. AJNR Am. J. Neuroradiol. 1997; 18: 699–704.

Beck RW, Cleary PA. Optic neuritis treatment trial. One-year follow-up results. Arch Ophthalmol 1993; 111: 773–5.

Beecham AH, Patsopoulos NA, Xifara DK, Davis MF, Kemppinen A, Cotsapas C, et al. Analysis of immune-related loci identifies 48 new susceptibility variants for multiple sclerosis. Nat. Genet. 2013; 45: 1353–1360.

Bellmann-Strobl J, Stiepani H, Wuerfel J, Bohner G, Paul F, Warmuth C, et al. MR spectroscopy (MRS) and magnetisation transfer imaging (MTI), lesion load and clinical scores in early relapsing remitting multiple sclerosis: a combined cross-sectional and longitudinal study. Eur. Radiol. 2009; 19: 2066–2074.

Bermel RA, Weinstock-Guttman B, Bourdette D, Foulds P, You X, Rudick RA. Intramuscular interferon beta-1a therapy in patients with relapsing-remitting multiple sclerosis: a 15-year follow-up study. Mult. Scler. 2010; 16: 588–596.

Bjartmar C, Kidd G, Mork S, Rudick R, Trapp BD. Neurological disability correlates with spinal cord axonal loss and reduced N-acetyl aspartate in chronic multiple sclerosis patients. Ann. Neurol. 2000; 48: 893–901.

Bjartmar C, Kinkel RP, Kidd G, Rudick RA, Trapp BD. Axonal loss in normal-appearing white matter in a patient with acute MS. Neurology 2001; 57: 1248–1252.

Bø L, Vedeler CA, Nyland HI, Trapp BD, Mørk SJ. Subpial demyelination in the cerebral cortex of multiple sclerosis patients. J. Neuropathol. Exp. Neurol. 2003; 62: 723–732.

Boggild MD, Williams R, Haq N, Hawkins CP. Cortical plaques visualised by fluid-attenuated inversion recovery imaging in relapsing multiple sclerosis. Neuroradiology 1996; 38 Suppl 1: S10-3.

Carmosino MJ, Brousseau KM, Arciniegas DB, Corboy JR. Initial evaluations for multiple sclerosis in a university multiple sclerosis center: Outcomes and role of magnetic resonance imaging in referral. Arch. Neurol. 2005; 62: 585–590.

Castriota-Scanderbeg A, Fasano F, Filippi M, Caltagirone C. T1 relaxation maps allow differentiation between pathologic tissue subsets in relapsing-remitting and secondary progressive multiple sclerosis. Mult. Scler. Houndmills Basingstoke Engl. 2004; 10: 556–561.

Cercignani M, Bozzali M, Iannucci G, Comi G, Filippi M. Magnetisation transfer ratio and mean diffusivity of normal appearing white and grey matter from patients with multiple sclerosis. J Neurol Neurosurg Psychiatry 2001; 70: 311–7.

Charcot JM. Lectures on the diseases of the nervous system. The New Sydenham Society; 1881.

Charil A, Dagher A, Lerch JP, Zijdenbos AP, Worsley KJ, Evans AC. Focal cortical atrophy in multiple sclerosis: relation to lesion load and disability. NeuroImage 2007; 34: 509–17.

Choi SR, Howell OW, Carassiti D, Magliozzi R, Gveric D, Muraro PA, et al. Meningeal inflammation plays a role in the pathology of primary progressive multiple sclerosis [Internet]. Brain 2012[cited 2012 Nov 19] Available from: http://brain.oxfordjournals.org/content/early/2012/08/18/brain.aws189

Coles A. Multiple sclerosis. Pract. Neurol. 2009; 9: 118–126.

Comi G, Filippi M, Barkhof F, Durelli L, Edan G, Fernández O, et al. Effect of early interferon treatment on conversion to definite multiple sclerosis: a randomised study. The Lancet 2001; 357: 1576–1582.

Compston A, Confavreux C. The distribution of multiple sclerosis. In: McAlpine's multiple sclerosis. Churchill Livingstone Elsevier; 2005. p. 71–111.

Confavreux C, Aimard G, Devic M. Course and prognosis of multiple sclerosis assessed by the computerized data processing of 349 patients. Brain 1980; 103: 281–300.

Confavreux C, Vukusic S, Adeleine P. Early clinical predictors and progression of irreversible disability in multiple sclerosis: an amnesic process. Brain 2003; 126: 770–782.

Confavreux C, Vukusic S, Moreau T, Adeleine P. Relapses and progression of disability in multiple sclerosis. N. Engl. J. Med. 2000; 343: 1430–8.

Damian MS, Schilling G, Bachmann G, Simon C, Stöppler S, Dorndorf W. White matter lesions and cognitive deficits: relevance of lesion pattern? Acta Neurol. Scand. 1994; 90: 430–436.

Davie CA, Barker GJ, Thompson AJ, Tofts PS, McDonald WI, Miller DH. 1H magnetic resonance spectroscopy of chronic cerebral white matter lesions and normal appearing white matter in multiple sclerosis. J. Neurol. Neurosurg. Psychiatry 1997; 63: 736–742.

Dawson JW. The histology of disseminated sclerosis. Trans R Soc Edinb 1916; 50: 517–740.

De Stefano N, Filippi M. MR spectroscopy in multiple sclerosis. J. Neuroimaging Off. J. Am. Soc. Neuroimaging 2007; 17 Suppl 1: 31S–35S.

De Stefano N, Matthews PM, Filippi M, Agosta F, De Luca M, Bartolozzi ML, et al. Evidence of early cortical atrophy in MS: relevance to white matter changes and disability. Neurology 2003; 60: 1157–62.

De Stefano N, Matthews PM, Fu L, Narayanan S, Stanley J, Francis GS, et al. Axonal damage correlates with disability in patients with relapsing-remitting multiple sclerosis. Results of a longitudinal magnetic resonance spectroscopy study. Brain 1998; 121: 1469–77.

De Stefano N, Narayanan S, Francis SJ, Smith S, Mortilla M, Tartaglia MC, et al. Diffuse axonal and tissue injury in patients with multiple sclerosis with low cerebral lesion load and no disability. Arch Neurol 2002; 59: 1565–71.

DeGraba TJ. The role of inflammation after acute stroke Utility of pursuing anti-adhesion molecule therapy. Neurology 1998; 51: S62–S68.

DeLuca GC, Williams K, Evangelou N, Ebers GC, Esiri MM. The contribution of demyelination to axonal loss in multiple sclerosis. Brain 2006; 129: 1507–16.

Díaz-Sánchez M, Mayra Gómez-Moreno S, Asunción Morales-Otal M, Ramos-González A, Benito-León J. Accuracy of MRI criteria for dissemination in space for the diagnosis of multiple sclerosis in patients with clinically isolated syndromes. Mult. Scler. 2010; 16: 576–580.

Dixon JE, Simpson A, Mistry N, Evangelou N, Morris PG. Optimisation of T(2)(*)-weighted MRI for the detection of small veins in multiple sclerosis at 3T and 7T [Internet]. Eur. J. Radiol. 2011[cited 2012 Jan 13] Available from: http://www.ncbi.nlm.nih.gov/pubmed/22138119

Dousset V, Brochet B, Vital A, Gross C, Benazzouz A, Boullerne A, et al. Lysolecithin-induced demyelination in primates: preliminary in vivo study with MR and magnetization transfer. Am. J. Neuroradiol. 1995; 16: 225–231.

Duyn JH. The future of ultra-high field MRI and fMRI for study of the human brain. Neuroimage 2012; 62: 1241–1248.

Dyment DA, Ebers GC, Dessa Sadovnick A. Genetics of multiple sclerosis. Lancet Neurol. 2004; 3: 104–110.

Ebers GC, Traboulsee A, Li D, Langdon D, Reder AT, Goodin DS, et al. Analysis of clinical outcomes according to original treatment groups 16 years after the pivotal IFNB-1b trial. J. Neurol. Neurosurg. Psychiatry 2010; 81: 907–912.

Evangelou N, Konz D, Esiri MM, Smith S, Palace J, Matthews PM. Regional axonal loss in the corpus callosum correlates with cerebral white matter lesion volume and distribution in multiple sclerosis. Brain 2000; 123 (Pt 9): 1845–9.

Evangelou N, Konz D, Esiri MM, Smith S, Palace J, Matthews PM. Size-selective neuronal changes in the anterior optic pathways suggest a differential susceptibility to injury in multiple sclerosis. Brain J. Neurol. 2001; 124: 1813–1820.

Fazekas F, Barkhof F, Filippi M, Grossman RI, Li DKB, McDonald WI, et al. The contribution of magnetic resonance imaging to the diagnosis of multiple sclerosis. Neurology 1999; 53: 448.

Filippi M, Agosta F. Magnetization transfer MRI in multiple sclerosis. J. Neuroimaging Off. J. Am. Soc. Neuroimaging 2007; 17 Suppl 1: 22S–26S.

Filippi M, Bozzali M, Rovaris M, Gonen O, Kesavadas C, Ghezzi A, et al. Evidence for widespread axonal damage at the earliest clinical stage of multiple sclerosis. Brain 2003; 126: 433–7.

Filippi M, Horsfield MA, Hajnal JV, Narayana PA, Udupa JK, Yousry TA, et al. Quantitative assessment of magnetic resonance imaging lesion load in multiple sclerosis. J. Neurol. Neurosurg. Psychiatry 1998; 64 Suppl 1: S88-93.

Filippi M, Iannucci G, Tortorella C, Minicucci L, Horsfield MA, Colombo B, et al. Comparison of MS clinical phenotypes using conventional and magnetization transfer MRI. Neurology 1999; 52: 588–94.

Filippi M, Rocca MA. MRI evidence for multiple sclerosis as a diffuse disease of the central nervous system. J. Neurol. 2005; 252 Suppl 5: v16-24.

Filippi M, Rocca MA. Magnetic resonance imaging techniques to define and monitor tissue damage and repair in multiple sclerosis. J. Neurol. 2007; 254 Suppl 1: I55–I62.

Filippi M, Tortorella C, Bozzali M. Normal-appearing white matter changes in multiple sclerosis: the contribution of magnetic resonance techniques. Mult. Scler. Houndmills Basingstoke Engl. 1999; 5: 273–282.

Fog T. On the Vessel-Plaque Relationships in the Brain in Multiple Sclerosis. Acta Neurol. Scand. 1964; 40: SUPPL 10:9-15.

Fog T. The topography of plaques in multiple sclerosis with special reference to cerebral plaques. Acta Neurol. Scand. 1965; 15: 1–161.

Fog. Topographic distribution of plaques in the spinal cord in multiple sclerosis. Arch. Neurol. Psychiatry 1950; 63: 382–414.

Fu L, Matthews PM, De Stefano N, Worsley KJ, Narayanan S, Francis GS, et al. Imaging axonal damage of normal-appearing white matter in multiple sclerosis. Brain 1998; 121 (Pt 1): 103–13.

Ganter, Prince, Esiri. Spinal cord axonal loss in multiple sclerosis: a post-mortem study. Neuropathol. Appl. Neurobiol. 1999; 25: 459–467.

Gay D, Esiri M. Blood-brain barrier damage in acute multiple sclerosis plaques. An immunocytological study. Brain J. Neurol. 1991; 114 (Pt 1B): 557–572.

Geurts JJG, Blezer ELA, Vrenken H, van der Toorn A, Castelijns JA, Polman CH, et al. Does high-field MR imaging improve cortical lesion detection in multiple sclerosis? J. Neurol. 2008; 255: 183–191.

Geurts JJG, Bö L, Pouwels PJW, Castelijns JA, Polman CH, Barkhof F. Cortical lesions in multiple sclerosis: combined postmortem MR imaging and histopathology. AJNR Am. J. Neuroradiol. 2005; 26: 572–577.

Gilmore CP, Geurts JJG, Evangelou N, Bot JCJ, van Schijndel RA, Pouwels PJW, et al. Spinal cord grey matter lesions in multiple sclerosis detected by post-mortem high field MR imaging. Mult. Scler. Houndmills Basingstoke Engl. 2009; 15: 180–188.

Goldstein LSB, Yang Z. Microtubule-Based Transport Systems in Neurons: The Roles of Kinesins and Dyneins. Annu. Rev. Neurosci. 2000; 23: 39–71.

Gonzalez-Toledo E, Kelley RE, Minagar A. Role of magnetic resonance spectroscopy in diagnosis and management of multiple sclerosis. Neurol. Res. 2006; 28: 280–283.

Greenberg BM, Balcer L, Calabresi PA, et al. Interferon beta use and disability prevention in relapsing-remitting multiple sclerosis. JAMA Neurol. 2013; 70: 248–251.

Greenfield J. Greenfield's neuropathology ed. by Seth Love ... [et al.]. 8th ed. London: Arnold; 2008.

Griffin CM, Chard DT, Parker GJM, Barker GJ, Thompson AJ, Miller DH. The relationship between lesion and normal appearing brain tissue abnormalities in early relapsing remitting multiple sclerosis. J. Neurol. 2002; 249: 193–199.

Haacke EM, Mittal S, Wu Z, Neelavalli J, Cheng Y-CN. Susceptibility-Weighted Imaging: Technical Aspects and Clinical Applications, Part 1. Am. J. Neuroradiol. 2009; 30: 19–30.

Hollenbeck PJ, Saxton WM. The axonal transport of mitochondria. J. Cell Sci. 2005; 118: 5411–5419.

Hurley AC, Al-Radaideh A, Bai L, Aickelin U, Coxon R, Glover P, et al. Tailored RF pulse for magnetization inversion at ultrahigh field. Magn. Reson. Med. Off. J. Soc. Magn. Reson. Med. Soc. Magn. Reson. Med. 2010; 63: 51–58.

Jacobs LD, Beck RW, Simon JH, Kinkel RP, Brownscheidle CM, Murray TJ, et al. Intramuscular interferon beta-1a therapy initiated during a first demyelinating event in multiple sclerosis. CHAMPS Study Group. N. Engl. J. Med. 2000; 343: 898–904.

Jenkinson M, Bannister P, Brady M, Smith S. Improved optimization for the robust and accurate linear registration and motion correction of brain images. Neuroimage 2002; 17: 825–41.

Kangarlu A, Bourekas EC, Ray-Chaudhury A, Rammohan KW. Cerebral cortical lesions in multiple sclerosis detected by MR imaging at 8 Tesla. Ajnr 2007; 28: 262–6.

Kappos L, Freedman MS, Polman CH, Edan G, Hartung H-P, Miller DH, et al. Effect of early versus delayed interferon beta-1b treatment on disability after a first clinical event suggestive of multiple sclerosis: a 3-year follow-up analysis of the BENEFIT study. The Lancet 2007; 370: 389–397.

Kates R, Atkinson D, Brant-Zawadzki M. Fluid-attenuated inversion recovery (FLAIR): clinical prospectus of current and future applications. Top. Magn. Reson. Imaging TMRI 1996; 8: 389–396.

Keiper MD, Grossman RI, Hirsch JA, Bolinger L, Ott IL, Mannon LJ, et al. MR identification of white matter abnormalities in multiple sclerosis: a comparison between 1.5 T and 4 T. AJNR Am. J. Neuroradiol. 1998; 19: 1489–1493.

Kelly SB, Chaila E, Kinsella K, Duggan M, Walsh C, Tubridy N, et al. Using atypical symptoms and red flags to identify non-demyelinating disease. J. Neurol. Neurosurg. Psychiatry 2012; 83: 44–48.

Khaleeli Z, Sastre-Garriga J, Ciccarelli O, Miller DH, Thompson AJ. Magnetisation transfer ratio in the normal appearing white matter predicts progression of disability over 1 year in early primary progressive multiple sclerosis. J. Neurol. Neurosurg. Psychiatry 2007; 78: 1076–1082.

Kidd D, Thorpe JW, Thompson AJ, Kendall BE, Moseley IF, MacManus DG, et al. Spinal cord MRI using multi-array coils and fast spin echo. II. Findings in multiple sclerosis. Neurology 1993; 43: 2632–2637.

Kilsdonk ID, Jonkman LE, Klaver R, Veluw SJ van, Zwanenburg JJM, Kuijer JPA, et al. Increased cortical grey matter lesion detection in multiple sclerosis with 7 T MRI: a post-mortem verification study. Brain 2016: aww037.

Kilsdonk ID, Wattjes MP, Lopez-Soriano A, Kuijer JPA, de Jong MC, de Graaf WL, et al. Improved differentiation between MS and vascular brain lesions using FLAIR* at 7 Tesla. Eur. Radiol. 2014; 24: 841–849.

Kingwell E, Leung AL, Roger E, Duquette P, Rieckmann P, Tremlett H. Factors associated with delay to medical recognition in two Canadian multiple sclerosis cohorts. J. Neurol. Sci. 2010; 292: 57–62.

Kister I, Herbert J, Zhou Y, Ge Y. Ultrahigh-field MR (7 T) imaging of brain lesions in neuromyelitis optica [Internet]. Mult. Scler. Int. 2013; 2013[cited 2015 Sep 1] Available from: http://www.hindawi.com/journals/msi/aip/398259/

Kollia K, Maderwald S, Putzki N, Schlamann M, Theysohn JM, Kraff O, et al. First clinical study on ultra-high-field MR imaging in patients with multiple sclerosis: comparison of 1.5T and 7T. AJNR Am. J. Neuroradiol. 2009; 30: 699–702.

Kremenchutzky M. Primary Progressive MS. Int MS J 2003; 10: 89–95.

Kremenchutzky M, Rice GP, Baskerville J, Wingerchuk DM, Ebers GC. The natural history of multiple sclerosis: a geographically based study 9: observations on the progressive phase of the disease. Brain 2006; 129: 584–94.

Kurtzke JF. Rating neurologic impairment in multiple sclerosis: an expanded disability status scale (EDSS). Neurology 1983; 33: 1444–52.

Kutzelnigg A, Lucchinetti CF, Stadelmann C, Brück W, Rauschka H, Bergmann M, et al. Cortical demyelination and diffuse white matter injury in multiple sclerosis. Brain J. Neurol. 2005; 128: 2705–2712.

Kwon EE, Prineas JW. Blood-brain barrier abnormalities in longstanding multiple sclerosis lesions. An immunohistochemical study. J. Neuropathol. Exp. Neurol. 1994; 53: 625–636.

Larsson HBW, Thomsen C, Frederiksen J, Stubgaard M, Henriksen O. In vivo magnetic resonance diffusion measurement in the brain of patients with multiple sclerosis. Magn. Reson. Imaging 1992; 10: 7–12.

Lassmann H, Wekerle H. The pathology of multiple sclerosis. In: McAlpine's multiple sclerosis. Churchill Livingstone Elsevier; 2005.

Lee MA, Blamire AM, Pendlebury S, Ho KH, Mills KR, Styles P, et al. Axonal injury or loss in the internal capsule and motor impairment in multiple sclerosis. Arch. Neurol. 2000; 57: 65–70.

Levin N, Mor M, Ben-Hur T. Patterns of misdiagnosis of multiple sclerosis. Isr. Med. Assoc. J. IMAJ 2003; 5: 489–490.

Lipton HL, Liang Z, Hertzler S, Son K-N. A specific viral cause of multiple sclerosis: One virus, one disease. Ann. Neurol. 2007; 61: 514–523.

Lummel N, Boeckh-Behrens T, Schoepf V, Burke M, Brückmann H, Linn J. Presence of a central vein within white matter lesions on susceptibility weighted imaging: a specific finding for multiple sclerosis? Neuroradiology 2011; 53: 311–317.

Mac Innes M, Arnold DL. The Relevance of Normal-Appearing White Matter Pathology in Multiple Sclerosis. In: Normal-appearing White and Grey Matter Damage in Multiple Sclerosis. Milan: Springer; 2004. p. 92–97.

Mainero C, Benner T, Radding A, van der Kouwe A, Jensen R, Rosen BR, et al. In vivo imaging of cortical pathology in multiple sclerosis using ultra-high field MRI. Neurology 2009; 73: 941–948.

McDonald WI, Compston A, Edan G, Goodkin D, Hartung HP, Lublin FD, et al. Recommended diagnostic criteria for multiple sclerosis: guidelines from the International Panel on the diagnosis of multiple sclerosis. Ann Neurol 2001; 50: 121–7.

McDonnell GV, Hawkins SA. Clinical study of primary progressive multiple sclerosis in Northern Ireland, UK. J. Neurol. Neurosurg. Psychiatry 1998; 64: 451–4.

Miki Y, Grossman RI, Udupa JK, Wei L, Kolson DL, Mannon LJ, et al. Isolated U-fiber involvement in MS: preliminary observations. Neurology 1998; 50: 1301–1306.

Miller DH, Rudge P, Johnson G, Kendall BE, Macmanus DG, Moseley IF, et al. Serial gadolinium enhanced magnetic resonance imaging in multiple sclerosis. Brain 1988; 111 (Pt 4): 927–39.

Mistry N, Dixon J, Tallantyre EC, Tench C, Abdel-Fahim R, Jaspan T, et al. Central veins in brain lesions visualized with high-field magnetic resonance imaging: a pathologically specific diagnostic biomarker for inflammatory demyelination in the brain. JAMA Neurol. 2013; 70: 623–628.

Mistry N, Tallantyre EC, Dixon JE, Galazis N, Jaspan T, Morgan PS, et al. Focal multiple sclerosis lesions abound in 'normal appearing white matter'. Mult. Scler. J. 2011; 17: 1313–1323.

Molyneux PD, Tubridy N, Parker GJ, Barker GJ, MacManus DG, Tofts PS, et al. The effect of section thickness on MR lesion detection and quantification in multiple sclerosis. AJNR Am. J. Neuroradiol. 1998; 19: 1715–1720.

Moore GRW, Laule C. Neuropathologic Correlates of Magnetic Resonance Imaging in Multiple Sclerosis. J. Neuropathol. Exp. Neurol. 2012; 71: 762–778.

Moraal B, Roosendaal SD, Pouwels PJW, Vrenken H, Schijndel RA van, Meier DS, et al. Multi-contrast, isotropic, single-slab 3D MR imaging in multiple sclerosis. Eur. Radiol. 2008; 18: 2311–2320.

Moreau T, Coles A, Wing M, Isaacs J, Hale G, Waldmann H, et al. Transient increase in symptoms associated with cytokine release in patients with multiple sclerosis. Brain J. Neurol. 1996; 119 (Pt 1): 225–237.

Moriarty DM, Blackshaw AJ, Talbot PR, Griffiths HL, Snowden JS, Hillier VF, et al. Memory dysfunction in multiple sclerosis corresponds to juxtacortical lesion load on fast fluid-attenuated inversion-recovery MR images. AJNR Am. J. Neuroradiol. 1999; 20: 1956–1962.

Mühlau M, Buck D, Förschler A, Boucard CC, Arsic M, Schmidt P, et al. White-matter lesions drive deep gray-matter atrophy in early multiple sclerosis: support from structural MRI [Internet]. Mult. Scler. J. 2013[cited 2013 May 12] Available from: http://msj.sagepub.com/content/early/2013/03/12/1352458513478673

Neema M, Goldberg-Zimring D, Guss ZD, Healy BC, Guttmann CRG, Houtchens MK, et al. 3 T MRI relaxometry detects T2 prolongation in the cerebral normal-appearing white matter in multiple sclerosis. NeuroImage 2009; 46: 633–641.

Neto SP, Alvarenga RM, Vasconcelos CC, Alvarenga MP, Pinto LC, Pinto VL. Evaluation of pattern-reversal visual evoked potential in patients with neuromyelitis optica. Mult. Scler. J. 2013; 19: 173–178.

Newcombe J, Hawkins CP, Henderson CL, Patel HA, Woodroofe MN, Hayes GM, et al. Histopathology of multiple sclerosis lesions detected by magnetic resonance imaging in unfixed postmortem central nervous system tissue. Brain 1991; 114 (Pt 2): 1013–23.

Nielsen AS, Kinkel RP, Madigan N, Tinelli E, Benner T, Mainero C. Contribution of cortical lesion subtypes at 7T MRI to physical and cognitive performance in MS. Neurology 2013; 81: 641–649.

Nijeholt GJ, Bergers E, Kamphorst W, Bot J, Nicolay K, Castelijns JA, et al. Post-mortem high-resolution MRI of the spinal cord in multiple sclerosis: a correlative study with conventional MRI, histopathology and clinical phenotype. Brain 2001; 124: 154–66.

Okuda DT, Vrenken H. Metabolite changes in radiologically isolated syndrome More pathology than meets the eye? Neurology 2013; 80: 2084–2085.

Ormerod IEC, Miller DH, McDONALD WI, Boulay EPGHD, Rudge P, Kendall BE, et al. The Role of Nmr Imaging in the Assessment of Multiple Sclerosis and Isolated Neurological Lesions. Brain 1987; 110: 1579–1616.

Patsopoulos NA, Barcellos LF, Hintzen RQ, Schaefer C, Duijn CM van, Noble JA, et al. Fine-Mapping the Genetic Association of the Major Histocompatibility Complex in Multiple Sclerosis: HLA and Non-HLA Effects. PLOS Genet 2013; 9: e1003926.

Peterson JW, Bo L, Mork S, Chang A, Trapp BD. Transected neurites, apoptotic neurons, and reduced inflammation in cortical multiple sclerosis lesions. Ann Neurol 2001; 50: 389–400.

Polman CH, Reingold SC, Banwell B, Clanet M, Cohen JA, Filippi M, et al. Diagnostic criteria for multiple sclerosis: 2010 revisions to the McDonald criteria. Ann. Neurol. 2011; 69: 292–302.

Polman CH, Reingold SC, Edan G, Filippi M, Hartung H-P, Kappos L, et al. Diagnostic criteria for multiple sclerosis: 2005 revisions to the 'McDonald Criteria'. Ann. Neurol. 2005; 58: 840–846.

Poser CM, Paty DW, Scheinberg L, McDonald WI, Davis FA, Ebers GC, et al. New diagnostic criteria for multiple sclerosis: Guidelines for research protocols. Ann. Neurol. 1983; 13: 227–231.

Pretorius PM, Quaghebeur G. The role of MRI in the diagnosis of MS. Clin. Radiol. 2003; 58: 434–448.

Reidel MA, Stippich C, Heiland S, Storch-Hagenlocher B, Jansen O, Hähnel S. Differentiation of multiple sclerosis plaques, subacute cerebral ischaemic infarcts, focal vasogenic oedema and lesions of subcortical arteriosclerotic encephalopathy using magnetisation transfer measurements. Neuroradiology 2003; 45: 289–294.

Rice CM. Disease modification in multiple sclerosis: an update. Pract. Neurol. 2014; 14: 6–13.

Rocca MA, Agosta F, Sormani MP, Fernando K, Tintore M, Korteweg T, et al. A three-year, multi-parametric MRI study in patients at presentation with CIS. J Neurol 2008; 255: 683–91.

Rocca MA, Mastronardo G, Rodegher M, Comi G, Filippi M. Long-Term Changes of Magnetization Transfer–Derived Measures from Patients with Relapsing-Remitting and Secondary Progressive Multiple Sclerosis. Am. J. Neuroradiol. 1999; 20: 821–827.

Rolak LA, Fleming JO. The differential diagnosis of multiple sclerosis. The Neurologist 2007; 13: 57–72.

Rovaris M, Bozzali M, Santuccio G, Iannucci G, Sormani MP, Colombo B, et al. Relative contributions of brain and cervical cord pathology to multiple sclerosis disability: a study with magnetisation transfer ratio histogram analysis. J Neurol Neurosurg Psychiatry 2000; 69: 723–7.

Rovaris M, Filippi M. Diffusion Tensor MRI in Multiple Sclerosis. J. Neuroimaging 2007; 17: 27S–30S.

Rovaris M, Gambini A, Gallo A, Falini A, Ghezzi A, Benedetti B, et al. Axonal injury in early multiple sclerosis is irreversible and independent of the short-term disease evolution. Neurology 2005; 65: 1626–1630.

Rudick RA, Miller AE. Multiple sclerosis or multiple possibilities The continuing problem of misdiagnosis. Neurology 2012; 78: 1904–1906.

Ruiz-Peña JL, Piñero P, Sellers G, Argente J, Casado A, Foronda J, et al. Magnetic resonance spectroscopy of normal appearing white matter in early relapsing-remitting multiple sclerosis: correlations between disability and spectroscopy. BMC Neurol. 2004; 4: 8.

Sadovnick AD, Armstrong H, Rice GPA, Bulman D, Hashimoto L, Party DW, et al. A population-based study of multiple sclerosis in twins: Update. Ann. Neurol. 1993; 33: 281–285.

Sajja BR, Wolinsky JS, Narayana PA. Proton magnetic resonance spectroscopy in multiple sclerosis. Neuroimaging Clin. N. Am. 2009; 19: 45–58.

Sanchez-Panchuelo RM, Besle J, Beckett A, Bowtell R, Schluppeck D, Francis S. Within-Digit Functional Parcellation of Brodmann Areas of the Human Primary Somatosensory Cortex Using Functional Magnetic Resonance Imaging at 7 Tesla. J. Neurosci. 2012; 32: 15815–15822.

Sastre-Garriga J, Ingle GT, Chard DT, Ramio-Torrenta L, McLean MA, Miller DH, et al. Metabolite changes in normal-appearing gray and white matter are linked with disability in early primary progressive multiple sclerosis. Arch. Neurol. 2005; 62: 569–73.

Sati P, George IC, Shea CD, Gaitan MI, Reich DS. FLAIR*: A Combined MR Contrast Technique for Visualizing White Matter Lesions and Parenchymal Veins. Radiology 2012; 265: 926–932.

Sati P, Thomasson DM, Li N, Pham DL, Biassou NM, Reich DS, et al. Rapid, high-resolution, whole-brain, susceptibility-based MRI of multiple sclerosis. Mult. Scler. J. 2014; 20: 1464–1470.

Sawcer S, Franklin RJM, Ban M. Multiple sclerosis genetics. Lancet Neurol. 2014; 13: 700–709.

Sawcer S, Hellenthal G, Pirinen M, Spencer CCA, Patsopoulos NA, Moutsianas L, et al. Genetic risk and a primary role for cell-mediated immune mechanisms in multiple sclerosis. Nature 2011; 476: 214–219.

Sawcer S, Jones HB, Feakes R, Gray J, Smaldon N, Chataway J, et al. A genome screen in multiple sclerosis reveals susceptibility loci on chromosome 6p21 and 17q22. Nat. Genet. 1996; 13: 464–468.

Scalfari A, Neuhaus A, Daumer M, DeLuca GC, Muraro PA, Ebers GC. Early relapses, onset of progression, and late outcome in multiple sclerosis. JAMA Neurol. 2013; 70: 214–222.

Schmierer K, Parkes HG, So P-W, An SF, Brandner S, Ordidge RJ, et al. High field (9.4 Tesla) magnetic resonance imaging of cortical grey matter lesions in multiple sclerosis. Brain J. Neurol. 2010; 133: 858–867.

Schmierer K, Scaravilli F, Altmann DR, Barker GJ, Miller DH. Magnetization transfer ratio and myelin in postmortem multiple sclerosis brain. Ann. Neurol. 2004; 56: 407–415.

Schmierer K, Wheeler-Kingshott CAM, Tozer DJ, Boulby PA, Parkes HG, Yousry TA, et al. Quantitative magnetic resonance of postmortem multiple sclerosis brain before and after fixation. Magn. Reson. Med. Off. J. Soc. Magn. Reson. Med. Soc. Magn. Reson. Med. 2008; 59: 268–277.

Scolding N, Barnes D, Cader S, Chataway J, Chaudhuri A, Coles A, et al. Association of British Neurologists: revised (2015) guidelines for prescribing disease-modifying treatments in multiple sclerosis. Pract. Neurol. 2015; 15: 273–279.

Secondary Progressive Efficacy Clinical Trial of Recombinant Interferon-beta-1a in MS (SPECTRIMS) Study Group. Randomized controlled trial of interferon- beta-1a in secondary progressive MS Clinical results. Neurology 2001; 56: 1496–1504.

Sepulcre J, Goni J, Masdeu JC, Bejarano B, Velez de Mendizabal N, Toledo JB, et al. Contribution of white matter lesions to gray matter atrophy in multiple sclerosis: evidence from voxel-based analysis of T1 lesions in the visual pathway. Arch Neurol 2009; 66: 173–9.

Sepulcre J, Sastre-Garriga J, Cercignani M, Ingle GT, Miller DH, Thompson AJ. Regional gray matter atrophy in early primary progressive multiple sclerosis: a voxel-based morphometry study. Arch. Neurol. 2006; 63: 1175–80.

Sinnecker T, Dörr J, Pfueller CF, Harms L, Ruprecht K, Jarius S, et al. Distinct lesion morphology at 7-T MRI differentiates neuromyelitis optica from multiple sclerosis. Neurology 2012; 79: 708–714.

Stevenson VL, Miller DH, Rovaris M, Barkhof F, Brochet B, Dousset V, et al. Primary and transitional progressive MS: a clinical and MRI cross-sectional study. Neurology 1999; 52: 839–45.

Tallantyre EC, Bø L, Al-Rawashdeh O, Owens T, Polman CH, Lowe J, et al. Greater loss of axons in primary progressive multiple sclerosis plaques compared to secondary progressive disease. Brain 2009; 132: 1190–1199.

Tallantyre EC, Bø L, Al-Rawashdeh O, Owens T, Polman CH, Lowe JS, et al. Clinico-pathological evidence that axonal loss underlies disability in progressive multiple sclerosis. Mult. Scler. Houndmills Basingstoke Engl. 2010; 16: 406–411.

Tallantyre EC, Brookes MJ, Dixon JE, Morgan PS, Evangelou N, Morris PG. Demonstrating the perivascular distribution of MS lesions in vivo with 7-Tesla MRI. Neurology 2008; 70: 2076–8.

Tallantyre EC, Dixon JE, Donaldson I, Owens T, Morgan PS, Morris PG, et al. Ultra-high-field imaging distinguishes MS lesions from asymptomatic white matter lesions. Neurology 2011; 76: 534–539.

Tallantyre EC, Morgan PS, Dixon JE, Al-Radaideh A, Brookes MJ, Evangelou N, et al. A comparison of 3T and 7T in the detection of small parenchymal veins within MS lesions. Invest. Radiol. 2009; 44: 491–494.

Tallantyre EC, Morgan PS, Dixon JE, Al-Radaideh A, Brookes MJ, Morris PG, et al. 3 Tesla and 7 Tesla MRI of multiple sclerosis cortical lesions. J. Magn. Reson. Imaging 2010; 32: 971–977.

Tan IL, van Schijndel RA, Pouwels PJ, van Walderveen MA, Reichenbach JR, Manoliu RA, et al. MR venography of multiple sclerosis. AJNR Am J Neuroradiol 2000; 21: 1039–42.

The IFNB Multiple Sclerosis Study Group. Interferon beta-1b is effective in relapsing-remitting multiple sclerosis I. Clinical results of a multicenter, randomized, double-blind, placebo-controlled trial. Neurology 1993; 43: 655–655.

The North American Study Group on Interferon beta-1b in Secondary Progressive MS. Interferon beta-1b in secondary progressive MS Results from a 3-year controlled study. Neurology 2004; 63: 1788–1795.

Thompson AJ, Kermode AG, MacManus DG, Kendall BE, Kingsley DP, Moseley IF, et al. Patterns of disease activity in multiple sclerosis: clinical and magnetic resonance imaging study. BMJ 1990; 300: 631–634.

Thompson AJ, Montalban X, Barkhof F, Brochet B, Filippi M, Miller DH, et al. Diagnostic criteria for primary progressive multiple sclerosis: a position paper. Ann Neurol 2000; 47: 831–5.

Thompson AJ, Polman CH, Miller DH, McDonald WI, Brochet B, Filippi M, et al. Primary progressive multiple sclerosis. Brain 1997; 120 (Pt 6): 1085–96.

Thorpe JW, Kidd D, Kendall BE, Tofts PS, Barker GJ, Thompson AJ, et al. Spinal cord MRI using multi-array coils and fast spin echo. I. Technical aspects and findings in healthy adults. Neurology 1993; 43: 2625–2631.

Tintore M, Rovira A, Martinez MJ, Rio J, Diaz-Villoslada P, Brieva L, et al. Isolated demyelinating syndromes: comparison of different MR imaging criteria to predict conversion to clinically definite multiple sclerosis. AJNR Am J Neuroradiol 2000; 21: 702–6.

Tintoré M, Rovira A, Río J, Tur C, Pelayo R, Nos C, et al. Do oligoclonal bands add information to MRI in first attacks of multiple sclerosis? Neurology 2008; 70: 1079–1083.

Traboulsee A, Dehmeshki J, Peters KR, Griffin CM, Brex PA, Silver N, et al. Disability in multiple sclerosis is related to normal appearing brain tissue MTR histogram abnormalities. Mult. Scler. Houndmills Basingstoke Engl. 2003; 9: 566–573.

Trapp BD, Peterson J, Ransohoff RM, Rudick R, Mork S, Bo L. Axonal transection in the lesions of multiple sclerosis. N Engl J Med 1998; 338: 278–85.

Trapp BD, Ransohoff R, Rudick R. Axonal pathology in multiple sclerosis: relationship to neurologic disability. Curr Opin Neurol 1999; 12: 295–302.

Uğurbil K, Adriany G, Andersen P, Chen W, Garwood M, Gruetter R, et al. Ultrahigh field magnetic resonance imaging and spectroscopy. Magn. Reson. Imaging 2003; 21: 1263–1281.

Uhlenbrock D, Sehlen S. The value of T1-weighted images in the differentiation between MS, white matter lesions, and subcortical arteriosclerotic encephalopathy (SAE). Neuroradiology 1989; 31: 203–12.

VanAmerongen BM, Dijkstra CD, Lips P, Polman CH. Multiple sclerosis and vitamin D: an update. Eur. J. Clin. Nutr. 2004; 58: 1095–109.

Vaughan J t., Garwood M, Collins C m., Liu W, DelaBarre L, Adriany G, et al. 7T vs. 4T: RF power, homogeneity, and signal-to-noise comparison in head images. Magn. Reson. Med. 2001; 46: 24–30.

van Waesberghe JH, Kamphorst W, De Groot CJ, van Walderveen MA, Castelijns JA, Ravid R, et al. Axonal loss in multiple sclerosis lesions: magnetic resonance imaging insights into substrates of disability. Ann Neurol 1999; 46: 747–54.

Weinshenker BG, Bass B, Rice GP, Noseworthy J, Carriere W, Baskerville J, et al. The natural history of multiple sclerosis: a geographically based study. I. Clinical course and disability. Brain 1989; 112: 133–46.

Willis MD, Harding KE, Pickersgill TP, Wardle M, Pearson OR, Scolding NJ, et al. Alemtuzumab for multiple sclerosis: Long term follow-up in a multi-centre cohort. Mult. Scler. J. 2015: 1352458515614092.

Wilson M, Tench CR, Morgan PS, Blumhardt LD. Pyramidal tract mapping by diffusion tensor magnetic resonance imaging in multiple sclerosis: improving correlations with disability. J. Neurol. Neurosurg. Psychiatry 2003; 74: 203–207.

Wuerfel J, Sinnecker T, Ringelstein EB, Jarius S, Schwindt W, Niendorf T, et al. Lesion morphology at 7 Tesla MRI differentiates Susac syndrome from multiple sclerosis. Mult. Scler. J. 2012; 18: 1592–1599.

Young IR, Hall AS, Pallis CA, Bydder GM, Legg NJ, Steiner RE. NUCLEAR MAGNETIC RESONANCE IMAGING OF THE BRAIN IN MULTIPLE SCLEROSIS. The Lancet 1981; 318: 1063–1066.

Zeis T, Graumann U, Reynolds R, Schaeren-Wiemers N. Normal-appearing white matter in multiple sclerosis is in a subtle balance between inflammation and neuroprotection. Brain J. Neurol. 2008; 131: 288–303.

Zivadinov R, Bergsland N, Stosic M, Sharma J, Nussenbaum F, Durfee J, et al. Use of perfusion- and diffusion-weighted imaging in differential diagnosis of acute and chronic ischemic stroke and multiple sclerosis. Neurol. Res. 2008; 30: 816–826.

“Holmes gives a demonstration”

“You will not apply my precept,” he said, shaking his head. “How often have I said to you that when you have eliminated the impossible, whatever remains, *however improbable*, must be the truth? We know that he did not come through the door, the window, or the chimney. We also know that he could not have been concealed in the room, as there is no concealment possible. Whence, then, did he come?”

An excerpt from *The Sign of Four*

By Sir Arthur Conan Doyle